The Role of the Stargazin-like Protein Gamma 7

David John Cox

University College London, UK

Ph.D.

ProQuest LLC
789 East Eisenhower Parkway
P.O. Box 1346
Ann Arbor, MI 48106-1346

Abstract

Voltage-dependent calcium channel (VDCC) γ -subunits were first identified by their co-purification with VDCC α_1-subunits from skeletal muscle. Since then a further seven γ-subunits have been identified by their homology to γ1. Their role however is not limited to interaction with VDCCs. The second γ-subunit identified, γ2 (also known as Stargazin), along with γ3, γ4 and γ8 have been shown to be involved in regulation of α-amino-3-hydroxy-5-methyl-4-isoxazolepropionic acid (AMPA) receptor trafficking. Also, recent work has shown that expression of the VDCC α_1 subunit, $Ca_V2.2$, is reduced when it is co-transfected with γ7. The objectives of this study were to investigate the mechanism by which this reduction of $Ca_V2.2$ expression takes place and identify the role of γ7.

Several truncated γ7 subunits were made to examine if potential endoplasmic reticulum (ER) retention motifs, present in the C-terminal region of γ7, are involved in the reduction of $Ca_V2.2$ expression. Truncation of γ7 from Y217 (including both potential ER retention (RXR) motifs) did not alter its distribution compared to full length γ_7, both being localised in the ER in transiently transfected COS7 cells. This suggests that these ER retention motifs are not critical in the effect of γ7 on $Ca_V2.2$ expression. However, western blotting experiments, also using transiently transfected COS7 cells, show that the C-terminal region of γ7 is necessary and sufficient for the reduction of $Ca_V2.2$ expression. This was confirmed electrophysiologically using a *Xenopus* oocyte overexpression system

To aid in the elucidation of its role binding partners for γ7 were sought. PC12 cells, a rat pheochromocytoma cell line, were used a potential source of binding partners. RT-PCR and immunocytochemistry were used to show that γ7 is endogenously expressed in PC12 cells. Immunoprecipitation of HA tagged

γ7 from a stably transfected PC12 cell line identified three ribonucleotide binding proteins as potential binding partners.

Acknowledgements

I would like to thank my supervisors, Prof. Annette Dolphin and Prof. Steve Bolsover, for their assistance, guidance, and support throughout the course of my PhD. I would also like to thank them for their help with the correction of this thesis.

I would also like to thank everyone in the group, who have been so helpful and supportive during my PhD. I am especially grateful to Prof. Annette Dolphin and Dr Jerome Leroy for their collaborations with the electrophysiological experiments. In addition I would like to thanks the Proteomics and Peptide Facility at the MRC Clinical Science Centre, Imperial College for their help with the peptide mass fingerprinting.

Table of Contents

List of Figures and Tables

Figures

Tables

List of Abbreviations

A2RE	hnRNP A2 response element
ABP	α-binding pocket
ADAR	Adenosine deaminases acting on RNA
Aga	Agatoxin
AID	α interaction domain
AMPA	α-amino-3-hydroxy-5-methyl-4-isoxazole propionic acid
ARC	Activity-related cytoskeleton-associated protein
ASK1	Apoptosis-signalling kinase 1
ATF6	Activating transcription factor 6
BCA	Bicinchoninic acid
BHK	Baby hamster kidney
BSA	Bovine serum albumin
CaMKII	Calcium/calmodulin-dependent protein kinase II
CBF	CAAT-binding factor
CFP	Cyan fluorescent protein
CHOP	C/EBP homologous protein
CIAP	Calf Intestinal Alkaline Phosphatase
Ctx	Conotoxin
DAPI	4',6-Diamidino-2-phenylindole
DHP	Dihydropyridine
DMEM	Dulbecco's Modified Eagle Medium
DTT	Dithiothreitol
EEG	Electroencephalography
eIF2	Translation initiation factor 2
EMP	Epithelial membrane protein
ER	Endoplasmic reticulum
ERAD	ER-associated degradation
ERSE	ER stress element
EST	Expressed Sequence Tag

FBS	Foetal Bovine Serum
FITC	Fluorescein isothiocyanate
GABA	γ-aminobutyric acid
GFP	Green fluorescent protein
GluR	Glutamate receptor
HA	Hemagglutinin
hnRNP	Heterogeneous nuclear ribonucleoprotein
HVA	High voltage activated
IRE1	Inositol-requiring-1
JIK	Jun N-terminal inhibitory kinase
LC2	Light chain 2 of microtubule-associated protein
LVA	Low voltage activates
MAGUK	Membrane-associated guanylate kinase
MBP	Myelin basic protein
MP20	Membrane protein 20
NGF	Nerve growth factor
NMDA	N-methyl-D-asparate
nPIST	Neuronal isoform of protein-interacting specifically with TC10
PAGE	Polyacrylamide gel electrophoresis
PBS	Phosphate buffered slaine
PCR	Polymerase Chain Reaction
PDI	Protein Disulphide Isomerase
PDVF	Polyvinylidene fluoride
PDZ	Postsynaptic density-95/Discs large/zona occludens-1
PERK	PKR-like ER kinase
PKA	Protein kinase A
PKC	Protein kinase C
PMP22	Peripheral myelin protein 22
PP(1/2B)	Protein Phosphatase (1/2B)
PSD-95	Postsynaptic density protein 95
QPCR	Quantitative polymerase chain reaction (real time)
RPMI	Roswell Park Memorial Institute 1640
RNP	Ribonucleoprotein
RT-PCR	Reverse transcriptase PCR

SCG	Superior cervical ganglion
SDS	Sodium dodecyl sulphate
SR	Sarcoplasmic reticulum
TAE	Tris, acetic acid, EDTA
TBS	Tris buffer saline
TARP	Transmembrane AMPA receptor regulatory protein
TLS	Translocated in liposarcomas
TNF	Tumor necrosis factor
UPR	Unfolded protein response
VDCC	Voltage-dependent calcium channel
VDIC	Voltage-dependent ion channel
XBP	X-box binding protein
YFP	Yellow fluorescent protein

Chapter 1 - Introduction

1.1. Excitable Cells and Action Potentials

Excitable cells are cells that respond regeneratively to a small change in membrane potential. They are essential in a range of roles from movement (in the case of muscle cells) to conscious thought (in the case of neurons). Key to the functions of excitable cells are changes in ion concentrations across the plasma membrane. I will begin by explaining how the resting membrane potential is maintained and how changes in ion concentration can generate action potentials.

1.1.1. The Resting Membrane Potential

All cells have a resting membrane potential due to a local imbalance of charge across the membrane. In neurons the resting membrane potential is between -50 and -80 mV. This is maintained by several factors, most important of which is the electrogenic sodium/potassium pump. This pump, at the expense of energy in the from of ATP, moves two potassium ions into the cell and three sodium ions out thus creating a net negative charge inside the cell. This leads to a high potassium concentration within the cell compared to outside ($[K^+]$ inside = 100 mM, $[K^+]$ outside = 5 mM). The reverse is true for sodium concentration ($[Na^+]$ inside = 15 mM, $[Na^+]$ outside = 150 mM). Using the Nernst equation one can find the equilibrium potential for each ion, E_K = -80 mV and E_{Na} = 62 mV.

In the absence of the sodium/potassium pump, if the membrane was impermeable to both K^+ and Na^+ ions then there could be no movement of ions and thus no membrane potential. If the membrane was only permeable to Na^+ then the membrane potential would be equal to E_{Na} (62 mV). Likewise if the membrane was only permeable to K^+ then the membrane potential would be -80 mV. This suggests that the resting membrane potential is due to a combination of permeability of both ions with K^+ being the major contributor. Using the Constant Field Equation (also known as the Goldman-Hodgkin-Katz equation), which takes into account the permeability of the membrane, one can calculate the membrane potential. If the membrane was equally permeable to both ions then V_m = 7.97 mV. However, if the membrane is taken to be 40 times more

permeable to K^+ than Na^+ then V_m is approximately equal to the observed value of -65 mV. This calculation however is an oversimplification. It can be improved by taking into account other ions (most notably calcium and chloride ions). Anionic proteins, a common constituent of cells, also affect the resting membrane potential.

1.1.2. The Action Potential

The changes in membrane potential during an action potential can roughly be split into 4 stages (shown in Fig. 1.1.). Firstly, after stimulation, there is the rising phase during which there is rapid depolarisation of the membrane. At the peak of this depolarisation the membrane potential reaches about + 40 mV. The point at which the membrane potential is greater than 0 mV is known as the overshoot. The falling phase of the action potential is a rapid repolarisation, past the resting membrane potential, until the membrane is actually more negative than the resting potential. The stage at which the membrane potential is less than the resting potential is known as the undershoot. There is then a relatively slow return to the resting membrane potential. Overall the action potential from beginning to end takes about 2 msec.

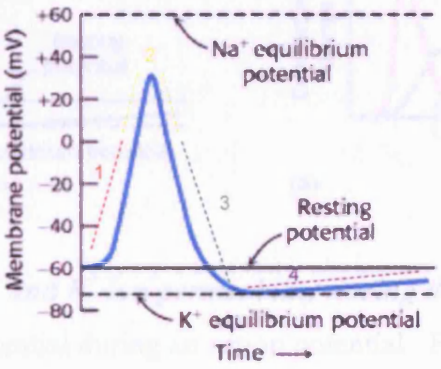

Fig. 1.1. Changes in membrane potential at a single point during an action potential. After stimulation the membrane depolarises (1, rising phase), reaches a peak (2, overshoot) and begins to repolarise (3, falling phase) passing, and then slowing returning to the resting membrane potential (4 undershoot). Adapted from Lodish *et al* (1).

A series of experiments by Hodgkin and Huxley in the 1950's showed that the ionic current flow through the axon membrane was largely accounted for by changes in its conductance to Na^+ and K^+ ions. They went on to propose a model of the action potential in which sites for ionic flow were opened as a result of membrane potential change (2-5). During the rising phase the inside of the membrane has a negative electrical potential with a large driving force on Na^+ ions. Na^+ ions enter the cell causing rapid depolarisation of the membrane. During the overshoot phase the relative permeability of the membrane favours sodium and the membrane potential goes close to E_{Na}. During the falling phase the membrane permeability to sodium reduces and the permeability to potassium increases. K^+ ions leave, causing the membrane potential to become negative again. During the undershoot phase the membrane potential moves towards E_K. The membrane then becomes less permeable to K^+ and, due to the action of the electrogenic sodium/potassium pump, the resting potential is restored. These changes in ion permeability during the action potential are shown in Fig. 1.2. The sites of ionic flow proposed by Hodgkin and Huxley have now been shown to be voltage-dependent ion channels (VDICs).

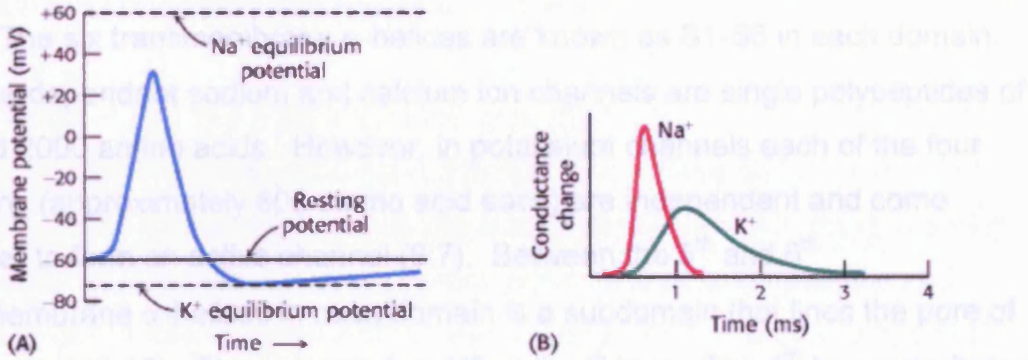

Fig. 1.2. Changes in Na^+ and K^+ ion permeability during the action potential. A) Changes in membrane potential during an action potential. B) Corresponding changes in Na^+ and K^+ permeability. After stimulation the cell membrane transiently becomes more permeable to Na^+ resulting in depolarisation. The subsequent reduction in Na^+ permeability and increase in K^+ permeability results in hyperpolarisation. Adapted from Lodish *et al (1)*.

1.2. Voltage-Dependent Ion Channels

All VDICs serve similar functions and there is a high degree of similarity between their structures. Firstly they required a voltage senor to detect changes in the membrane potential. Upon detecting a change they need to open to allow ions to flow across the membrane. It is also vital that they contain a specificity filter to ensure that only the required ions can pass through. Finally, when required, they need to return to a closed state to prevent further ions passing through. Here I will try to describe common features shared between VDICs

1.2.1. The Molecular Structure of the Voltage-Dependent Ion Channels

All VDICs cloned thus far have a similar structure. They can be thought of as consisting of two main parts. Firstly, the pore, through which the ions pass. Secondly, the voltage sensor, the movement of which results in opening or closing of the channel depending on the membrane potential. All VDICs contain twenty four transmembrane α-helices separated into four domains (Fig. 1.3.). The six transmembrane α-helices are known as S1-S6 in each domain. Voltage-dependant sodium and calcium ion channels are single polypeptides of around 2000 amino acids. However, in potassium channels each of the four domains (approximately 600 amino acid each) are independent and come together to form an active channel (6;7). Between the 5^{th} and 6^{th} transmembrane α-helices in each domain is a subdomain that lines the pore of the channel (8-10). This is termed as H5 or the P loop. The 4^{th} transmembrane α-helix in each domain has multiple positively charged amino acids and is thought to function as the voltage sensor (Fig. 1.3.).

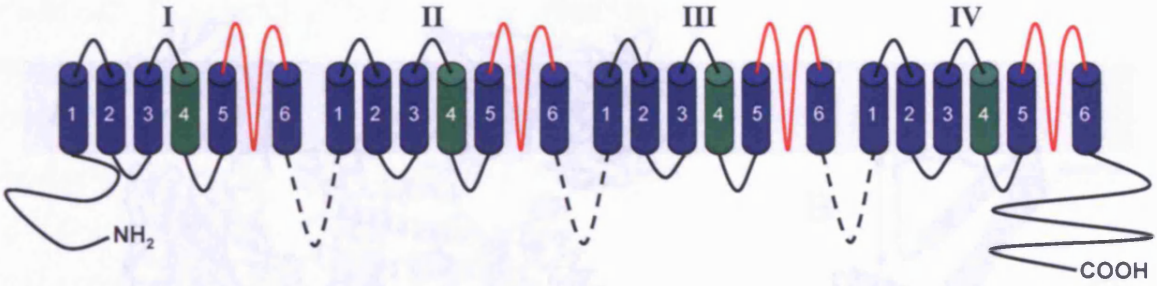

Fig. 1.3. A diagrammatic representation of voltage-dependent ion channels. Transmembrane domains are shown in blue. The S4 domain, thought to be the voltage sensor is shown in green. The P-loop, believed to line the pore of the channel is shown in red. Dashed lines represent the intracellular loops that connect the individual domains in voltage-dependent sodium and calcium channels. These are absent in voltage-dependent potassium channels.

Recent work by Jiang *et al* (11) determined the crystal structure of a voltage-dependent potassium channel from the archaebacterial *Aeropyrum pernix* (Fig. 1.4).

1.2.2. Channel Opening and the Voltage Sensor

Hodgkin and Huxley had previously predicted 'some component of the membrane which behaves as though it had a large charge or dipole moment' (2). The movement of which should generate a small current during the gating of the channel. Detection of these "gating currents" was achieved and has proven useful in testing models of voltage dependent ion channel function (12).

Upon the deduction of the primary structure of a voltage-dependent sodium channel from *Electrophorus electricus,* Noda *et al* (13) suggested the possible importance of the highly positively charged S4 segment in detecting changes in membrane potential and gating of the channel. Site directed mutagenesis experiments, in which these positively charged amino acids were replaced, confirmed a relationship between these charges and the membrane potential at which the channels opened (14;15).

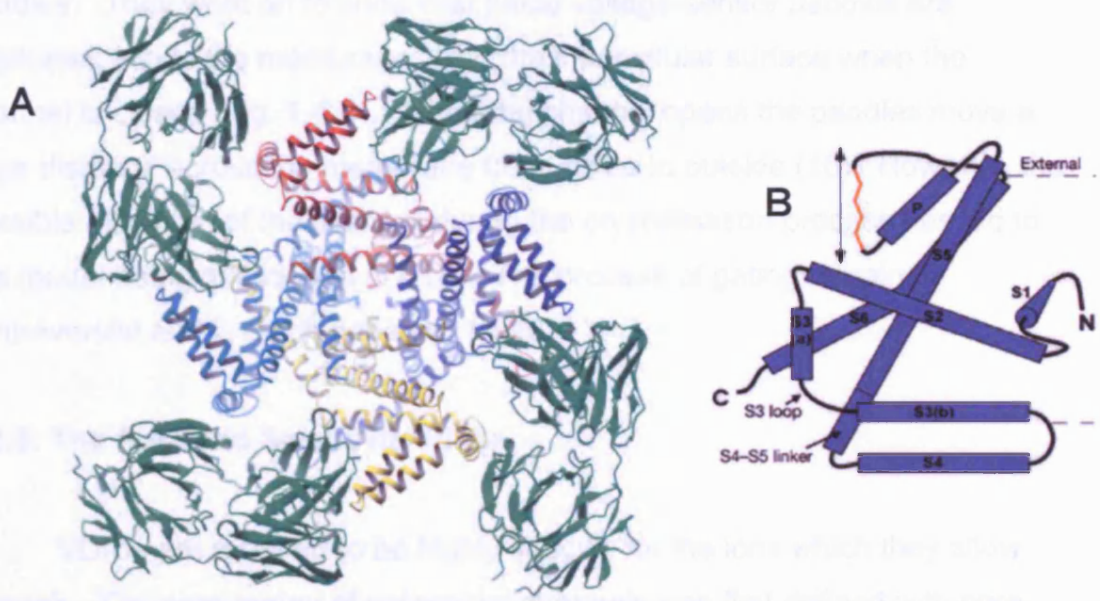

Fig. 1.4. A diagrammatic representation of the voltage-dependent potassium channel. **A.** Structure of the K_VAP channel (blue, yellow, cyan and red helical structures) bound to four Fab fragments (green), viewed down the four-fold axis from the intracellular side. **B.** A schematic diagram of the KvAP subunit topology is shown with an orange selectivity filter and an arrow to indicate the ion pathway. Adapted from Jiang *et al* (11).

There is an energetic problem of moving charged amino acids through the low dielectric environment of the membrane lipid bilayer. The conventional model of how this occurs places the majority of S4 charges in the gating pore, a highly solvated aqueous environment, formed largely by S1–S3 segments peripherally and the pore domain centrally. The positive charges on the S4 segment are paired with negative charges on the other segments. Upon depolarisation of the membrane the S4 segment moves outwards exposing positive charges to the outside of the membrane and negative charges to the inside. Thus, the S4 charges cross the membrane with minimal contact with the hydrophobic core of the bilayer.

With the determination of a crystal structure of a voltage-dependent potassium channel a new model of how the voltage sensor works was proposed. Jiang *et al* (11) found that each S4 segment formed half of a cationic, helix–turn–helix structure. These were termed 'voltage-sensor

paddles'. They went on to show that these voltage-sensor paddles are positioned inside the membrane, near the intracellular surface when the channel is closed (Fig. 1.4.B). When the channel opens the paddles move a large distance across the membrane from inside to outside (16). However, the possible distortion of the channel during the crystallisation process has led to this model being questioned (17;18). The process of gating remains controversial and is much debated (19-22).

1.2.3. The Pore and Selectivity Filter

VDICs are required to be highly specific for the ions which they allow through. The pore-region of potassium channels was first defined with pore-blocking scorpion toxins (23). Further detail was obtained with the generation of a crystal structure of a potassium channel from *Streptomyces lividans*, KcsA, a two transmembrane spanning protein with homology to the S5-S6 region of voltage-dependant potassium channels.

This crystal structure led to a model where the pore is constructed as an inverted cone, with the selectivity filter held at its base. The narrow selectivity filter is only 12 Å long, whereas the remainder of the pore is wider and has a relatively inert hydrophobic lining. These structural and chemical properties favour a high K^+ throughput by minimising the distance over which K^+ interacts strongly with the channel. A large water-filled cavity and helix dipoles are thought to help to overcome the high electrostatic energy barrier facing a cation in the low dielectric membrane centre. The K^+ selectivity filter is lined by carbonyl oxygen atoms, which provide multiple closely spaced sites. The filter is constrained in an optimal geometry so that a dehydrated K^+ ion fits with proper coordination but the Na^+ ion is too small. Two K^+ ions at close proximity in the selectivity filter will repel each other. This repulsion overcomes the otherwise strong interaction between ion and protein and allows rapid conduction in the setting of high selectivity. These properties select for monovalent cations by providing a polar environment with a partial negative charge, and give just the right diameter to select for K^+ over cations of different size.

The outer vestibule and selectivity region of the sodium and calcium channels must be different from the K^+ channel structure to account for their different selectivity properties. In sodium channels mutation studies have revealed that the most important structural feature is the two rings of charged amino acids around the narrow selectivity filter, responsible for the channel's affinity for sodium ions (24-27). Specifically, four highly conserved amino acids in the same relative position in the Na^+ channel P loops of domains I-IV participate in the formation of the selectivity filter, Asp-384, Glu-942, Lys-1422, and Ala-1714 (the DEKA motif), using the rat brain residue channel numbers.

The P loops of domains I-IV of high voltage activated (HVA) voltage-dependent calcium channels contain a highly conserved pattern in positions corresponding to those of the DEKA motif. These residues are Glu-393, Glu-736, Glu-1145, and Glu-1446 (the EEEE motif), using the numbers of the rabbit cardiac L-type channel (rabbit $Ca_v1.2$). In low voltage activated (LVA) calcium channels, there are two glutamates and two aspartates at the corresponding positions. The current model of calcium channel selectivity is that the pore acts like an ion exchange resin, with the four closely spaced negative charges attracting an equal number of positive charges (28). The high density of negative charge in the pore is crucial for selectivity for divalent cations. Indeed, in the absence of divalents, calcium channels are non-selective cation channels that allow even relatively large organic cations to permeate (29). Much work has been performed upon exactly how ions pass though the pore of ion channels. However, it is beyond the scope of this study and will not be discussed further here.

1.2.4. Inactivation

A further characteristic of voltage-dependent ion channels is that after maintained depolarisation of the membrane they inactivate. They spontaneously close and will not reopen until the membrane is repolarised. In potassium channels it was proposed that a "ball and chain" model of inactivation, in which a mobile part of the protein moves so as to block the pore, takes place (30). This is also known as N-type inactivation as the ball and chain are at the N-terminus of the protein. Support for this model was provided by

Zagotta *et al* (31) who showed that 1) removal of the "ball" removed inactivation 2) that shortening of the chain speed up inactivation and 3) that expression of the "ball" alone was sufficient to block the channel. There is also C-type inactivation involving the S6 and H5 regions which is likely to be associated with a change in the permeability characteristics of the pore (32;33). In addition, the β-subunits of mammalian voltage-dependent potassium channels have also been shown to be involved in inactivation (34).

Inactivation of sodium and calcium channels involves different mechanisms. Stühmer *et al* (14) and West *et al* (35) showed that in sodium channels a region of conserved positively charged and hydrophobic amino acids in the cytoplasmic section between domains III and IV was involved in inactivation. It is believed that this region works similarly to the ball in potassium channels. Both auxiliary β-subunits (36) and the S4 segment (37) have also been shown to be involved. In calcium channels the S6 segment of Domain I has been shown to be involved in inactivation (38). The auxiliary subunits of voltage-dependent calcium channels have also been shown to be involved, as will be discussed later.

The kinetics of inactivation will not be extensively discussed here. A model based on the work of Kou and Bean (39) on voltage-dependent sodium channels and furthered by Serrano *et al* (40) working on voltage-dependent calcium channels ($Ca_V3.1$) channels is given in Fig. 1.5. They assume that all four voltage sensors must activate before the channel can open. However, inactivation can occur directly from closed states.

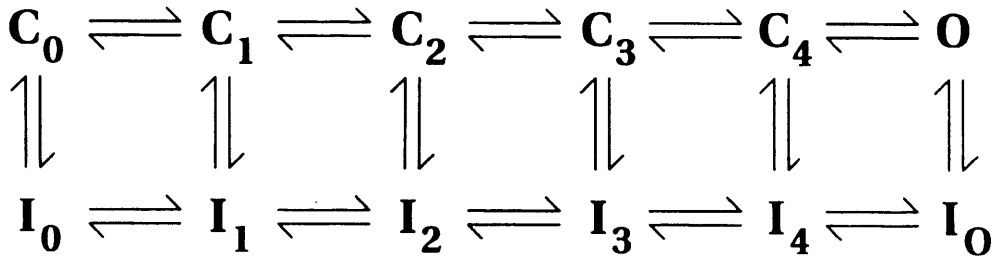

Fig. 1.5. A model of gating of voltage dependent calcium channels. The gating of VDCC channels is modelled by a number of stages. They open (C_0 to O), inactivate (O to I_0) and recover (back to C_0). In the open state all four voltage sensors are activated. C = closed, I = inactivated, O = Open. Adapted from Serrano *et al* (40)

1.3. Voltage-Dependent Calcium Channels

As a member of the VDIC family voltage-dependent calcium channels (VDCCs) are primarily composed of a pore forming subunit. However, when VDCC were first purified from the transverse tubule membranes of skeletal muscle (41) along with the pore forming (α) subunit additional proteins (β, γ) were also identified.

More detailed biochemical analyses revealed an additional $\alpha_2\delta$ subunit co-migrating with the $\alpha 1$ subunit (42). These auxiliary proteins have been shown to be important in calcium channel function and will be discussed further in section 1.3.4. Biochemical analysis led to a model comprising a 190 kDa principal transmembrane α_1 subunit associated with a disulfide-linked $\alpha_2\delta$ hetrodimer of 170 kDa and a 33 kDa transmembrane γ subunit. The 55 kDa β subunit was not predicted to have any transmembrane domains and was thus thought to be intracellular (Fig. 1.6).

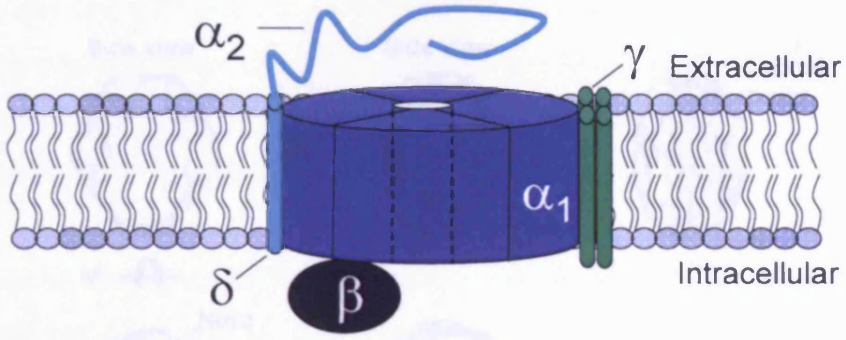

Fig. 1.6. A diagrammatic representation of a voltage-dependent calcium channel. The channel is primarily composed by the pore forming α_1 subunit. In addition to this there is an intracellular β subunit, an extracellular α_2 subunit connected by disulphide bonds to a single transmembrane δ subunit and a four transmembrane γ subunit.

While no crystal structure of a VDCC has been obtained Wang *et al* (43;44) have used electron microscopy to obtain three-dimensional structures of skeletal and cardiac VDCCs. The skeletal muscle VDCCs were isolated as dimers composed of two arch-shaped monomers ~210 Å across and ~75 Å thick, that interact very tightly at each end of the arch. The roughly toroidal structure of the two monomers enclosed a cylindrical space of ~80 Å diameter, which is then closed on each side by two dome-shaped protein densities reaching over from each monomer arch. The dome-shaped domains had a length of ~80–90 Å and a maximum height of ~45 Å. Small orifices punctuated their exterior surface. The cardiac VDCC (Fig. 1.7) was found to have a similar structure with a major difference being apparent in the putative transmembrane region, which would be consistent with the absence of the γ subunit.

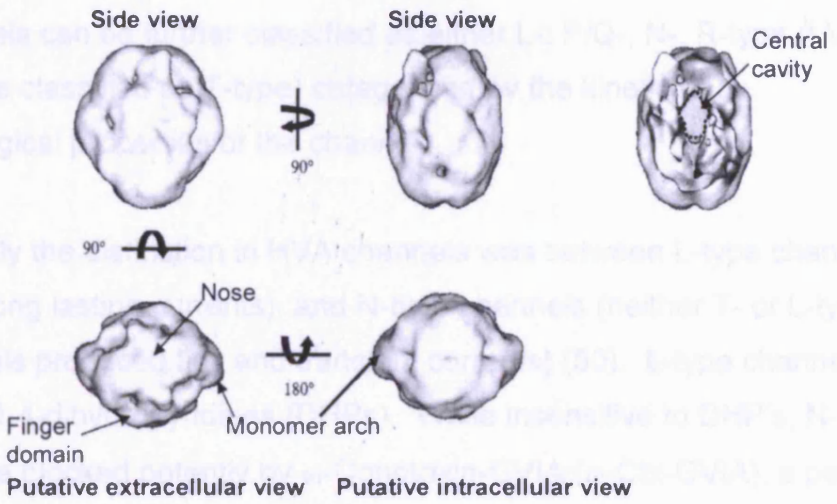

Fig. 1.7. A three-dimensional structure of the cardiac voltage-dependant calcium channel. The complex has a total width of 14.5 nm with a central chamber that encloses a volume with a height and width 5 x 3 nm, respectively, and depth of 4 nm. They can be thought of as being comprised of three regions 1) the monomer arches. 2) the finger domains, which are protein densities protruding from the monomer arches that surround a central aqueous compartment. 3) The nose region which is formed by the intimate association of the monomer arches creating a narrow bridge, with some contribution from the tips of the finger domains. Adapted from Wang *et al* (44).

1.3.1. Identification and Classification of Voltage-Dependent Calcium Channels

The first work on calcium channels was performed by Bernard Katz, Paul Fatt and Bernard Ginsborg in the 1950's on the large muscle cells of crab (45) and crayfish (46). Due to their importance in many physiological processes much work has been performed on identifying VDCCs and attempting to elucidate their mechanisms of action. Now, in mammalian genomes, 10 VDCCs have been identified and more than 20 putative genes have been identified which may encode functional calcium channel subunits (47;48).

The primary distinction between channel types is the voltage at which the channel operates. Low voltage-activated channels (LVA) are activated by weak depolarisation and rapidly inactivate, whereas high voltage-activated (HVA)

channels require stronger depolarisation and have variable inactivation (49). HVA channels can be further classified as either L-, P/Q-, N-, R-type (LVA channels are classified as T-type) categorised by the kinetic and pharmacological properties of the channel.

Initially the distinction in HVA channels was between L-type channels (large and long lasting currents), and N-type channels (neither T- or L-type: T-type channels produced tiny and transient currents) (50). L-type channels are blocked by 1,4-dihydropyridines (DHPs). While insensitive to DHP's, N-type channels are blocked potently by ω-Conotoxin-GVIA (ω-Ctx-GVIA), a peptide isolated from the venom of a cone snail *Conus geographus* (51).

Regan *et al* (52;53) discovered neuronal HVA channels that were not blocked by DHPs or by ω-Ctx-GVIA, thus fitting into neither category. Named P-type channels (originally characterized in Purkinje neurons of the cerebellum (54)) they were found to be blocked by the toxin ω-Agatoxin-IVA (ω-Aga-IVA), a peptide from the venom of the funnel-web spider (*Agelenopsis aperta*) (55). Zhang *et al* (56) identified a further set of channels that were also resistant to DHP's and ω-Ctx-GVIA but were blocked less rapidly and/or potently by ω-Aga-IVA. These were named Q-type channels. Due to the difficulty in determining a distinction between P- and Q-type channels they are often grouped together and termed P/Q-type channels. Also, there is HVA current that is resistant to DHP's, ω-Ctx-GVIA and ω-Aga-IVA. Named R-type channels (resistant), they inactivate more rapidly than the other HVA currents and may activate at more negative voltages (56;57) and may include multiple channel subtypes (58).

The different types of VDCC currents are, primarily defined by different α_1 subunits. The first α_1 subunit to be cloned was the L-type channel of skeletal muscle. Six other HVA α_1 subunits were cloned by homology. Later three LVA α_1 subunits were cloned. The cloned α_1 subunits were originally designated classes A through I, with S used for the α_1 subunit from skeletal muscle. This single-letter notation for the α_1 subunits has now, for the most part, been superseded by the Ca_V classification proposed by Ertel *et al* (59). This scheme

classified VDCCs by the structural relationship between the α1 subunits and splits them into three families Ca_V1, Ca_V2 and Ca_V3 (Fig. 1.8.).

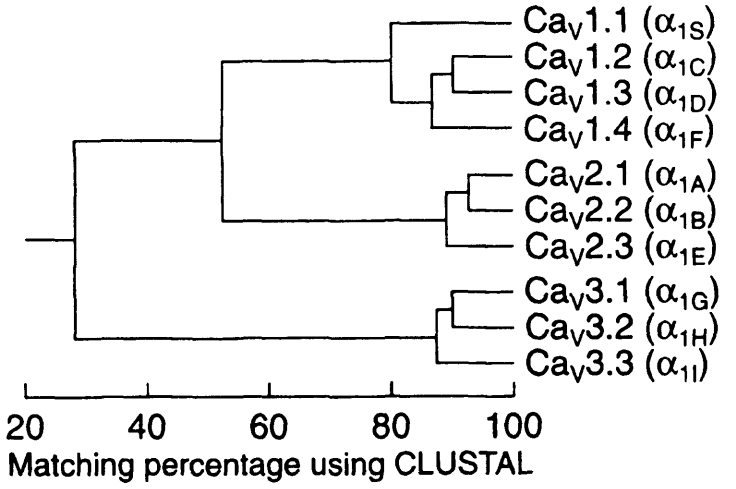

Fig. 1.8. Phylogeny of voltage-dependent calcium channel α_1 subunits. Comparison of all sequence pairs defined three families with intrafamilial sequence identities above 80% ($Ca_V1.x$, $Ca_V2.x$, $Ca_V3.x$). A consensus sequence was defined for each family, and these three sequences were compared to one another, with interfamily sequence identities of ~52% ($Ca_V1.x$ versus $Ca_V2.x$) and 28% ($Ca_V3.x$ versus $Ca_V1.x$ or $Ca_V2.x$). Only the membrane-spanning segments and the pore loops (~350 amino acids) were compared. Adapted from Ertel *et al* (59).

Expression of the cloned α_1 subunits in mammalian cells or *Xenopus* oocytes and analysis of their pharmacological and biophysical profiles has allowed the correlation between the α_1 subunits and the type of current they produce. The HVA channels are produced by the $Ca_V1.x$ and $Ca_V2.x$ α_1 subunits. $Ca_V1.1$, $Ca_V1.2$, $Ca_V1.3$, and $Ca_V1.4$ are L-type channels (60-65). $Ca_V2.1$ is thought to encode both P- and Q-type channels by alternative splicing of the same gene (66-69). The N-type calcium channel is produced by $Ca_V2.2$ (63;68;70;71). $Ca_V2.3$ likely constitutes a variant of the R-type calcium channel family (58;72-75). The LVA T-type channels are produced by $Ca_V3.1$, $Ca_V3.2$, and $Ca_V3.3$ (76-83) The various methods of classification of each of the α_1 subunits are given in Table 1.

1.3.2. Calcium as a Signalling Molecule

Ca^{2+} ions are required for the proper functioning of many extracellular and intracellular processes, including muscle contraction, nerve conduction, hormone release, and blood coagulation. In addition, the Ca^{2+} ion plays a unique role in intracellular signalling and is involved in the regulation of many enzymes.

Both the extracellular and intracellular concentrations of Ca^{2+} are tightly regulated by bidirectional Ca^{2+} transport across the plasma membrane of cells and by the membranes of intracellular organelles such as the endoplasmic reticulum, the mitochondria, and the sarcoplasmic reticulum of muscle cells. This results in remarkably low intracellular Ca^{2+} concentration ($\approx 10^{-7}$ M) compared to the extracellular concentration ($\approx 10^{-3}$ M) and allows the opening of a relatively small number of calcium channels to cause a large transient change in intracellular Ca^{2+} concentration.

Upon opening of the channel the Ca^{2+} concentration in the area near the inner mouth of a calcium channel ("nanodomain") can approach millimolar levels and near the membrane, but away from the channel ("microdomain") it reaches micromolar levels. While these highly localised Ca^{2+} gradients cannot be measured directly they can be estimated from simulations of Ca^{2+} diffusion and binding (84-89).

1.3.3. The Function of Voltage-Dependent Calcium Channels

A range of cellular responses are triggered by the influx of Ca^{2+} through VDCCs including neurotransmitter release (90), neuronal excitability (91), neurite outgrowth (92) and Ca^{2+} release from cytoplasmic stores (93). It has also been implicated in synaptic plasticity, the regulation of calcium-dependent second messenger cascades (such as cyclic adenosine monophosphate and inositol 1,4,5-trisphosphate) and in the regulation of gene expression (94;95).

Ca_V Classification	Single-letter Notation	Gene Name	Physiological Classification	Voltage Activation
$Ca_V1.1$	α_{1S}	*CACNA1S*	L	HVA
$Ca_V1.2$	α_{1C}	*CACNA1C*	L	HVA
$Ca_V1.3$	α_{1D}	*CACNA1D*	L	HVA
$Ca_V1.4$	α_{1F}	*CACNA1F*	L	HVA
$Ca_V2.1$	α_{1A}	*CACNA1A*	P/Q	HVA
$Ca_V2.2$	α_{1B}	*CACNA1B*	N	HVA
$Ca_V2.3$	α_{1E}	*CACNA1E*	R	HVA
$Ca_V3.1$	α_{1G}	*CACNA1G*	T	LVA
$Ca_V3.2$	α_{1H}	*CACNA1H*	T	LVA
$Ca_V3.3$	α_{1I}	*CACNA1I*	T	LVA

Table 1. Classification of the VDCC α_1 subunits

As the structural relationship would suggest, the primary division in the roles of VDCCs is between HVA channels, crucial for muscle contraction and neurotransmitter release and LVA channels, involved in generation of repetitive electrical activity.

In skeletal muscle, $Ca_V1.1$ acts as a voltage sensor, coupling membrane depolarisation to release of calcium from the sarcoplasmic reticulum (SR). Franzini-Armstrong and Protasi (96) showed that this involves a direct physical interaction between the $Ca_V1.1$ channels and the ryanodine receptor of the SR. $Ca_V1.2$ is involved in excitation-contraction coupling in cardiac muscle. In contrast to $Ca_V1.1$, it is the influx of calcium through $Ca_V1.2$ which produces highly localised calcium influx, which triggers Ca^{2+}-induced Ca^{2+} release from the cardiac SR (89;97).

L-type VDCCs are also widespread in neurons. They are typically confined to cell bodies (98) where they likely regulate calcium dependent enzymes, gene expression and integration of synaptic inputs (99). However, some specialized synapses use L-type channels (100) and there is some evidence for functional coupling of neuronal L-channels to ryanodine receptors (101). L-type VDCCs are also present in secretory cells such as endocrine cells where they initiate release of hormones (102).

Other HVA channels (notably N and P/Q channels) seem to be restricted to neurons and related endocrine cells, and are the primary calcium channels involved in the release of neurotransmitters at most synapses (90). N- and P/Q-type calcium channels show highest expression levels at presynaptic terminals and are directly coupled to neurotransmitter release (103-105). R-type calcium channels are expressed on proximal dendrites and may, in some neurons, participate in neurotransmitter release (106).

In addition to the effects of increasing the intracellular calcium concentration the inward current produced by VDCCs also contributes to the action potential. The electrical component of the calcium influx is especially important in the LVA VDCCs, which are involved in the generation of repetitive activity in several cell types, including cardiac pacemaker cells and thalamic

neurons (107). Briefly, hyperpolarisation removes the resting inactivation from LVA channels. This causes the channels to activate, producing a low-threshold spike, which in turn triggers a burst of sodium-dependent action potentials. Rapid inactivation of the LVA channels (and also activation of various potassium channels) leads to termination of this burst. Providing that the subsequent hyperpolarisation is sufficient to once again remove the inactivation from the channels, the cell can burst repetitively.

1.3.4. Auxiliary Subunits of Voltage-Dependent Calcium Channels

As mentioned previously, although the α_1 subunit is sufficient to form a functional channel (108) it is believed that endogenously it is associated with ancillary $\alpha_2\delta$, β and γ subunits. These ancillary subunits have been shown to modulate various properties of the channel (such as activation and inactivation) and also are thought to be involved in the trafficking of the channel to the cell membrane (109-117). The structures and functions of the $\alpha_2\delta$ and β subunits will be briefly discussed here and with γ subunits discussed later.

1.3.4.1. β subunits of Voltage-Dependent Calcium Channels

Ruth *et al* (118) were the first to clone a β subunit (the same β as purified by Takahashi *et al* (42)). A further three β subunit were identified by homology and subsequently cloned (81;111;112;119). The proteins encoded by these genes are further diversified by splice variants of each of these subunits. Their expression varies depending upon tissue type with all four genes being expressed within the brain. There does not appear to be an exclusive pairing between any one α_1 and β subunit (120).

All four β subunit genes encode intracellular proteins comprised of two domains connected by a flexible linker (121) (Fig. 1.9). These two domains were subsequently noted to be homologous to the SH3 and the guanylate kinase families (122;123). Recent crystallographic analyses confirmed these findings and showed β subunits to be a members of the membrane-associated guanylate kinase (MAGUK) protein family (124-126).

Pragnell *et al* (127) showed that β subunits bind with high affinity to the cytoplasmic intracellular linker between domains I and II of all HVA calcium channels, via an 18 amino acid motif called the α interaction domain (AID) on the I–II linker. This interacts with the β subunit through a conserved hydrophobic cleft (named the α-binding pocket, ABP) in the guanylate kinase domain. Other, lower affinity, β subunit interaction sites have been identified on various α subunits (128-131). However, it has not yet been established whether the β subunit is an invariable stoichiometric subunit of the calcium channel, or whether it reversibly associates.

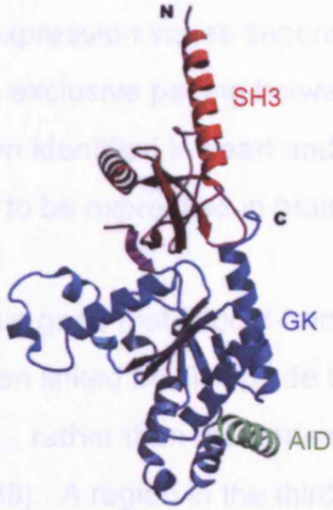

Fig. 1.9. The structure of the VDCC β subunit. Structure of VDCC β functional core in complex with the AID ribbon. Domain I, domain II, and the AID are represented in red, blue, and green, respectively. Adapted from Opatowsky *et al* (125).

Lacerda *et al* (109) reported that co-expression of the β subunit with the skeletal $Ca_V1.1$ enhances the level of expression and confers gating properties more like endogenous channels. Co-expression of β subunits with the cardiac and neuronal α_1 subunits also had a large effect on the level of α_1 expression and the voltage dependence and kinetics of gating of the channel. Generally in expression systems co-expression of β subunits increases the level of expression of the α_1 subunit (reviewed in (132)), and in its absence the majority of the α_1 that remains is in the ER (133). These findings have led to the

hypothesis that one role of the β subunit is to act as a chaperone assisting the trafficking of the channel to the plasma membrane. In addition to increased levels of α_1 expression the kinetics of the channel are also altered. Generally the voltage dependence of activation and inactivation is shifted to more negative membrane potentials, and the rate of inactivation is increased (reviewed in (120).

1.3.4.2. $\alpha_2\delta$ subunits of Voltage-dependent Calcium Channels

Thus far four genes encoding $\alpha_2\delta$ subunits ($\alpha_2\delta$-1- $\alpha_2\delta$-4) have been identified (115;134-136), further diversity is introduced by alternative splicing. Similarly to the β subunits $\alpha_2\delta$ expression varies depending upon tissue type and there does appear to be an exclusive pairing between any one α_1 and $\alpha_2\delta$ subunit. All four $\alpha_2\delta$'s have been identified in heart and skeletal muscle and $\alpha_2\delta$-1 - $\alpha_2\delta$-3 have been shown to be expressed in brain (115;135-138).

$\alpha_2\delta$ is a product of a single gene that is post-translationally cleaved into α_2 and δ peptides, which are then linked by disulphide bridges (139-141). It is believed that the extracellular α_2, rather than the transmembrane δ subunit, interacts with the α_1 subunit (138). A region in the third domain of the α_1 subunit (in the first extracellular loop between the 5th and 6th transmembrane regions) is thought to be the corresponding primary site of interaction. The α_2 subunit is extensively glycosylated (134) and these sugar residues have been shown to be important in maintaining the stability of the interaction with α_1 and in $\alpha_2\delta$'s effect on the channel kinetics (138).

The role of $\alpha_2\delta$ subunits is still unclear. Generally expression results in increasing the current through the channel and as with the β subunit co-expression of $\alpha_2\delta$-1 was shown to increase the membrane trafficking of the α_1 subunit (142). Further effects on the kinetics of the channels have also be identified, but with no general trend between the four $\alpha_2\delta$ subunits (reviewed in (143)).

1.3.5. Channelopathies of Voltage-Dependent Calcium Channels

Mutations in VDCCs can cause a range of pathologies. These can be useful in discovering more about VDCC and will be briefly discussed here (reviewed in (144)).

Several pathologies have been linked to mutations in $Ca_V2.1$. For example familial hemiplegic migraine, which is associated with headaches accompanied by aura, ataxia and nystagmus, has been linked to numerous missense mutations causing defects in the $Ca_V2.1$ subunit (145). Further mutations have been found to be responsible for episodic ataxia-2, which is associated with ataxia, nystagmus, dysarthria, vertigo and cerebella atrophy and migraine are also common to this condition (146).

The presence of an expanded CAG repeat in the C-terminus of $Ca_V2.1$ leads to autosomal dominant spinocerebellar ataxia 6. This is characterized by ataxia, nystagmus, dysarthria, and neuronal loss in the cerebellum, the dentate and inferior olivary nuclei (147). Two mouse models have also been identified, *tottering* (characterised by seizures and mild ataxia) and *leaner* (characterized by severe ataxia) both due to single nucleotide substitutions (148-150).

Missense mutation, deletions, and frameshifts with premature stop codons in $Ca_V1.4$ are thought to be responsible for human incomplete X-linked congenital stationary night blindness. This is a heterogeneous, non-progressive disorder with impairment of night vision and variably reduced day vision, which is thought to result from altered synaptic transmission from photoreceptor cells to second-order neurons (151;152). Missense mutations in $Ca_V1.1$ result in hypokalemic periodic paralysis which presents as episodic weakness of the trunk and limbs, generally without myotonia, which can last hours to days (153-155).

Mutations in auxiliary subunits are also involved in pathologies. An insertion of four nucleotides into a splice donor site of the mouse gene encoding β4 results in the *lethargic* (ataxia and absence seizures, but without apparent

neuronal degeneration (156)) phenotype (157). Mutations in the mouse $\alpha_2\delta$-2 gene result in the *ducky* and *ducky*^{2J} phenotypes (epilepsy and ataxia) (158) and also in the *entla* phenotype (ataxia, paroxysmal dyskinesia, and absence seizures) (159). Mutation of the γ2 subunit results in the *Stargazer* phenotype, which will be discussed further below.

1.4. γ Subunits of Voltage-Dependent Calcium Channels

It remains controversial as to whether γ subunits form part of a functional VDCC or not. Compared to $\alpha_2\delta$ and β subunit their effect on VDCC expression and kinetics is slight (with the exception of the γ7 subunit). Indeed it is accepted that a primary role of at least some of the γ subunit family is involved in the trafficking of AMPA receptors (160).

Eight γ subunits have thus far been identified ranging between 222 and 426 amino acids in length. They are all part of the PMP-22/EMP/MP20/Claudin family. They share a conserved four transmembrane domain structure with amino- and carboxyl- termini located intracellularly. The first extracellular loop contains conserved sites for N-glycosylation and also a GLWXXC motif. The first extracellular loops also contain conserved cysteine residues which may form disulphide bonds. The carboxyl-termini of γ2, γ3, γ4 and γ8 all contain a type I PDZ-binding motif (the consensus sequence for which is S/T-X-Φ, where Φ is any hydrophobic residue (161)). γ5 and γ7 share a similar SS/TSPC motif.

1.4.1. Identification of γ Subunits

As mentioned previously γ subunits were first identified as they were co-purified with the $Ca_V1.1$ from skeletal muscle T-tubule membranes. This γ subunit was subsequently cloned by Jay *et al* (162) from rabbit skeletal muscle cDNA revealing a 666 nucleotide sequence. This translates to a 222 amino acid protein with a calculated molecular weight of approximately 25 kDa. These finding were confirmed by Bosse *et al* (163).

The human orthologue (*CANCG1*) was identified from cDNA library derived from foetal skeletal muscle. Both Powers *et al* (164) and Iles *et al* (165) went on to map the gene to 17q11.2-q24. This is the same region which contains the gene for the β1 subunit (166). The rat orthologue was identified by Eberst *et al* (167) which encoded a 223 amino acid protein that shares 79% and 84% identity to the rabbit and human γ1 subunits respectively.

For sometime it was thought that there was only one γ subunit which formed part of skeletal calcium channels. However, Letts *et al* (168) identified a second neuronal γ subunit, the mutation of which was responsible for the "stargazer" phenotype in the stargazer mutant mouse strain. This protein was subsequently named stargazin (also known as γ2).

Mouse γ2 encodes a 323 amino acid protein with a molecular weight of approximately 36 kDa. The human orthologue of γ2 (located on chromosome 22q13.1) was identified by Black and Lennon (169) by a search of an EST database for sequences homologous to mouse γ2 and subsequent (polymerase chain reaction (PCR) of a cerebellum cDNA library. Similarity between γ1 and γ2 is low (only 18% identity) but they do share similar hydrophobicity plots, gene structure and intron size (four exons with a large first intron). A third γ subunit (γ3) was also identified by Black and Lennon (169). They went on to map γ3 to chromosome 16p12-p13.1. The deduced 315-amino acid transmembrane protein is 98% identical to γ2, but only 17% identical to γ1. Once again the gene contained four exons with a large first intron.

The mouse orthologue of γ3 was identified by Klugbauer *et al* (170), who also identified 2 other potential γ subunits, γ4 and γ5. However, this γ5 had a different gene structure to the other members of the family, containing only 2 exons. Additionally only one common sequence motif (GLWXXC) was shared between this protein and other members of the family. This motif is not exclusive to γ subunits but is shared with other tetraspannin proteins. These differences led Chu *et al* to propose that this gene should be referred to as mouse protein distantly related to the γ subunit Cancg genes (pr) (171).

Burgess *et al* (172) mapped the human orthologue of γ4 to chromosome 17q24. They also identified a novel γ subunit (γ5) located on chromosome 17q24. Subsequently, Burgess *et al* (173) went on to identify a further 3 γ subunits (γ6, γ7 and γ8) clustered on chromosome 19q13.4. Interestingly γ8 contains an unusual start codon, AXXCTGG (the consensus sequence for initiation of translation in vertebrates (also called Kozak sequence) is: ACCATGG). This is conserved in the rat, mouse and human genes.

γ5, γ6, γ7 and γ8 were independently identified by Chu *et al* (171) and γ5 and γ7 were also independently identified by Moss *et al* (174). Furthermore both Chu *et al* and Moss *et al* suggested a different gene structure for γ5 and γ7 from that proposed by Burgess *et al*. For both genes there was evidence of a five exon structure as opposed to the four exon structure originally purposed. A short form of γ6 was also found by both Burgess *et al* (173) and Chu *et al (171)*. They predicted that this short form is assembled by three exons rather than four, resulting in the encoded protein being shorter by 46 amino acids than the long isoform. Hydropathy analysis suggested that this short isoform would contain only two transmembrane domains (171).

The phylogenetic relationship between the γ subunits is given in Fig.1.10. Briefly, they can be grouped by homology into 3 sets: 1) γ1 and γ6; 2) γ2, γ3, γ4 and γ8; 3) γ5 and γ7. There may also exist γ subunits yet to be identified. By analysis of the mouse representative transcript and protein set for molecules involved in brain function Gustincich *et al* (175) identified two potential members of the γ subunit family γ9 and γ10.

	Gene Name	Chromosome/cytoband	Exons	Translation Length
γ1	*CACNG1*	17q24	4	222
γ2 (Stargazin)	*CACNG2*	22	4	323
γ3	*CACNG3*	16p12-p13.1	4	315
γ4	*CACNG4*	17q24	4	327
γ5	*CACNG5*	17q24	5	275
γ6	*CACNG6*	19q13.4	4	260
γ7	*CACNG7*	19q13.4	5	275
γ8	*CACNG8*	19q13.4	4	426

Table 2. γ subunits genes

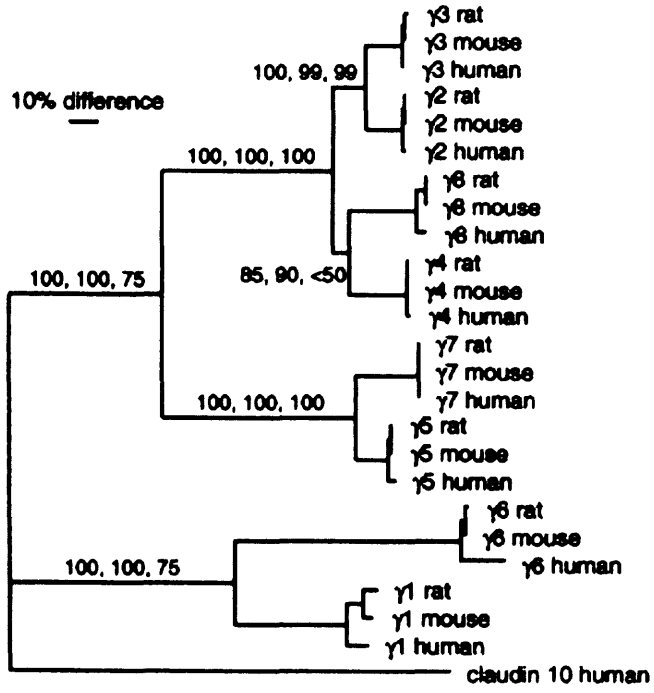

Fig. 1.10. The phylogenetic relationship of mouse rat and human γ subunits. The scale bar shows a 10% difference in corrected distance (using the entire alignment). Numbers above branches indicate the support in percentage of bootstrap replications for nodes joining different gamma subunits in the distance, maximum likelihood, and maximum parsimony analyses, respectively. The tree was rooted with human claudin 10. Adapted from Chu *et al* (171)

Chu *et al* (171) proposed two possible models of the evolutionary pathway of the generation of the eight γ subunits. The first contained four evolutionary steps in which following a single round of tandem gene duplication and chromosome duplication, an unequal crossing-over event led to a gene cluster with 3 paralogous γ genes and an additional single γ gene on another chromosome. This was followed by a final chromosome duplication event to generate a second homologous gene cluster as well as a second homologous γ gene. The second model comprised five steps with two rounds of tandem duplications resulting in a gene cluster with three ancestral γ subunit genes. The first round of chromosome duplication generated another homologous gene cluster. The deletion of two genes from one of the gene clusters was followed by another round of chromosome duplication to give the eight γ subunits. The lack of any γ subunits in the *Caenorhabditis elegans* genome, which contains

the other calcium channel subunits, led them to conclude an independent evolution of the γ subunits from the other calcium channel subunits.

1.4.2. Tissue Expression of γ Subunits

The tissue distribution of γ subunits remains controversial with different results obtained between different groups (as detailed below). Overall at least one γ subunit has been detected in almost all tissues. The brain has been shown to express all of the identified γ subunits with the exception of γ1.

Using RT-PCR Powers *et al* (164), Burgess *et al* (173)and Chu *et al* (171) all found γ1 to be expressed in skeletal muscle. Chu *et al* also found expression at low levels in the aorta whereas Burgess *et al* found low levels of expression in bone marrow, thymus, foetal brain and trachea.

Using Northern blotting and *in situ* hybridization Letts *et al* (168) showed γ2 mRNA to be expressed abundantly in adult mouse brain the with the highest expression in cerebellum, olfactory bulb, cerebral cortex, thalamus, and CA3 and dentate gyrus of the hippocampus by in situ hybridisation. A similar expression profile was observed by Moss *et al* (176). This was confirmed by Klugbauer *et al* (170) who used Northern blotting and *in situ* hybridization detected γ2 in the brain with high expression in the cerebellum and moderate expression in the hippocampus, cerebral cortex thalamus, and olfactory bulb. Tomita *et al* (177) also found γ2 mRNA to be concentrated in the cerebellum and cerebral cortex. They went on to show that γ2 mRNA is expressed in the neurons of cerebral cortex, granule cells of dentate gyrus, pyramidal cells of the hippocampus, interneurons of hilus of dentate gyrus and in stratum oriens and stratum radiatum.

γ2 expression has also been investigated using various PCR techniques. Chu *et al* (171) and Green *et al* (178) only detected γ2 expression in the brain. Further analysis by Green *et al* showed that γ2 was expressed in all brain regions with higher expression in the cerebellum and nucleus accumbens. Foetal brain also showed high expression. Burgess *et al* (173) also found

expression of γ2 in the brain, but in contrast to the previous results they also found γ2 expression in the adrenal gland, spinal cord, foetal liver, foetal brain, testes, small intestine and liver.

Sharp *et al* (117) used western blotting and immunohistochemistry to investigate γ2 expression at the protein level. They found expression in mouse forebrain and cerebellum but not the thymus, heart, lung, skeletal muscle, liver or kidney. γ2 expression was highest in the cerebellum and cortex; moderate in midbrain thalamus hippocampus and striatum and low in pons and brain stem. This was confirmed by Tomita *et al* (177), who also identified low levels of expression in the olfactory bulb. Immunoblotting for γ2 in rat pups showed expression was first detectable at postnatal day 4 and increased until adulthood.

Northern blotting and *in situ* hybridization showed γ3 expression only in the brain (restricted to the forebrain) with strong expression in the hippocampus and cerebral cortex and moderate expression in the olfactory bulb and caudate putamen (170;177). PCR techniques also found γ3 expression in both adult and foetal brain (171;173;178). At the protein level the highest levels of γ3 expression was found in the cortex, with moderate expression in the midbrain, hippocampus and striatum and low expression in thalamus and hippocampus (117;177). Expression was first detectable in rat pups at postnatal day 16 and increased until adulthood.

Northern blotting showed γ4 to be only expressed in the brain (170). *In situ* hybridization showed γ4 mRNA to be diffusely expressed throughout the brain with higher levels of expression in the caudate putamen, olfactory bulb, habenula and moderate expression in the cerebellum and thalamus (177). PCR techniques confirmed the expression of γ4 in the brain with high expression in the caudate nucleus, putamen and thalamus. γ4 was found to be expressed strongly in foetal brain. Lower levels of expression were also found in a range of tissues including lung, heart, prostate, pancreas, placenta, small intestine, stomach, testes and uterus (171;173;178). At the protein level γ4 expression was found in the olfactory bulb, cortex midbrain, hippocampus, striatum and at

lower levels in the thalamus, pons brainstem and cerebellum (117;176;177). In rat pups expression was detectable from embryonic day 20 and increased to a peak at postnatal day 6 then reduced again to low levels at adulthood. Kious *et al* (179) found γ4 to be expressed early in the cranial neural plate, and later in the cranial and dorsal root ganglia in developing chick embryos. The timing of this expression correlated precisely with the onset of neuronal differentiation and led them to suggest that γ4 may promote differentiation via regulation of intracellular calcium levels.

Expression of γ5 has of yet only been examined by RT-PCR. Chu *et al* (171) only found γ5 mRNA in the brain. Burgess *et al* (173) also found expression in kidney, thymus, prostrate, testes, foetal brain and spinal cord.

The two splice variants of γ6 show different expression profiles. Burgess *et al* (173) found that in skeletal muscle, bone marrow, salivary gland and adrenal gland the long (four exon) isoform predominates whereas expression of the short (three exon) isoform is found in the small intestine, spleen and spinal cord. Chu *et al* (171) found expression of the long isoform in skeletal muscle, and the short isoform in aorta, brain and lung. Both isoforms were expressed in both the atrium and ventricle.

Burgess *et al* (173) found γ7 mRNA to be expressed in a range of tissues with high level of expression in the brain, foetal brain, spinal cord, testis and foetal liver. Lower level of expression were found in kidney, liver, lung, colon, small intestine, spleen, stomach, thymus, prostrate skeletal muscle, trachea, adrenal and mammary tissue. Chu *et al* (171) also found γ7 mRNA to be expressed in the brain and also found high expression in the lung and testes with lower levels of expression in the atrium, ventricle and skeletal muscle. Using Northern blotting Moss *et al* found γ7 mRNA to be only expressed in the brain (174). Two transcripts (~2.4 and 3.0 kb) were found in all regions probed with the short transcript expressed at greater levels in the cerebellum, amygdala, hippocampus and thalamus.

Unpublished data from experiments performed in our laboratory by Dr. M. Niteo-Rostro found widespread expression of γ7 mRNA in mouse brain with stronger expression in the olfactory bulb, cerebellum and CA1, CA3 and dentate gyrus regions of the hippocampus. Within the cerebellum γ7 mRNA was strongly expressed in the Purkinje cell layer and also in the granule cell layer. Immunohistochemical studies of mouse cerebellum found γ7 localisation in individual Purkinje cells and their dendrites (Appendix A.4.2. Fig. A.1).

Finally γ8 mRNA was detected in brain, foetal brain and testes (171;173). In situ hybridization detected high levels of expression in the hippocampus and moderate expression in the cortex and olfactory bulb. In rat pups protein was detectable from postnatal day 4 increasing until adulthood. The highest level of expression was found in the hippocampus with lower levels in the cerebral cortex and olfactory bulb (177).

1.4.3. Effects of γ Subunits on Voltage-Dependent Calcium Channels

1.4.3.1. Effects on Calcium Current Properties

γ1 Subunits

Wei *et al* (180) showed that in *Xenopus* oocytes co-expression of γ1 did not have a significant effect on currents elicited by $Ca_V1.2$. However, when the subunit was co-expressed with $Ca_V1.2$ and β1, both peak currents and rates of activation at more negative potentials were increased. They suggested that rather than simply amplifying expression of α_1 subunits, heterologous skeletal muscle β and γ subunits could modulate the biophysical properties of $Ca_V1.2$.

Lerche *et al* (181) showed that in mammalian HEK 293 cells co-transfection of the γ1 with $Ca_V1.2$ shifted the inactivation curves by -20 mV. Similarly Eberst *et al* (167) showed that co-expression of γ1 with the $Ca_V1.2$, β2a and $\alpha_2\delta$-1 complex in HEK 293 cells shifted the inactivation curve to negative potentials and accelerated current inactivation without changing other

voltage-dependent properties of the channel. Again in HEK293 cells Klugbauer *et al* (170) showed that co-expression of γ1 with $Ca_V1.2$, β2a and $\alpha_2\delta$-1 resulted in a -30 mV shift in the steady-state inactivation curve with accelerated current inactivation. Using a *Xenopus* oocyte expression system Kang *et al* (182) showed co- expression of γ1 with $Ca_V2.2$, β3 and $\alpha_2\delta$ resulted in decelerated activation kinetics.

Mice that lack γ1 by targeted deletion are viable, fertile and show no obvious phenotype. The other components of skeletal muscle VDCCs are expressed at normal levels (183) and the channel is maintained as a complex (184). There is a increase in L-type current density, deceleration of the inactivation, and a shift in the steady state inactivation to more positive potentials. However, there was no observed effect on skeletal excitation-contraction coupling (185). Transient expression of the γ1 subunit, but not the γ2 subunit, in primary cultured muscle cells from γ1-deficient mice shifted the steady-state inactivation approximately -15 mV, thereby restoring wild type steady-state inactivation and current amplitude (186).

γ2 Subunits

In the initial experiments performed by Letts *et al* (168) co-expression of γ2 in a BHK cell line stably transfected with $Ca_V2.1$, β1a and $\alpha_2\delta$-1 resulted in current amplitudes that were decreased as the channels became increasing inactivated. γ2 accentuated inhibition by shifting the voltage-dependence of channel availability towards more negative potentials. Also, the midpoint voltage was more negative in cells transfected with γ2 resulting in a hyperpolarising shift of approximately 7 mV. However, the peak current-voltage relationship was unchanged.

Klugbauer *et al* (170) showed that co-expression of γ2 with $Ca_V2.1$, β1a and $\alpha_2\delta$-1 in HEK293 cells resulted in a small, but significant, shift of the voltage-dependent activation to more positive potentials and also shifted the steady state inactivation curve towards a more hyperpolarised potential. Substitution of the β1a subunit (skeletal) with the β2a subunit (cardiac) resulted

in the negative shift in voltage-dependence of inactivation which only occurred when Ca^{2+} was used as the charge carrier. If Ba^{2+} was used as the charge carrier a shift to more positive potentials was observed. Co-expression of γ2 with $Ca_V1.2$, β2a and $\alpha_2\delta$-1 resulted in small shifts of the voltage-dependence of activation and inactivation. Co-expression of γ2 with the LVA VDCC $Ca_V3.1$ slowed the speed of recovery from voltage-dependent inactivation.

Rousset *et al* (116) found that co-expression of γ2 with $Ca_V2.1$ and $\alpha_2\delta$-1 induced a small negative shift in the inactivation curve and an acceleration of the inactivation kinetics. When β subunits were co-expressed these effects were still generally present (116). They also observed that γ2 increased the proportion of β expressing oocytes that displayed unusually slow inactivation. Also in a *Xenopus* oocyte expression system Kang *et al* showed co-expression of γ2 with $Ca_V2.2$, β3 and $\alpha_2\delta$-1 resulted in decelerated activation kinetics (182). A decrease in current amplitude was observed, though this effect was dependent upon the presence of the $\alpha_2\delta$ subunit.

Green *et al* (178) observed no effect on current amplitude, current activation, steady-state inactivation or the rate of inactivation upon the co-expression of γ2 with $Ca_V3.3$ in HEK293 cells. However, deactivation was significantly slowed. When co-expressed in *Xenopus* oocytes with a $Ca_V2.1$/β4 VDCC complex, either in the absence or presence of an $\alpha_2\delta$-2 subunit γ2 did not significantly modulate the VDCC peak current amplitude, voltage-dependence of activation or voltage-dependence of steady-state inactivation (176).

γ3 Subunits

As with γ2, Rousset *et al* (116), found that co-expression of γ3 with $Ca_V2.1$and $\alpha_2\delta$ induced a small negative shift of the inactivation curve and an acceleration of the inactivation kinetics. When β subunits were co-expressed these effects were still generally present. They also observed that γ3 increased the proportion of β expressing oocytes that displayed unusually slow inactivation.

Green *et al* (178) found co-expression of γ3 with $Ca_V3.3$ in HEK 293 cells had no effect on current amplitude, current activation, steady-state inactivation or the rate of inactivation. Unlike the case for γ2, deactivation was not significantly slowed by γ3.

γ4 Subunits

Klugbauer *et al* (170) showed that co-expression of γ4 with $Ca_V2.1,\beta_{1a}$ and $\alpha_2\delta$-1 shifted the steady state inactivation curve towards a more hyperpolarised potential. Co- expression γ4 with $Ca_V3.1$ resulted in a significant shift of steady state inactivation curves to more positive voltages and slowed the speed of recovery from voltage-dependent inactivation.

In contrast Green *et al* (178), also using HEK293 cells found no effect on current amplitude, current activation, steady-state inactivation or the rate of inactivation, when γ4 was co-expressed with $Ca_V3.3$. Co-expression of γ4 with a $Ca_V2.1$/β4 VDCC complex, either in the absence or presence of an $\alpha_2\delta$-2 subunit in *Xenopus* oocytes did not significantly modulate the VDCC peak current amplitude, voltage-dependence of activation or voltage-dependence of steady-state inactivation (176). γ4 was also found to have no significant effect on $Ca_V3.1$ current (187).

γ6 subunits

Hansen *et al* (187) observed that co-expression of both the long and short isoforms of γ6 with $Ca_V3.1$ in HEK293 cells significantly decreased the current density by 49% and 69% respectively. Neither the long nor the short isoform significantly affected the voltage dependency of activation or inactivation or the kinetics of $Ca_V3.1$ current. Expression of the long isoform of γ6 was shown not to affect the level of $Ca_V3.1$ mRNA or the total protein expressed in HEK 293 cells. Transient expression of the long isoform of γ6 was also found to reduce the endogenous low voltage-activated current by 63% in HL-1 cells, an immortalised arterial cell line (187).

γ7 subunits

In our laboratory Moss *et al* (174) showed that co-expression of γ7 with $Ca_V2.2$, β1B and $\alpha_2\delta$-2 resulted in almost complete abolition of N-type current in both *Xenopus* oocytes and mammalian cell expression system. This effect was shown to be not dependent upon co-expression of $\alpha_2\delta$-2. γ7 was also shown to significantly reduce the current through both $Ca_V1.2$ and $Ca_V2.1$ by 48% and 52% respectively with no significant effects of γ7 on the voltage dependence of activation. However, endogenous N-type currents in sympathetic neurones of the rat superior cervical ganglion were unaffected by the transient transfection of γ7. They went on to show that co-expression of γ7 resulted in a large reduction of expression of $Ca_V2.2$ rather than interfering with trafficking or biophysical properties of the channel. Hansen *et al* (187) found that γ7 had no significant effect on the voltage dependency of activation or inactivation or the kinetics of $Ca_V3.1$ when co-expressed in HEK293 cells.

1.4.3.2. Biochemical Interactions

Biochemical association between γ subunits and the other VDCC subunits has been less widely examined than the biophysical effects. As mentioned previously γ1 subunits were found to co-purify with $Ca_V1.1$, β1a and $\alpha_2\delta$-1. Arikkath *et al* (184) showed that $Ca_V1.1$, β1a and $\alpha_2\delta$-1 subunits are still associated in γ1 null mice. Transiently transfected γ1 subunits (but not γ2 subunits) incorporated into γ1 null L-type channels in skeletal muscle of γ1 null mice. In addition $Ca_V1.1$ and γ1 were found to form a complex when transiently transfected in tsA-201 cells. They went on to identify that it is the first half of γ1, including the first two transmembrane domains, that is important for subunit interaction.

γ2 and γ3 have also been shown to associate with other neuronal VDCC subunits. Using sucrose gradient fractionation of rabbit cerebellum $Ca_V2.1$, $Ca_V2.2$, $\alpha_2\delta$-2, β3 and β4 were found to co-sediment with both γ2 and γ3 (182).

These interactions were confirmed by co-immunoprecipitation. Sharp *et al* (117) also found interaction between γ subunits and α_1 subunits. Using antibodies against a highly conserved C-terminal epitope present in γ2, γ3 and γ4 they immunoprecipitated $Ca_V2.2$ α_1 subunits from mouse brain.

1.4.4. Non-Voltage-Dependant Calcium Channel Roles of γ Subunits

Along with their effects on VDCCs there is increasing evidence that γ subunits have other roles. It has been proposed that γ2, γ3, γ4 and γ8 are all involved in the trafficking of AMPA type glutamate receptors and should be defined as transmembrane AMPA receptor regulatory proteins (TARP's) (177). AMPA receptors are of fundamental importance in the brain. They are responsible for the majority of fast excitatory synaptic transmission. They are hetero-tetramers composed of variable combinations of four subunits, glutamate receptor 1 (GluRl–GluR4) (188;189). Glutamate is the primary excitatory neurotransmitter in the central nervous system, regulating numerous cellular signalling pathways and controlling the excitability of central synapses both pre- and postsynaptically. AMPA receptors have been shown to be involved in synapse formation and stabilisation, and regulation of functional AMPA receptors is the principal mechanism underlying synaptic plasticity (reviewed Palmer *et al* (190)). The interaction between γ subunits and AMPA receptors was revealed through investigation of the *Stargazer* mutant mouse strain which will now be discussed.

1.4.4.1. The Stargazer Mutant Mouse Line

The *stargazer* mutation in mice arose spontaneously in the A/J Mouse strain in the Animal Resources colony of the Jackson Laboratory in the 1980s. It was originally identified by its distinctive head-tossing activity, ataxic gait spike wave seizures and behavioural arrest (191). This phenotype is characteristic of absence epilepsy in humans.

As mentioned previously Letts *et al* found this phenotype is due to a mutation in the *cacng2* gene which encodes for γ2. *Stargazer* mice harbour a

transposon insertion in the second intron of *cacng2*, disrupting transcription of the gene (117;168;182;192). Subsequently, two allelic variants of stargazer have arisen, *Waggler* and *Stargazer* ^{3J}. All three mutations affect the *cacng2* mRNA levels as they all arise from disruptions within the introns of this gene. The mutations cause reduced *cacng2* mRNA and protein levels. *Stargazer* and *Waggler* mice have the least amount of mRNA and undetectable protein, whereas *Stargazer*^{3J} appears to be the mildest allele, both in terms of the phenotype and protein expression (192).

Electroencephalography (EEG) studies demonstrated frequent polyspike discharges and staring spells that could be suppressed with anticonvulsants effective against absence epilepsy (191-193). Electrophysiological studies have shown hyperexcitability of thalamic and cortical neurons as a potential source of the absence spells (194;195), and anatomical studies have suggested that the frequent seizures result in aberrant sprouting of mossy fibres and loss of hilar interneurons in the hippocampus(196).

The anatomy of the stargazer cerebellum is normal, except for a 14% reduction in cerebellar size (191;197). However, there is a loss of brain-derived neurotrophic factor during development, and delayed disappearance of external granule cells (197;198). In addition, there is a loss of γ-aminobutyric acid (GABA) synapses among Purkinje and Golgi cells (199;200) and an impairment of AMPA-mediated glutamate transmission onto cerebellar granule cells (201;202).

1.4.4.2. The Role of γ Subunits in AMPA Receptor Trafficking

Using immunocytochemical staining and immunogold electron microscopic analysis Chen *et al* (202) revealed a lack of synaptic labelling of AMPA receptor subunits despite the presence of cytoplasmic staining in cerebellar granule cells of *Stargazer* mice. They went on to show that γ2 co-immunoprecipitates with GluR1, 2, and 4 in co-transfected COS cells. Sharp *et al* (117) also confirmed the co-immunoprecipitation of γ2 with GluR1 from solubilised mouse brain homogenates. Interestingly GluR1 could also be co-

immunoprecipitated with $Ca_V2.2$. Furthermore, Chen *et al* (202) showed that transfection of γ2 into stargazin mutant granule cells led to recovery of AMPA receptor mediated synaptic currents.

In addition to binding to AMPA receptors γ2 was also found to bind to synaptic PDZ proteins, such as PSD-95, SAP-97 and SAP-102 through its C-terminal PDZ binding motif. Chen *et al* (202) proposed a model in which the interaction of γ2 with AMPA receptor subunits was essential for delivering functional receptors to the surface membrane of granule cells, whereas its binding with PSD-95 and related PDZ proteins is required for targeting AMPA receptors to synapses.

Using phosphorylation site-specific γ2 antibodies Choi *et al* (203) showed that the C terminus of γ2 is phosphorylated within the PDZ binding motif at the Thr-321 residue in heterologous cells and *in vivo*. γ2 phosphorylation was enhanced by the catalytic subunit of cAMP-dependent protein kinase A (PKA). Mutations mimicking stargazin phosphorylation (T321E and T321D) resulted in elimination of yeast two-hybrid interactions, in vitro co-immunoprecipitation, and co-clustering between γ2 and PSD-95. Phosphorylated γ2 showed a selective loss of co-immunoprecipitation with PSD-95 in heterologous cells and limited enrichment in postsynaptic density fractions of rat brain.

Similar experiments were performed by Chetkovich *et al* (204). *In vitro* peptide phosphorylation assays and western blot analysis with phospho-stargazin-specific antibodies confirmed phosphorylation of Thr-321 by protein kinase A. These results led both groups to suggest that phosphorylation of the γ2 C-terminus by PKA regulates its interaction with PSD-95 and synaptic targeting of AMPA receptors. Furthermore NMDA receptor activity can induce both stargazin phosphorylation, via activation of CaMKII and PKC, and γ2 dephosphorylation, by activation of PP1 downstream of PP2B (205).

Schnell *et al* (206) used hippocampal slice cultures and biolistic gene transfections to study the targeting of the AMPA receptor to synapses. They showed that AMPA receptors are localised to synapses through direct binding

of the first two PDZ domains of synaptic PSD-95 to γ2. Increasing the level of synaptic PSD-95 caused the recruitment of new AMPA receptors to synapses without changing the number of surface AMPA receptors. Additionally γ2 over expression drastically increased the number of extra-synaptic AMPA receptors, but did not alter synaptic currents if synaptic PSD-95 levels were kept constant. Chen *et al* (207) showed that surface delivery of kainate receptors, which are structurally very similar to AMPA receptors, was independent of γ2.

Tomita *et al* (177) showed that other γ subunits (γ3, γ4 and γ8) are also involved in AMPA receptor trafficking and proposed that this group of proteins should be defined as TARP's. γ1, γ5 and the related protein claudin-1 were all shown not to be involved in AMPA trafficking. TARPs interact with AMPA receptors at the postsynaptic density, and surface expression of mature AMPA receptors requires a TARP. In a further series of experiments Tomita *et al* (160) showed that TARPs were stable at the plasma membrane, whereas AMPA receptors were internalized in a glutamate-regulated manner. Upon binding to glutamate, AMPA receptors detached from TARPs. This did not require ion flux or intracellular second messengers. They proposed that this allosteric mechanism for AMPA receptor dissociation from TARPs may participate in glutamate-mediated internalisation of receptors in synaptic plasticity.

Interaction between γ2 and AMPA receptors involved both extra- and intracellular determinants of TARPs. Cuadra *et al* (208) identified a novel domain corresponding to residues 243-283 within the cytoplasmic C terminus of γ2 that is also required for γ2 and AMPA receptor synaptic clustering. Using a yeast two-hybrid assay they showed that this domain binds to nPIST (neuronal isoform of protein-interacting specifically with TC10), a Golgi-enriched protein implicated in trafficking of transmembrane proteins. Using a range of techniques they confirmed this interaction in the brain. Interestingly over expression of nPIST in hippocampal neurons enhances AMPA receptor clustering, whereas transfection of a dominant-negative nPIST construct attenuates AMPA receptor synaptic clustering. These led them to propose the model of AMPA receptor trafficking below (Fig 1.11)

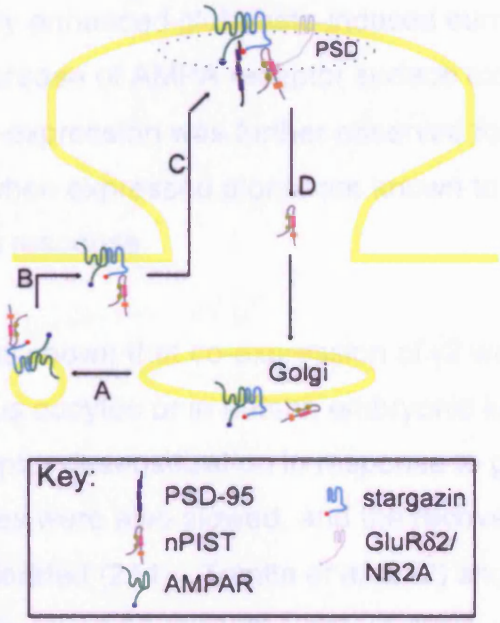

Fig. 1.11. A mode of the regulation of AMPA Recptors at synapses. γ2-AMPA receptor complexes interact with nPIST in the Golgi and exit the Golgi in vesicles (*A*). The vesicles fuse at extrasynaptic sites (*B*), and nPIST chaperones the γ2- AMPA recptor complex to the PSD, where it interacts with synaptic proteins such as GluRδ2, NR2A, or directly with PSD-95, allowing the γ2 C terminus to bind PSD-95 and stabilize the AMPA recptor at the synapse (*C*). nPIST is recycled to the Golgi to repeat the cycle (*D*). Adapted from Cuadra *et al* (208)

Furthermore, Ives *et al* (209) identified a series of proteins that interact with γ2 including the non-PDZ domain containing protein light chain 2 of microtubule-associated protein 1 (LC2). They went on to show that LC2 co-associates with γ2 as part of a tripartite complex comprising LC2-γ2-GluR2. As the extracted complex was found to be devoid of PSD95, SAP97, and actin they proposed that LC2 is involved in trafficking of AMPA receptors before they are anchored at the synapse.

1.4.4.3. TARPs as Modulators of AMPA Receptor Activity

Yamazaki *et al* (210) showed that in addition to the importance of TARPs in the trafficking of AMPA receptors they also directly modulated AMPA receptor activity. Co-expression of any of the TARPs with GluR 1 in HEK293 cells and

Xenopus oocytes markedly enhanced glutamate-induced currents. The effect was not just due to the increase of AMPA receptor surface expression. The enhancing effect by γ2 co-expression was further observed for homomeric GluR2 channels, which, when expressed alone, are known to produce only a small or negligible current response.

Subsequently it was shown that co-expression of γ2 with AMPA receptor subunits, either in *Xenopus* oocytes or in human embryonic kidney 293 cells, significantly reduced receptor desensitization in response to glutamate. Receptor deactivation rates were also slowed, and the recovery from desensitization was accelerated (211). Tomita *et al* (212) showed that γ2 can alter AMPA receptor kinetics by increasing the rate of channel opening. This effect of γ2 requires the first and second transmembrane domains and the first extracellular loop.

1.5. The Role of γ7

As mentioned previously Moss *et al* (174) showed that co-expression of γ7 with $Ca_V2.2$ resulted in almost complete abolition of N-type current in both *Xenopus* oocyte and mammalian cell expression systems. This was found to be due to γ7 causing a reduction in $Ca_V2.2$ expression. The aim of the work presented here is to try is to determine the mechanism by which γ7 causes the reduction of $Ca_V2.2$ expression and go on to identify the role of γ7.

The expression of a VDCC is a multi step process (Fig. 1.12). Firstly the RNA message for each of the subunits has to be transcribed from the corresponding gene on the chromosome (for endogenous expression) or from the vector (for transfected subunits). During (and post) transcription a range of ribonucleotide binding proteins (RNPs) bind to the mRNA. These proteins have a range of roles including mRNA export, localisation and stability (213).

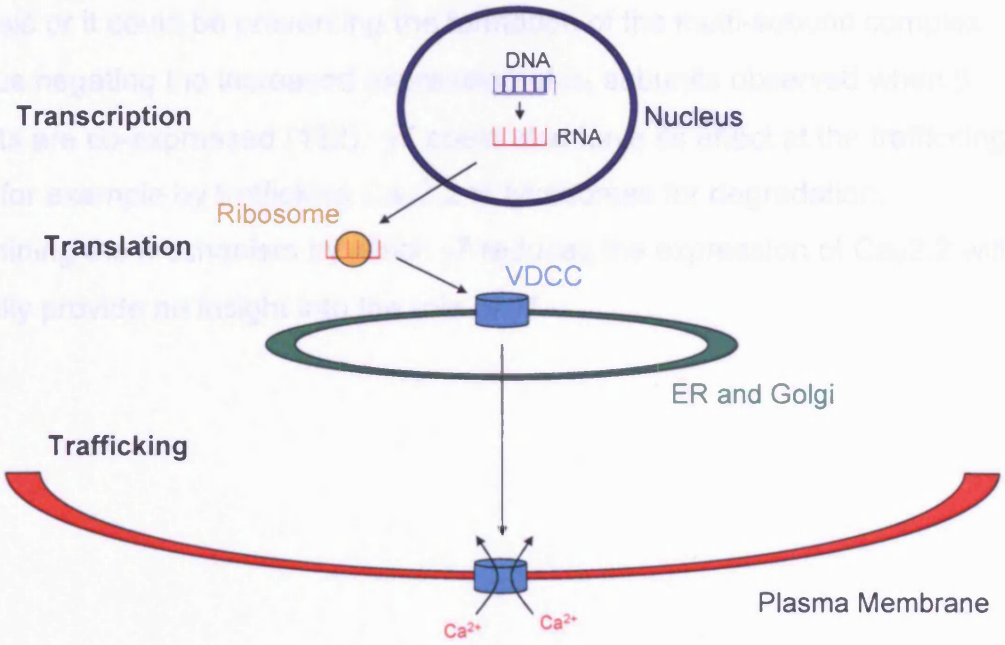

Fig. 1.12. A diagrammatic representation of the process of expression of a VDCC. The synthesis of a VDCC from DNA to a functional channel in the plasma membrane can be simplified into 3 stages. Transcription of DNA to RNA, translation of the RNA to protein (and subsequent modification of these proteins and their coming together to form a multi subunit protein) and finally trafficking of the proteins to the plasma membrane.

The mRNA is then translated on ribosomes with the transmembrane containing proteins being translated into the membrane of the ER. Proteins are then modified (e.g. disulphide bonds are formed and glycosylation takes place) in the ER and Golgi network. The individual subunits also assemble to form the multi-subunit complex. Finally the multi-subunit complex is trafficked to the plasma membrane. The VDCC complex is then localised to specific regions within the plasma membrane, such as the pre-synaptic terminal.

There are many points upon this pathway that γ7 could be having its effect on the expression of $Ca_V2.2$, a few of which are mentioned here. For example, at the transcription stage, promoter competition between γ7 and $Ca_V2.2$ (when expressed from plasmids) could result in a reduction of $Ca_V2.2$ mRNA being produced. Also, γ7 could interact with RNPs present on $Ca_V2.2$ mRNA resulting in the $Ca_V2.2$ mRNA becoming less stable. At the translation stage γ7 could be causing stress upon the ER resulting in reduced protein

synthesis or it could be preventing the formation of the multi-subunit complex and thus negating the increased expression of α_1 subunits observed when β subunits are co-expressed (132). γ7 could also have its effect at the trafficking stage, for example by trafficking $Ca_V2.2$ to lysosomes for degradation. Determining the mechanism by which γ7 reduces the expression of $Ca_V2.2$ will hopefully provide an insight into the role of γ7.

Chapter 2 – General Methods

2.1. cDNA's Constructs

The following cDNAs were used: human γ7(Moss), rabbit $Ca_V2.2$ Δ3'UTR (D14175), rat β1b (X61394, except R417S, V435A, V449A, W492R and V511A), a gift from Dr. T. P. Snutch, mouse $\alpha_2\delta$-2 (AF247139, common brain splice variant), rat Kv3.1b (M68880). All were used in the pMT2 expression vector (214) with the exception of KV3.1b which was used in the pRC-CMV expression vector.

2.2. Cell Culture

2.2.1. Culture of PC12 Cells

Rat pheochromocytoma cells (PC12) were a gift from Dr T. Shafer. They were maintained in Dulbecco's Modified Eagle's Medium (DMEM) supplemented with 7.5% horse serum and 7.5% foetal bovine serum (FBS) in a 5% CO_2 humidified atmosphere. Cells were passaged weekly. Three days after passaging 50% of the media was removed and replaced with fresh media. Before use PC12 cells were replated in DMEM supplemented with 10% FBS on to collagen coated 3.5 cm dishes or 3.5 cm dishes containing poly-L-lysine coated coverslips. To induce differentiation two hours after replating media was removed and replaced with serum free DMEM containing 100ng/ml Nerve Growth Factor (NGF)7S fragment (murine, natural). During differentiation medium was changed every other day and cells were left for at least 5 days before use.

2.2.2. Culture of tsA-201 Cells

tsA-201 cells (obtained from ECACC) are a SV40-transformed variant of the HEK293 human embryonic kidney cell line. They were maintained in Minimum Essential Medium supplemented with 10% FBS and 1% non-essential amino acids in a 5% CO_2 humidified atmosphere. Cells were passaged twice weekly. For transfection cells were used at 60-80% confluency and, unless otherwise stated, plated on to 3.5 cm dishes.

2.2.3. Culture of COS7 cells

COS7 cells are SV40 transformed african green monkey kidney cells (obtained from ECACC). They were maintained in DMEM supplemented with 10% FBS and in a 5% CO_2 humidified atmosphere. Cells were passaged twice weekly. For transfection cells were used at 60-80% confluency and, unless otherwise stated, plated on to 3.5 cm dishes.

2.3 Transfection

2.3.1. GenePORTER

Transient transfection of COS7 cells was performed using GenePORTER transfection reagent following the manufactures guidelines. Briefly, the DNA and GenePORTER reagent (2 µg:10 µl ratio – all DNA at 1 µg/µl) were each diluted in 500 µl of serum-free medium, mixed, incubated at room temperature for 1.5 hours, then applied to the cells. Transfections were stopped after 4 hours by the addition of 1ml of medium containing 20% serum. Unless otherwise stated a total of 2 µg of DNA was used to transfect one 3.5 cm dish of cells. All cells were incubated for 3 days at 37°C in a 5% CO_2 humidified atmosphere before use.

2.3.2. FuGENE

Transient transfection of tsA-201 and PC12 cells was performed using FuGENE 6 transfection reagent, following the manufactures guidelines. Briefly, for a 3.5 cm dish of cells, 3 µl of FuGENE was added to 97 µl of serum-free medium (MEM or DMEM for tsA201 and PC12 cells respectively) in a small, sterile tube and gently mixed. To this 2 µg of DNA solution (all DNA at 1 µg/µl) was added and gently mixed. Transfection mixes were then left to incubate for between 15 and 45 minutes at room temperature before being added to cells. Unless otherwise stated a total of 2 µg of DNA was used to transfect one 3.5 cm

dish of cells. All cells were incubated for 3 days at 37°C in a 5% CO_2 humidified atmosphere before use.

2.3.3. Nucleofection

Transient nucleofection of tsA201 was carried out using Amaxa's Nucleofector™ Device and Cell Line Nucleofector™ Kit V (Solution V). Nucleofection was performed according to manufactures guidelines for HEK-293 cells. Briefly, one T-75 flask of cells was used per nucleofection condition. Cells were harvested by incubating them in 5 ml of PBS and tapping the flask. Cells from all flasks were pooled and pelleted by centrifugation at 200 xg for 10 min at room temperature. This was done to remove and variability between individual flasks of cells. Pelleted cells were resuspended in 1ml of PBS per nucleofection condition and aliquoted into 15 ml Flacon tubes. Cells were then pelleted once again by centrifugation at 200 xg for 10 min at room temperature.

For each condition, the supernatant was discarded and pellet resuspended in 100 µl of Solution V to which 5 µg DNA (1 µg/µl) was added. The resuspended cells were then transferred into a cuvette and program A-23 used to nucleofect cells. 500 µl of pre-warmed (37°C) Roswell Park Memorial Institute 1640 (RPMI) medium supplemented with 10% FBS was added. For each condition two 6 cm plates containing 4 ml of RPMI supplemented with 10% FBS (pre-warmed to 37°C) were seeded with 250 µl of the nucleofected cell solution. Cells were cells were incubated at 37°C in a 5% CO_2 humidified atmosphere for 24 hours before use.

2.4. Generation of Constructs

During this study many constructs were generated. As the techniques used to generate each construct are very similar for brevity only the generation of $\gamma 7_{(1\text{-}217)}$ will be detailed here.

2.4.1, PCR to generate $\gamma 7_{(1\text{-}217)}$

The following primers were designed to amplify the first 651 bases (corresponding to amino acids 1-217) of human γ7:

Forward 5'-GACGAATTCACCATGAGTCACTGCAG-3';
Reverse 5'-ATAGAATTCCTCAGTAGAAGGCCGGGTGTGG-3'.

An EcoRI site was incorporated into each primer to allow cloning into the pMT2 expression vector.

The PCR reaction consisted of 25 mM dNTPs, 0.1 μg of γ7 in pMT2, 0.4 pmol/μl of each primer, 2.5 U of PfuTurbo® DNA Polymerase (Pfu), 20 mM Tris-HCl (pH 8.8).2 mM MgSO4.10 mM KCl,10 mM (NH4) 2SO4 0.1% Triton® X-100 and 0.1 mg/ml nuclease-free BSA in a total volume of 50μl. 0.1 μg of full length human γ7 in pMT2 was used as a template. PCR was performed using a Techne thermocylcer as follows:

Cycle1 (1x):	98°C for 3 min	Initial denaturation step
Cycle 2 (25x):	Step 1: 98°C for 30 sec	Denaturation step
	Step 2: 50°C for 40 sec	Annealing step
	Step 3: 75°C for 2 min 30sec	Extension step
Cycle 3 (1x)	75°C for 5 min	Final extension step
Cycle 4 (1x)	4°C for ∞	Cooling

A sample of the PCR reaction was combined with DNA sample loading buffer and separated by agarose gel electrophoresis on a 1% agarose gel using TAE as the running buffer. The gel was stained using ethidium bromide and DNA visualized under UV light using a UV transilluminator. An amplicon was identified corresponding to the expected size of $\gamma 7_{(1\text{-}217)}$. Unincorporated dNTP's and Pfu were removed from PCR reaction using a PCR clean up kit (following the manufacturer's guidelines) and the PCR product eluted in water.

2.4.2. Sub-cloning of $\gamma 7_{(1\text{-}217)}$ into the pMT2 Expression Vector

$\gamma 7_{(1\text{-}217)}$ was subcloned into the mammalian expression vector pMT_2 by the following method. Complementary sticky ends were produced for both the PCR product and pMT_2 vector by incubation at 37°C for 1 hour with the restriction endonuclease EcoRI. pMT_2 has a unique EcoRI site in the multiple cloning site upstream of the promoter sequence. The products of each of the restriction digests were combined with DNA sample loading buffer and separated by agarose gel electrophoresis on a 1% agarose gel. The gel was stained using ethidium bromide and DNA visualized under low UV light. Bands corresponding to $\gamma 7_{(1\text{-}217)}$ and linearised pMT_2 were excised from the gel and purified using an Invitrogen gel extraction kit (following the manufacture's guidelines). To reduce contamination by empty vector linearised pMT_2 was dephosphorylated by incubation for 2 hours at 37°C with Calf Intestinal Alkaline Phosphatase (CIAP). CIAP was removed using an Invitrogen PCR clean up kit and dephosphorylated linearised pMT_2 eluted in water. $\gamma 7_{(1\text{-}217)}$ and pMT_2 were ligated together using T4 ligase. An approximate ratio of 3 $\gamma 7_{(1\text{-}217)}$: 1 pMT_2 was used and incubation was carried out for 2 hours at room temperature. A control ligation was also set up in which was $\gamma 7_{(1\text{-}217)}$ was replaced with water. This provided an indication to the amount of pMT2 remaining that was either uncut or remained phosphorylated.

2.4.3. Transformation

Products of the ligation reactions were then used to transform Library efficiency DH5α competent bacteria (Invitrogen) by the following protocol. Cells were thawed from storage at -80°C on wet ice, the products of the ligation reactions added and mixed gently. A further control in which no DNA was added to the cells was also performed to ensure that antibiotic selection took place. The cells were then incubated on ice for 30 minutes. Heat-shock was performed by placing the cells in a 42°C water bath for 45 seconds then returning them to ice for a further 2 minutes. S.O.C. medium, pre-warmed to 37°C, was added to the cells which were then incubated for 1 hour at 37°C with constant shaking. Cells were then spread onto LB agar plates containing 100 µg/ml ampicillin and left to incubate overnight at 37°C. Plates were then stored

at 4°C until required. Aseptic technique used through out to minimize the possible contamination.

2.4.4. Purification of $\gamma 7_{(1\text{-}217)}$ in pMT2 DNA

Individual colonies were picked from the plate and used to seed 5 ml of LB broth containing 100 µg/ml ampicillin. Cultures were grown overnight at 37°C with constant shaking. Plasmid DNA was purified from 1.5 ml (the remainder was stored at 4°C) of each culture using an Invitrogen miniprep kit following the manufactures guidelines. Briefly, bacteria were harvested by centrifugation. Bacteria are lysed under alkaline conditions, and the lysate is subsequently neutralized and adjusted to high-salt binding conditions before loading onto a spin column. The columns contain a silica-gel membrane that binds DNA under high salt conditions and allows it to be eluted under low salt conditions. RNA, cellular proteins, and metabolites are not retained on the membrane and are removed in the flow-through during the wash steps. A short lysis time allows maximum release of plasmid DNA without release of chromosomal DNA, while minimizing the exposure of the plasmid to denaturing conditions. DNA was eluted in water. A sample of each plasmid was restriction digested with NcoI for 1 hour at 37°C to examine if $\gamma 7_{(1\text{-}217)}$ was present and inserted in the correct orientation. Products of the restriction digests were mixed with DNA sample loading buffer and separated by electrophoresis on a 1% agarose gel. The gel was stained with ethidium bromide and visualised under UV.

The remaining culture from one of the clones identified as containing $\gamma 7_{(1\text{-}217)}$ in the correct orientation was used to seed 200ml of LB broth containing 100 µg/ml ampicillin. This culture was incubated overnight at 37°C with constant shaking. A sample of the culture was taken to make a glycerol stock which was subsequently frozen and stored at -80°C. The remainder of the cells were then pelleted by centrifugation and plasmid DNA purified using a Invitrogen megaprep kit following the manufactures guidelines. DNA was taken up in TE and DNA concentration estimated by absorbance at 260 nm using a DU 800 spectrophotometer. DNA concentration was adjusted to 1 µg/µl by the addition

of TE. The test restriction digests detailed above were repeated to confirm that the correct plasmid had been purified. Purified plasmid was stored at -20°C.

2.4.5. Sequencing

$\gamma7_{(1\text{-}217)}$ in pMT_2 was sequenced using the Big Dye Kit v3.1, using the primers complementary to the vector both upstream and downstream of the expected insert, by the following method. Each reaction consisted of 2 μl of DNA at 1 μg/μl, 2μl of water, 2μl of 5X BigDye sequencing buffer 2μl of primer at 2 pmol/μl and 2μl of BigDye v3.1 and the following PCR reaction performed on a Techne thermocyler:

Cycle1 (1x):	96°C for 2 min 30 sec	Initial denaturation step
Cycle 2 (25x):	Step 1: 96°C for 20 sec	Denaturation step
	Step 2: 50°C for 30 sec	Annealing step
	Step 3: 60°C for 4 min	Extension step
Cycle 3 (1x)	4°C for ∞	Cooling

PCR products were then precipitated with isopropanol taken up in sequencing loading buffer run on an Avant-3100 sequencer. Chromatograms were analysed using Chromas and sequence aliments performed using Omega.

Standard molecular biology methods were also used to make the following constructs $\gamma7_{(1\text{-}238)}$ in pMT_2; $\gamma7_{(1\text{-}271)}$ in pMT_2; $\gamma7_{(201\text{-}275)}$ in pMT_2; $\gamma7_{(201\text{-}275)}$ in pcDNA3; γ7_CFP in pECFP-N1; γ7_HA in pMT_2; γ7_HA in pcDNA3; HA_γ7 in pMT_2; $\gamma7_{(201\text{-}275)}$ _HA in pMT_2; γ7_STOP in pMT_2; γ2TM γ7Tail in pMT_2; γ7_PDZ in pMT_2 and γ7N45A in pMT_2. The primer pairs to design these constructs are given in the Appendix (A.3.1).

2.5. Immunocytochemistry

PC12 and COS7 cells were fixed and permeabilised for immunocytochemistry as follows. Coverslips were removed from 3.5 cm dishes and washed twice with TBS (Tris buffered saline: 20 mM Tris, 150 mM NaCl, pH

7.4) to remove any remaining media. Cells were fixed by treatment with 4% paraformaldehyde for 15 minutes at room temperature. Cells were then permeablised by incubation for 15 minutes at room temperature with TBS containing 0.02% Triton-X 100. Prior to incubation with antibodies the coverslips were incubated for 30 minutes at room temperature with blocking buffer (20% (v/v) goat serum, 4% (w/v) bovine serum albumin (BSA), and 0.1% D,L-lysine in TBS) to reduce the amount of non-specific binding. Cells were then incubated overnight at 4°C with the primary antibody in antibody diluent buffer (10% (v/v) goat serum, 2% (w/v) BSA, and 0.5% D,L-lysine in TBS). After 4 washes with blocking buffer, 5 minutes per wash, biotin-conjugated goat anti-rabbit or anti-mouse antibody was applied at 5 µg/ml in antibody diluent buffer and incubated for 2 hours at 4°C. Cells were then washed 4 times with TBS, 5 minutes per wash, before fluorescein isothiocyanate (FITC)-conjugated streptavidin in TBS was applied at 3.33µg/ml and incubated for 1 hour at room temperature. After washing once with TBS the cells were incubated with the nuclear dye 4',6-diamidino-2-phenylindole at 300 nM DAPI) in TBS for 5 minutes at room temperature. In experiments with differentiated PC12 cells actin was visualised by incubating the cells for 20 min with 6.6 µM TexasRed–phalloidin. Finally cells were extensively washed with TBS and mounted in VectorShield to reduce photobleaching.

2.6. Immunoprecipitation

Cells were washed with ice cold PBS and harvested in PBS with protease inhibitor cocktail. Cells were lysed and protein solublised by the addition of extraction buffer (1% (v/V) Igepal, 20mM Tris, 150mM NaCl, 1mM EDTA 0.5% (w/v) Cholic Acid, 0.1% (w/v) SDS, protease inhibitor cocktail (pH 7.4) and constant agitation maintained for 30 minutes at 4°C. Insoluble material was removed by centrifugation at 40,000 xg 4°C for 1 hour. The supernatant was cleared by the addition of Protein G linked to agarose beads and constant agitation maintained for 2 hours at 4°C. Beads were removed by centrifugation for 12,000 xg for 30 seconds. 2µg of High Affinity Anti-HA was added to the supernatant and left to incubate overnight at 4°C with constant agitation. Further Protein G linked to agarose beads was added and left to incubate for 2 hours at 4°C with constant agitation. Beads were washed twice with a high

detergent buffer (1% (v/v) Igepal, 20mM Tris, 150mM NaCl, 1mM EDTA, Complete™ protease inhibitor cocktail pH 7.4); twice with a high salt buffer (0.1% (v/v) Igepal, 20mM Tris, 500mM NaCl, 1mM EDTA protease inhibitor cocktail (pH 7.4)) and twice with a low salt buffer (0.1% (v/v) Igepal, 20mM Tris, 1mM EDTA, protease inhibitor cocktail (pH 7.4)). Protein was freed from the beads by the addition of SDS sample buffer containing reducing agent and heating to 70°C for 10 minutes. Samples were then run on 4-12% Bis-Tris gels and either coomassie or silver stained or analysed by western blotting. Samples not used immediately were stored at -20°C until required.

2.7. RNA Isolation and Reverse Transcription

2.7.1. RNA Purification

RNA was isolated from tsA-201 or PC12 cells using the Qiagen RNeasy kit following the manufactures guidelines. Briefly, the media was removed and cells washed with PBS prior to lysis. Lysed material was then homogenised using QIAshredder columns. Ethanol was added to the homogenised lysate prior to loading onto the spin-column to provide the correct binding conditions. On column DNase digestion, using RNase-free DNase (Qiagen), was performed to prevent DNA contamination. Columns were extensively washed to remove all contaminants and RNA was eluted in water. If RNA was not immediately used for cDNA synthesis it was stored at -80°C. RNA concentration was determined from absorbance at 260nm using a DU 800 spectrophotometer.

2.7.2. Reverse Transcription

First-strand cDNAs were generated from 2μg of RNA by using Moloney Murine Leukemia Virus Reverse Transcriptase (MMLRTV) in the presence of random hexamer primers and RNasin.

2.8. Quantitative PCR

cDNA generated from the RT reaction described previously were diluted 100 fold and combined with iQ SYBR supermix and primers to give QPCR reactions with a final concentration of each primer of 8 pmol/μl For every experiment a standard curve was generated from a serial dilution (4 fold (1^{-1} to 9.8^{-5}) or 10 fold (1^{1} to 1^{-6})) of a mix of all cDNAs used within that experiment. Each sample and standard reaction was set up in triplicate. QPCR was performed using an iCycler using the following protocol:

Cycle1 (1x):	98°C for 3 mins	Initial denaturation step
Cycle 2 (50x):	Step 1: 98°C for 30 sec	Denaturation step
	50°C for 40 sec	Annealing step

A melt curve was generated by raising the temperature from 54°C to 94°C over 80 30s cycles the temperature increasing 0.5 °C per cycle and the fluorescence measured at the end of each cycle.

2.9. Stable Cell Lines

PC12 cell lines stably transfected with γ7_HA or γ7_CFP were established as follows. Before transfection the minimum concentration of Geneticin required to ensure death of untransfected cells within 14 days was determined to be 400 μg/ml. To decrease the likelihood of the vector integrating into the genome in a way that would have disrupted the gene of interest or other elements required for expression in mammalian cells the expression vectors containing γ7_HA and γ7_CFP were linearised prior to transfection using PvuI. Cells were transfected with γ7_HA in pcDNA3 or γ7_CFP in pECFP-N1 using FuGENE as previously described. Cells transfected with empty pCDNA3 and untransfected cells were used as positive and negative controls respectively. 24 hours post transfection the cells were washed fresh media added. Cells were split 48 hours post transfection to 25% confluency into DMEM supplemented with 7.5% horse serum, 7.5% fetal bovine serum and 400μg/ml Geneticin. Selective medium was replaced every 3-4 days until foci of resistant

cells could be identified and no cells remained in untransfected cell control. To obtain clonally selected cell lines both γ7_HA and γ7_CFP cells were resuspended, counted then transferred to 96-well plates at a dilution so as to give 1 cell per well. Wells in which more than one cell could be identified were not used further. After sufficient growth clones were transferred to 6-well plates and finally to T-75 flasks. Expression of γ7_HA and γ7_CFP was confirmed by western blotting and epifluorescence microscopy respectively. Stably transfected cell lines were maintained as previously described for untransfected PC12 except that media is further supplemented with 400μg/ml of Geneticin

2.10. Western Blotting

2.10.1. Preparation of Samples

Cells were washed with ice cold PBS and harvested in PBS with Complete™ protease inhibitor cocktail. A BCA assay was carried out to determine the protein concentration of each sample. Samples were then taken up in SDS sample loading (50 mM Tris-HCl (pH 7.4), 2% (w/v) SDS, 0.1% bromophenol blue, 10 % (v/v) glycerol and 2% (v/v) β-mercaptoethanol) to give a final protein concentration for each sample of 50 μg/30 μl. Samples were then sonicated briefly (3 10 second pulses, on ice) and, unless otherwise stated, heated to 70°C for 10 minutes. Samples not used immediately were stored at -20°C until required. Prior to loading on the gel protein samples were warmed for several minutes in a 37°C water bath and then any insoluble material pelleted by centrifugation.

2.10.2. SDS-PAGE

Samples were separated by SDS-PAGE using 4-12% Bis-Tris gels (Invitrogen) with a running buffer consisting of 50 mM MOPS 50 mM Tris base, 0.1% (w/v) SDS 1 mM EDTA (pH 7.7). The anti-oxidant thioglycolic acid was added to the upper reservoir at a final concentration of 0.01% to prevent disulphide bond formation during the run and thus improve protein resolution. Gels were run under for 1 hour at 200 V with mA limiting using a Novex Minicell

gel apparatus. Unless otherwise stated 50 μg of protein per lane was loaded and 12 μl of rainbow molecular weight markers were used.

2.10.3 Electrotransfer

Separated protein was transferred electrophoretically to polyvinylidene fluoride (PVDF) membranes using a semi-dry transfer system. The transfer buffer consisted of 10% (v/v) methanol, 0.01% (v/v) thioglycolic acid, 25 mM Bicine, Bis-tris (free base), 0.1% (w/v) SDS 1mM EDTA (pH 7.2). PVDF membranes were cut to size and pre-incubated in methanol and then transfer buffer before use. Transfer conditions of 15V and 400 mA (voltage limiting) for 30 minutes were used.

2.10.4. Western blotting

After transfer the membranes were blocked with 3% BSA for 3 hours at room temperature and then incubated overnight at room temperature with primary antibody in antibody diluent buffer (3% (w/v) BSA, 0.5% (w/v) Ovalbumin, 10% (v/v) goat serum, 0.5% (v/v) Igepal). Membranes were then extensively washed with TBS containing 0.5% (v/v) Igepal. Secondary antibody (Anti-Rabbit-HRP) was added (1μg/ml in antibody diluent), and the membranes were incubated at room temperature for 2 hours. After extensive washing with TBS containing 0.5% (v/v) Igepal, bound antibodies were detected using enhanced chemiluminescence plus reagents. Chemiluminescence or fluorescence was detected using a Typhoon phosphoimager and resulting images were analysed using ImageQuant.

Chapter 3 – Confirmation of Previous Observations and Generation of Stable Cell Lines

3.1. Introduction

3.1.1. $Ca_V2.2$, But Not $K_V3.1b$, Expression is Suppressed by Co-expression of γ7

As mentioned earlier, Moss *et al* (174) showed that expression of $Ca_V2.2$ was suppressed by the co-expression of γ7. This was shown as both a reduction in N-type current in both mammalian cells and *Xenopus* oocyte overexpression systems and also by immunocytochemistry and western blotting. They went on to show that there was no change in currents through a control protein, the Shaw-like voltage dependent potassium channel $K_V3.1b$. There was also no reduction in $K_V3.1b$ expression when γ7 was co-transfected, as judged by immunocytochemistry.

3.1.2. Green Fluorescent Protein (GFP) and Influenza Hemagglutinin (HA) Tagged Proteins

Green fluorescent protein (GFP) was discovered by Shimomura *et al* (215), as a companion protein to aequorin, in the *Aquorea* jellyfish. Its role is to transduce, by energy transfer, the blue chemiluminescence (around 475 nm) from aequorin into green fluorescent light (around 509 nm) (216). Cloning of the GFP gene (217) allowed the generation of chimeric proteins containing a GFP tag. Such proteins have been of great use in investigating the cellular and subcellular distribution of proteins (218). Mutations of GFP have resulted in variants with differing excitation and emission profiles such as cyan fluorescent protein (CFP) and yellow fluorescent protein (YFP).

Influenza virus hemagglutinin (HA) is a type I transmembrane glycoprotein that is well characterized in terms of structure, function and intracellular transport. Amino acids 99-107 (YPYDVPDYA) have been shown to exceptionally antigenic (219) and they are often added to proteins as an epitope tag (220-222). There are many commercially available antibodies to the HA tag and high-specificity, high-affinity antibodies can be used. These properties allow immunoprecipitation of the tagged protein with minimum contamination.

3.1.3. Sub-cellular Distribution of γ7

Moss *et al* showed that γ7 transfected into COS7 cells was distributed throughout the cytoplasm but not specifically localised to the plasma membrane (174). This pattern of distribution was also shown by Hansen *et al* using a GFP tagged γ7 (187). Hansen *et al* also used differential centrifugation to show that γ7 is found within membranes, but did not show if these were internal or plasma membranes.

3.2. Aims

The aims of the work described in this chapter were firstly to confirm the suppression of $Ca_V2.2$ expression previously obtained with γ7. Secondly I wished to investigate the potential glycosylation of γ7, and thirdly I wanted to examine γ7's sub-cellular distribution.

3.3. Additional Methods

Experiments were performed as described in Chapter 2 with the following differences and additions.

3.3.1. Generation of Constructs

HA_γ7, γ7_HA, γ7N45A and γ7_CFP were made by standard molecular biological techniques using the primer pairs detailed in the Appendix (A.3.1). HA_γ7 and γ7_HA were cloned into the pMT2 expression vector. γ7_HA was also cloned into the pcDNA 3.1 expression vector, which contains a neomycin resistance gene, for generation of a stably transfected PC12 cell line. γ7_CFP was generated by cloning γ7 into pECFP-N1 expression vector.

3.3.2. Imaging

Confocal images were obtained using a Leica TCS SP confocal scanning laser microscope, except PDI co-localisation experiments which were obtained

using a Zeiss LSM 510 confocal microscope. In all experiments photomultiplier settings were kept constant in each experiment and all images were scanned sequentially. All images shown, except where stated, are single 0.5 μm sections through the cell. PC12 cells stably transfected with γ7_CFP were examined using a Zeiss LSM 510 microscope and an Improvision live cell imaging system. When examining co-localisation of γ7_CFP with PDI the PDI antibody was used at 1:200. In the comparison of γ7 in fixed PC12 cells and γ7_CFP in live PC12 cells, cultures were treated with 100ng/ml NGF for 24 hr before fixing or imaging to initiate process outgrowth.

3.3.3. Western Blotting

Protein samples for Western blotting were separated using 4-12% Bis-Tris gels except in the experiments examining expression of $Ca_V2.2$ which were run on 4-12% Tris-Glycine gels. Anti-$\gamma7_{(Tail)}$, anti-HA and Anti-$Ca_V2.2$ antibodies were used at 0.4 μg/ml, 0.8 μg/ml and 1.2 μg/ml respectively.

3.4. Results

3.4.1. The Expression of $Ca_V2.2$ is Suppressed by the Co-Expression of γ7

Previous work had shown that co-transfection of γ7 suppressed the expression of $Ca_V2.2$. It was decided to repeat experiments performed by Moss *et al* (174) to confirm the effect of γ7 on $Ca_V2.2$ expression at a protein level by western blotting with an antibody raised against the II/III loop of rabbit $Ca_V2.2$.

The suppression of $Ca_V2.2$ expression by γ7 at the protein level is shown in Fig. 3.1. A. There is a clear reduction in $Ca_V2.2$ expressed when γ7 is co-transfected with it. As a control the effect of γ7 on the six potassium channel $K_V3.1b$ was investigated. Western blotting with an antibody raised against $K_V3.1b$ showed that expression of $K_V3.1b$ was found to not to be suppressed by co-expression of γ7 (Fig. 3.1.B).

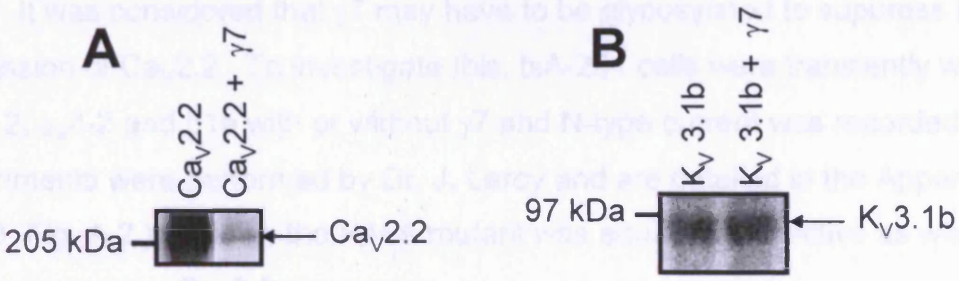

Fig. 3.1. $Ca_V2.2$ expression but not $K_V3.1b$ expression is suppressed by co-expression of γ7. Extracts of tsA-201 cells transfected with A. $Ca_V2.2 \pm \gamma7$ or B. $K_V3.1b \pm \gamma7$ were western blotted with antibodies raised against $Ca_V2.2$ and $K_V3.1b$ respectively.

3.4.2. γ7 is a Glycoprotein and is Glycosylated at N45

Glycosylation of the first extracellular loop is believed to be a conserved feature between the γ subunits (223). The asparagine at position 45 of γ7 has been predicted to be glycosylated and the following experiment was performed to confirm this. Primers were designed to generate a construct in which the asparagine at position 45 was converted to alanine thus preventing glycosylation taking place. Western blotting with the $\gamma7_{(Tail)}$ antibody showed a shift in molecular weight from a diffuse band between 32 and 37 kDa to a sharp band at the predicted molecular weight of around 31 kDa (Fig. 3.2).

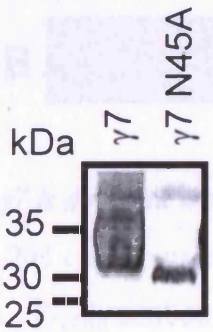

Fig. 3.2. Introduction of the mutation N45A in γ7 results in γ7 running at the expected molecular weight of 31 kDa. Extracts of tsA-201 cells transfected with γ7 or γ7 N45A were western blotted with the $\gamma7_{(Tail)}$ antibody.

It was considered that γ7 may have to be glycosylated to suppress the expression of $Ca_V2.2$. To investigate this, tsA-201 cells were transiently with $Ca_V2.2$, $\alpha_2\delta$-2 and β1b with or without γ7 and N-type current was recorded. Experiments were performed by Dr. J. Leroy and are detailed in the Appendix (A.4.3. Fig. A.2.). Briefly, the N45A mutant was equally as effective as wild type γ7 in suppressing $Ca_V2.2$ expression.

3.4.3. Generation and Characterisation of HA Tagged γ7 Constructs

Primers were designed to generate γ7 incorporating an HA tag at either the N or C-terminus. Expression of these constructs was confirmed by their transfection into tsA-201 cells and subsequent western blotting with the anti-γ7(Tail) antibody. Both the HA_γ7 and γ7_HA were detectable as can be seen in Fig. 3.3.A. However, western blotting with an antibody raised against the HA epitope only detected the γ7_HA construct (Fig. 3.3.B).

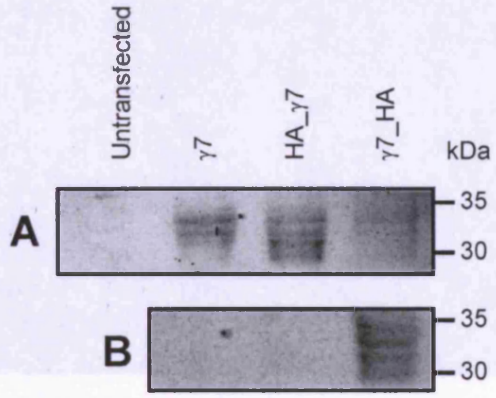

Fig. 3.3. N-terminally HA tagged γ7 is detected with the $\gamma7_{(Tail)}$ antibody but not the Anti-HA antibody. Extracts of tsA-201 cells transiently transfected with γ7, HA_γ7 or γ7_HA were western blotted with A. $\gamma7_{(Tail)}$ antibody B. Anti-HA antibody. Multiple bands seen may represent different glycosylation states.

Electrophysiological experiments in both *Xenopus* oocytes and tsA-201 cells, by Dr. J. Leroy and Prof. A. Dolphin respectively, were performed to confirm that the addition of a HA tag did not alter the suppression of $Ca_V2.2$ expression. Briefly *Xenopus* oocyte or tsA-201 cells were injected or transiently

transfected respectively with $Ca_V2.2$, $\alpha_2\delta$-2, β1b and either γ7_HA or a corresponding amount of empty vector. In both model systems γ7_HA was as effective as untagged γ7 in suppression of N-type current through $Ca_V2.2$.

3.4.4. Generation and Characterisation of a CFP Tagged γ7 Construct

Primers were designed to generate γ7 that could be cloned into pECFP-N1 to express γ7 with a C-terminal CFP tag. To confirm expression this construct was transiently transfected into COS7 cells and visualised by confocal microscopy (Fig. 3.4).

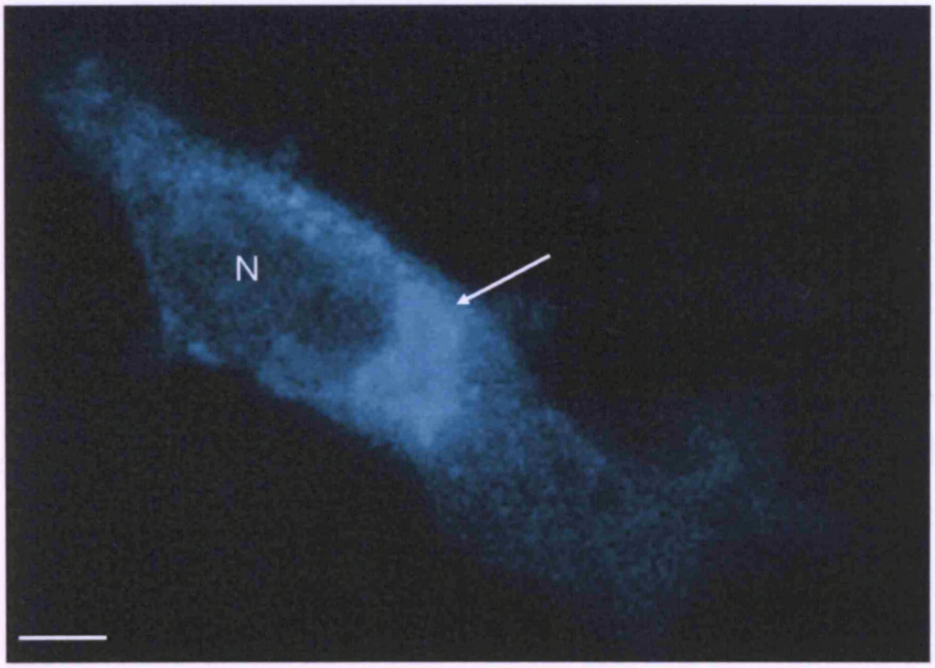

Fig. 3.4. Expression of γ7_CFP. γ7_CFP was transiently transfected into COS7 cells and three days post transfection its expression was examined by confocal microscopy. N indicates nucleus. The white arrow indicates the predominant perinuclear expression of γ7_CFP. Scale bar = 10 μm

γ7 showed a similar distribution to that previously described for untagged γ7 (174). Both showed perinuclear location with a weaker diffuse localisation throughout the cell. However, no discernable plasma membrane localisation was seen with either untagged or CFP-tagged γ7.

Electrophysiological experiments were performed by Dr. J. Leroy to confirm that γ7_CFP still suppressed $Ca_V2.2$ expression. Briefly tsA-201 cells were transiently transfected with $Ca_V2.2$, $\alpha_2\delta$-2 and β1b either plus γ7 or a corresponding amount of empty vector. γ7_CFP was as efficient as untagged γ7 in suppressing N-type current through $Ca_V2.2$ (Appendix. A.4.3. Fig. A.2.).

3.4.5. Generation of γ7_HA and γ7_CFP Stably Transfected PC12 Cell Lines

During the course of this study PC12 cell lines that stably expressed either γ7_HA or γ7_CFP were generated. The use of PC12 cells and their expression of γ subunits will be detailed Chapters 5 and 7. However, generation of these cell lines will be discussed here.

Briefly PC12 cells were transfected with either γ7_HA or γ7_CFP, and stably expressing cells were selected by addition of Geneticin, a neomycin analogue. Clones were selected and expression of γ7_HA detected by western blotting and immunodetection with the anti-HA antibody (Fig. 3.5) or by epifluorescence microscopy for γ7_CFP (Fig. 3.6). In both cases the majority of clonal cell lines that were tested did not express a γ7 construct at detectable levels despite being resistant to Geneticin.

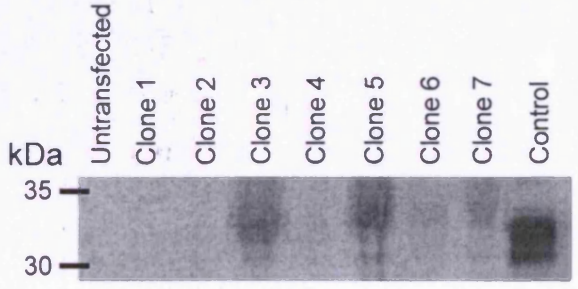

Fig. 3.5. Selection of γ7_HA expressing stably transfected PC12 cells. PC12 cells were transfected with γ7_HA. Cells were treated with neomycin and resistant cells clonally selected. γ7_HA expression was determined by western blotting with a anti-HA antibody. Extracts from tsA-201 cells transiently transfected with γ7_HA were used as a control.

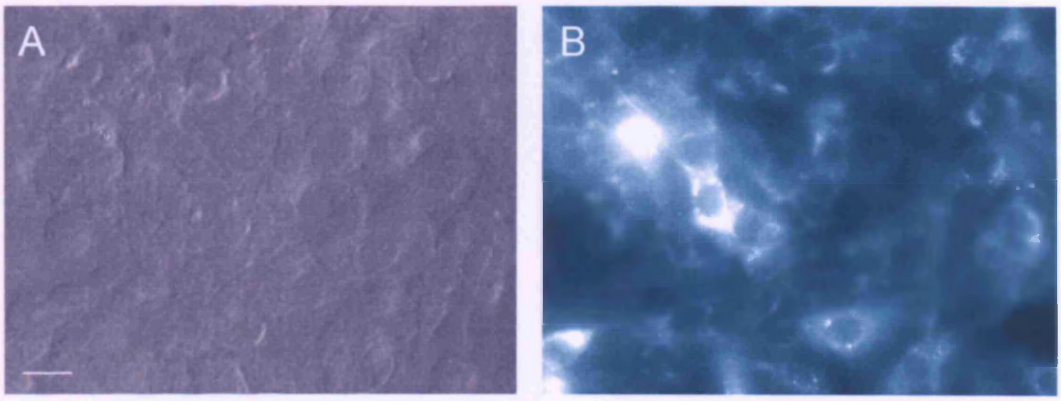

Fig. 3.6. Expression of γ7_CFP in expressing stably transfected PC12 cells. PC12 cells were transfected with γ7_CFP. Cells were treated with neomycin and resistant cells clonally selected. γ7_CFP expression was determined by epifluoresence microscopy. A. Bright field. B. CFP fluorescence. Scale Bar = 20 μm

3.4.6. Sub-cellular Distribution of γ7_CFP in PC12 Cells

The sub-cellular distribution of γ7_CFP was similar in fixed transiently transfected PC12 cells, live stably transfected PC12 cells and transiently transfected COS7 cells. All showed a predominantly perinuclear expression which was suggestive of localisation of γ7 to the ER and/or Golgi. In addition in PC12 cells which had extended processes γ7 often appeared to be concentrated at the end of the process (Fig. 3.7. White arrows).

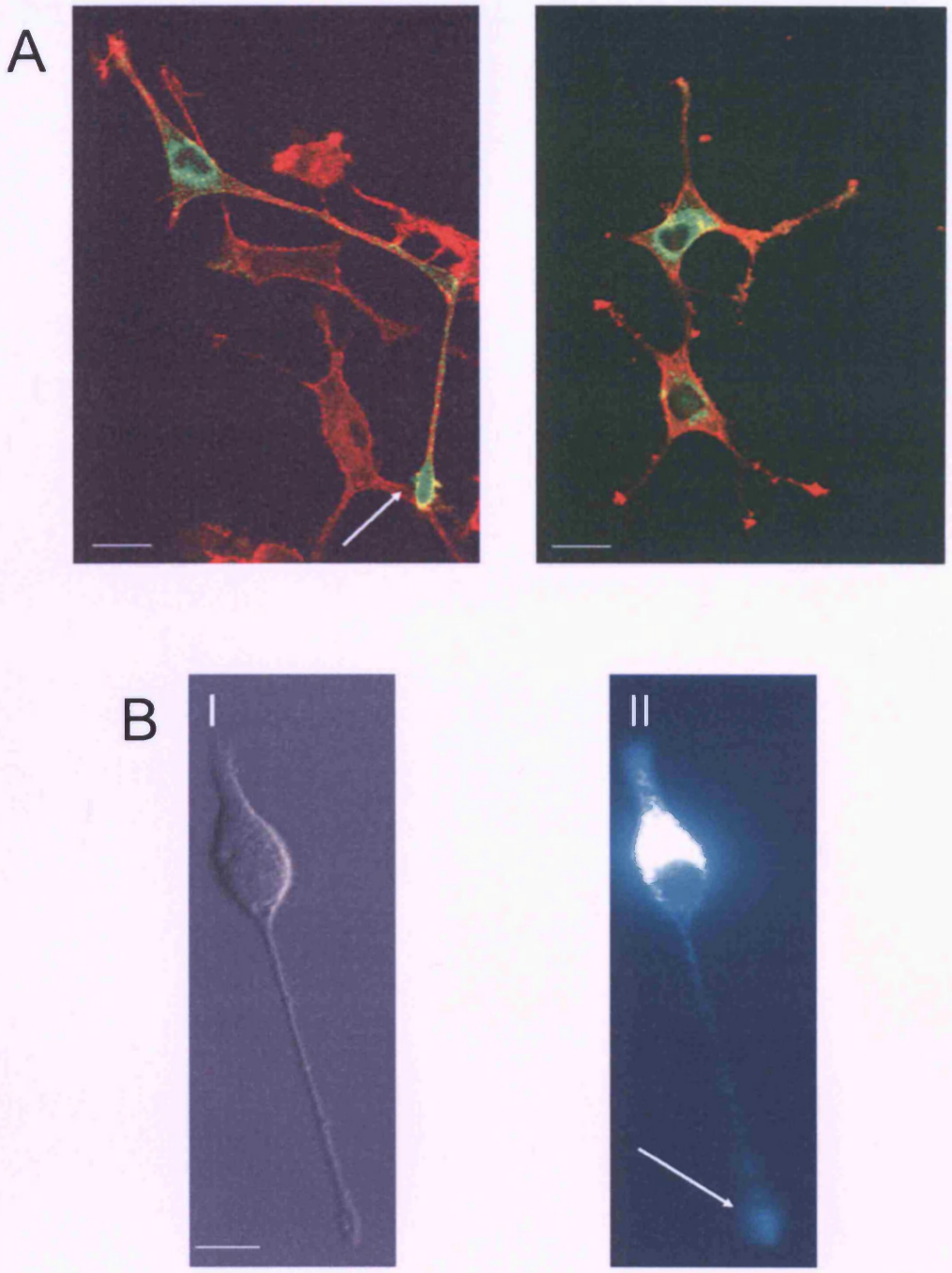

Fig. 3.7. Expression of γ7and γ7_CFP PC12 cells. A. PC12 cells were transiently transfected with γ7 and its cellular distribution detected by the $\gamma7_{(Tail)}$ antibody (Green). Texas-Red phalloidin was used to reveal F-actin. B. PC12 cells stably transfected with γ7_CFP I. Bright field. II. CFP fluorescence. White arrows indicate γ7 and γ7_CFP localised at the end of processes. Scale bars = 20 μm.

To investigate if the perinuclear distribution seen was due to γ7_CFP being present in the ER, γ7_CFP stably transfected PC12 cells were fixed and then probed with an antibody to Protein Disulphide Isomerase (PDI) as a

marker of ER (Fig. 3.8) (224). γ7 largely co-localises with the ER marker PDI (yellow).

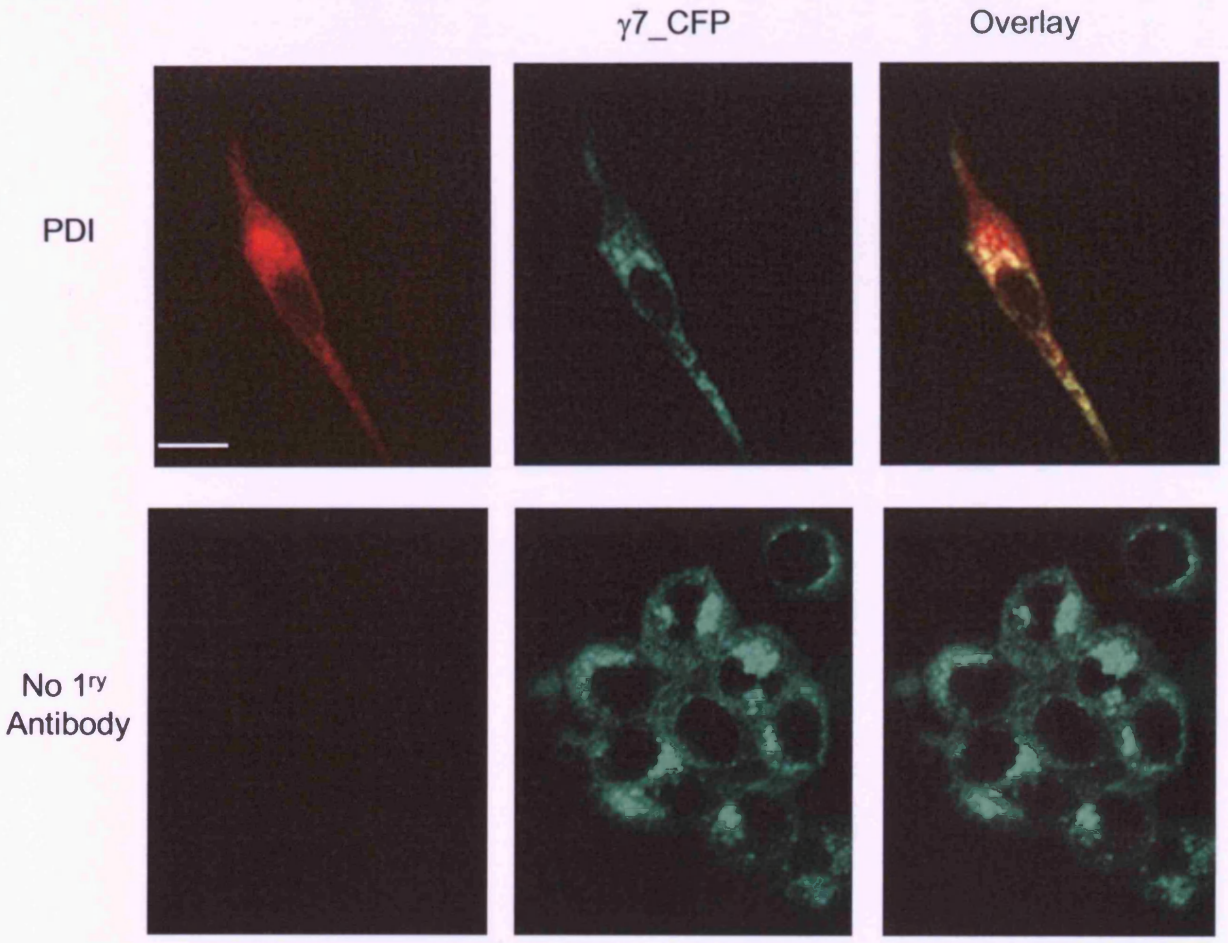

Fig. 3.8. Co-localisation of γ7_CFP with PDI, a marker of ER. PC12 cells stably transfected with γ7_CFP (Green) were fixed and probed with an antibody to PDI (Red). Yellow indicates where staining overlaps. Scale bar = 20 μm

3.5. Discussion

In agreement with the work previously performed by Moss *et al* (174) western blotting experiments here showed expression of $Ca_V2.2$ is suppressed when γ7 is co-transfected. This occurs even in the absence of β and $\alpha_2\delta$ subunits. Western blotting also showed that expression of $K_V3.1b$ was not reduced by the co-transfection of γ7. The lack of suppression of $K_V3.1b$, also a voltage gated ion channel suggests a degree of specificity of the action of γ7.

N-glycosylation has been shown for γ2, γ3 and γ4 (117) and all γ subunits have been predicted to have a glycosylation site at a preserved asparagine in the extracellular loop, N45 in γ7. Mutation of this asparagine to alanine resulted in a reduction in the apparent molecular weight of γ7 when separated by SDS PAGE. This would suggest that N45 is indeed glycosylated in native γ7. Treatment of wild type γ7 with endoglycosidases F or H could be performed in order to confirm this hypothesis.

Glycosylation is known to alter the running of proteins on SDS PAGE. The carbohydrate moiety alters the profile of the protein resulting in it being retarded differently by the gel and not running at the true weight of the protein. This may in part explain the broad range of molecular weights observed γ7 after SDS PAGE.

Electrophysiological experiments showed that glycosylation of γ7 is not important for the suppression of $Ca_V2.2$ expression. The N45A mutant was found to be as efficient as γ7 at suppressing N-type current through $Ca_V2.2$ in tsA-201 cells.

In agreement with other studies on the subcellular distribution of γ7 (174;187) these experiments show that γ7 appears to be located mainly on intracellular membranes. Subcellular distribution of γ7 and γ7_CFP appears to be identical in both COS7 and PC12 cells. In the stably transfected PC12 cells much of the γ7 co-locates with PDI, a marker of ER. However, due to the diffuse staining given by the PDI antibody it is hard to determine if γ7 is also

present outside the ER. The distribution of γ7_CFP in PC12 cells would suggest that γ7 moves from a perinuclear location to the end of the processes. However, the increased fluorescence seen at the end of the processes could be due to the increased volume of the cell there compared to the processes themselves. The movement of γ7_CFP could be further studied by live cell imaging of the stably transfected PC12 cell line.

It is possible that the N-terminal tail of γ7 is cleaved or modified. An HA tag placed at the N-terminius of γ7 was not detectable with an antibody to HA but was detectable with an antibody to an epitope in the C-terminal tail of γ7 (Fig.3.3B). This could be due to the N-terminal tag being not accessible to the Anti-HA antibody, not translated or cleaved from the protein. Sequencing revealed no problems with the construct that could account for the HA tag being missing.

Chapter 4 - γ7 and ER Stress

4.1. Introduction

4.1.1. Mechanisms of ER Stress

The ER is the principal site for synthesis, folding and maturation of transmembrane and secreted proteins. Perturbations that alter ER homeostasis, brought about by for example pathogenic infection, chemical insult, genetic mutation and nutrient deprivation can lead to accumulation of unfolded proteins.

The cellular response to ER stress is the activation of an intracellular signalling pathway – the unfolded protein response (UPR). The UPR is an integrated intracellular signalling pathway that transmits information about the protein folding status in the ER lumen to the cytoplasm and the nucleus. The UPR includes transcriptional induction of UPR genes, translational attenuation of global protein synthesis and ER-associated degradation (ERAD). If the protein-folding defect is not corrected, cells undergo apoptosis. The three major transducers of the UPR are PERK, ATF6 and IRE1 (225).

The ER chaperone BiP (immunoglobulin heavy chain-binding protein) is the regulator of the activation of the three major ER stress transducers – PERK, ATF6 and IRE. All three proteins contain a luminal domain that interacts with BiP. Under normal conditions, BiP serves as a negative regulator of PERK, ATF6 and IRE1activation. During ER stress, BiP binds to unfolded proteins, resulting in BiP release from the transducers. Upon BiP release from PERK and IRE1, they both undergo homodimerization and activation. BiP release from ATF6 permits its transport to the Golgi compartment for regulated intramembrane proteolysis. This BiP-regulated activation provides a direct mechanism to sense the folding capacity of the ER (225).

PERK is an ER transmembrane protein kinase that phosphorylates the α subunit of translation initiation factor 2 (eIF2) in response to ER stress (226). Phosphorylation of eIF-2α results in inhibition of the guanine nucleotide exchange factor eIF-2β, thereby reducing the rate of the GDP to GTP exchange that is required for eIF2 to carry out additional rounds of translation initiation

(227). This translational control provides an efficient mechanism to reduce the number of proteins entering into the ER.

ATF6 is an ER transmembrane-activating transcription factor. Upon ER stress, ATF6 and ATF6ß transit to the Golgi compartment where they are cleaved by S1P and S2P proteases to yield a cytosolic fragment (228). The free ATF6 fragment migrates to the nucleus to activate transcription.

IRE1 is an ER transmembrane glycoprotein which contains both kinase and RNase activities in the cytoplasmic domain (229). ER stress leads to its autophosphorylation and the subsequent activation of its RNase activity. The substrate of IRE1, XBP mRNA, encodes a basic leucine-zipper-containing transcription factor. Splicing of XBP mRNA is initiated by the RNase activity of IRE1 to generate mature XBP mRNA. Thus initiation of the UPR results in both an upregulation, and an increase in the amount, of mature, edited, XBP (230).

The signalling from downstream effectors of IRE1, PERK and ATF6 merges in the nucleus to activate transcription of UPR target genes. The mammalian ER stress element (ERSE) is present in the promoter regions of many, but not all, UPR target genes. XBP, ATF6 and the CAAT-binding factor (CBF), all of which bind to ERSE, along with ATF4, activate transcriptional induction of target genes (231). Generally these genes encode molecular chaperones and folding catalysts. Their upregulation increases the folding capacity of the ER.

The UPR also induces transcription of genes encoding proteins that mediate ERAD (232). This important component of the UPR stimulates the degradation and clearance of unfolded proteins in the ER lumen. This removal of these unfolded proteins further reduce stress upon the ER.

Prolonged UPR activation leads to apoptotic cell death, in which IRE1 serves a proapoptotic function. Activated IRE1 recruits Jun N-terminal inhibitory kinase (JIK) and TNF Receptor-Associated Factor 2 to activate apoptosis-signalling kinase 1 (ASK1), which in turn activates JNK and mitochondria/Apaf1-dependent caspases (233). In addition, UPR activation induces CHOP(C/EBP-

homologous protein) expression through the PERK and ATF6 pathways (234;235). CHOP is a proapoptotic transcription factor that potentiates apoptosis.

An overview of the cellular response is shown in Fig 4.1 (236)) and ER stress and the unfolded protein response has recently been comprehensively reviewed by Schroder & Kaufman. (225).

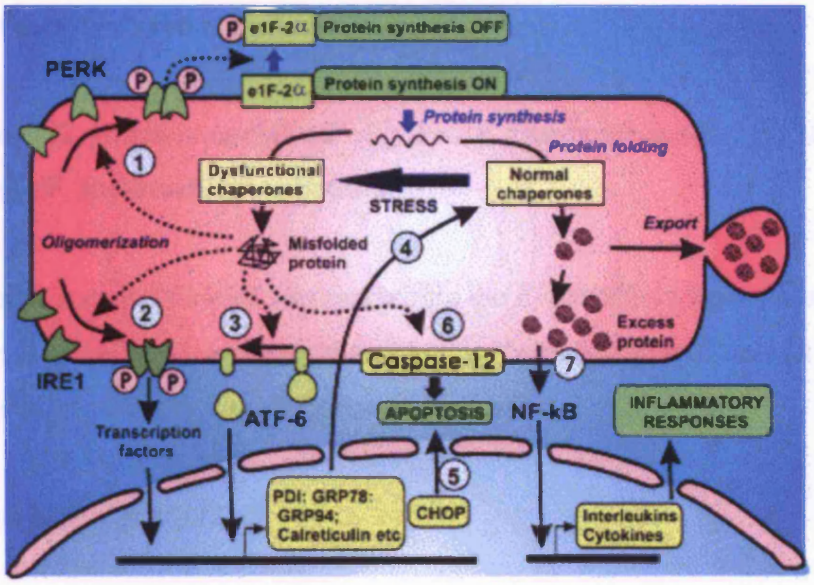

Fig. 4.1. ER stress signalling pathways. An accumulation of misfolded proteins or an excessive accumulation of normal proteins activate a number of signalling pathways. Chaperones within the ER lumen are responsible for folding newly synthesized proteins into their tertiary structures prior to their export to the Golgi. A variety of stress factors, including a decline in the luminal level of Ca^{2+}, results in dysfunctional chaperones and an accumulation of misfolded proteins that can activate a number of signalling pathways:

1. Oligomerization and autophosphorylation of PERK which sets off a phosphorylation cascade that culminates in the phosphorylation and inactivation of the translation initiation factor e1F-2 resulting in protein synthesis being switched off.

2. Oligomerization and autophosphorylation of IRE1 initiates one of the transcriptional signalling pathways responsible for the up regulation of the various chaperones.

3. Another of the transcriptional pathways depends upon the activation of the ER membrane-bound transcription factor ATF6, which is released from the ER to enter the nucleus where it interacts with the ER stress response element of the CHOP gene.

4. The various chaperones are then expressed within the ER where they participate in protein folding.

5. One of the genes activated during the stress response is CHOP, which acts as a transcription factor and can contribute to apoptosis.

6. The caspase-12, which is associated with the ER membrane is also activated and contributes to ER stress-induced apoptosis.

7. An excessive accumulation of proteins within the ER results in the activation of the transcription factor NF-KB, which acts to increase the production of interferons and cytokines so contributing to an inflammatory response.

Adapted from Berridge MJ (236)

4.1.2. Suppression of $Ca_V2.2$ Expression by the Co-Expression of Truncated $Ca_V2.2$ Constructs

Raghib et al (237) showed that functional expression of full-length $Ca_V2.2$ was significantly reduced by the co-expression of constructs which expressed domain I, domain I-II or domain III-IV of $Ca_V2.2$. Recording at the current level showed that this suppression was not due to differences in the biophysical properties of the channel. However, microscopy and western blotting were used to show that there was a decrease in $Ca_V2.2$ protein upon co-transfection with any of the truncated constructs. From these results they proposed that the mechanism of suppression of $Ca_V2.2$ by truncated constructs containing domain I involved inhibition of channel synthesis.

Page et al (238) went on to show that the UPR was involved in mechanism of $Ca_V2.2$ suppression of expression. They showed that co-transfection of a dominant negative PERK significantly reduced the suppression

of expression induced by domain I of $Ca_V2.2$. In addition treatment with thapsigargin, which induces ER stress, resulted in a similar reduction in N-type current and $Ca_V2.2$ protein as co-transfection of domain I of $Ca_V2.2$.

4.1.3. Measurement of Markers of ER Stress by QPCR

Recently QPCR has become an increasing popular method for quantifying changes in gene expression. In this study it was used to measure XBP editing and the expression of XBP and CHOP all of which are indicators of ER stress. A brief description of QPCR will be given here. An in depth review of QPCR experiments has recently been written by Bustin & Nolan (239).

QPCR follows the same methodology as standard PCR, with the exception that in addition one measures the binding of a fluorescent marker to the PCR product generated. At the start of a PCR reaction, reagents are in excess, and the template and product are at low enough concentrations that product renaturation does not compete with primer binding, so that amplification proceeds at a constant, exponential rate. As the point at which the reaction rate ceases to be exponential and enters a linear phase of amplification is variable, it is necessary to collect quantitative data at a point in which every sample is in the exponential phase of amplification. A threshold value, at which the PCR reaction is progressing exponentially, is set and the point at which the PCR reaction passes reaches this level is known as the Ct value. The lower the starting amount of mRNA the higher the Ct value will be. A typical QPCR graph is shown in Fig 4.2

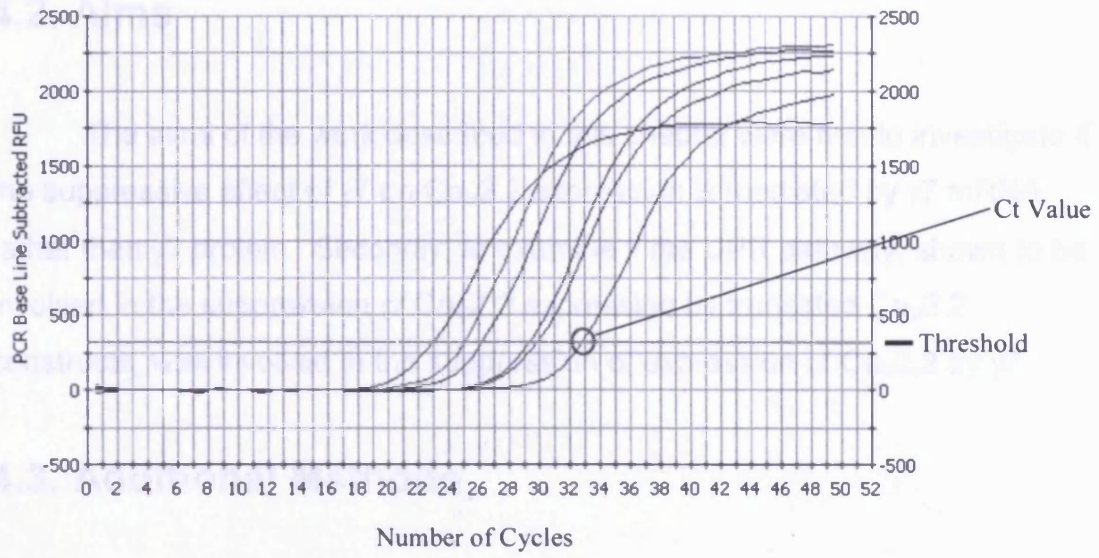

Fig. 4.2. An example of data generated by QPCR. Standards are shown by black lines. A sample with a high amount of target mRNA is shown by the red line and a sample with a lower amount of target mRNA is shown by the blue line. The threshold value is shown by the orange horizontal line. At this point the PCR is in the exponential phase. It is worth noting that the end point fluorescence varies greatly. The red circle highlights the point at which the fluorescence passes the threshold. This is termed the Ct value. Samples and standards are usually performed in triplicate but only one of the three reactions has been shown for clarity.

SYBR Green binding was used for detecting and quantifying PCR products. SYBR Green is a fluorophore that binds to double-stranded DNA. The amount of light emitted is far higher when bound to double stranded DNA then when unbound. Thus, as a PCR product accumulates, fluorescence increases. The advantages of SYBR Green are that it is inexpensive, easy to use, and sensitive. However, SYBR Green will bind to any double-stranded DNA in the reaction, including non-specific reaction products and primer-dimers. Therefore it is necessary to perform a melt curve after completion of the PCR run to confirm that only one product has been produced. Molecular beacons and Taqman probes, which bind specifically to the PCR product generated, can also be used but will not be discussed here.

4.2. Aims

The aims of the work described in this chapter were first to investigate if the suppressive effect of γ7 on $Ca_V2.2$ expression is mediated by γ7 mRNA rather than γ7 protein. Secondly, to examine if the UPR pathway, shown to be involved in the suppression of $Ca_V2.2$ expression by truncated $Ca_V2.2$ constructs, was involved in the suppression of expression of $Ca_V2.2$ by γ7

4.3. Additional Methods

Experiments were performed as described in Chapter 2 with the following differences and additions.

4.3.1. γ7_STOP

γ7_STOP was made by standard molecular biological techniques using the primer pairs detailed in the Appendix (A.3.1.) and subcloned into the pMT2 expression vector. γ7_STOP mRNA was identified by RT-PCR using the γ7_STOP RT primer pairs detailed in the Appendix (A.3.2.). Electrophysiological experiments on tsA-201cells were performed by Dr J. Leroy.

4.3.2. QPCR

tsA-201 cells were transfected or nucleofected with 2 μg or 5 μg respectively of a mix of $Ca_V2.2$, β_1b, $\alpha_2\delta$-2 and γ7 constructs at a 1:1:1:1 ratio. Where subunits were omitted they were replaced with empty pMT2 vector. RNA was harvested 24 hours post transfection. Inducers of ER stress were applied at a level shown previously to induce ER stress (230;240). Where tunicamycin was applied it was added to the growth medium of the cells to give a final concentration of 2.5 μg/ml six hours prior to harvesting RNA. Similarly in experiments where DTT was used it was added to the growth medium to give a final concentration of 10 mM 30 minutes prior to harvesting RNA. Primer pairs for CHOP, $XBP_{(Total)}$ and $XBP_{(Unedited)}$ are detailed in the Appendix (A.3.2.).

Preliminary experiments were performed to define the optimum PCR conditions for each primer pair and accordingly step two of the second PCR cycle was set to a temperature of 61°C, 56.7°C and 61.1°C for primer pairs for CHOP, $XBP_{(Total)}$ and $XBP_{(Unedited)}$, respectively.

Percentage XBP Edited was calculated as follows:

$$\frac{SQ_{Total} - SQ_{Unedited}}{SQ_{Total}} \times 100$$

4.4. Results

4.4.1 Suppression of $Ca_V2.2$ by γ7 Requires γ7 Protein

To investigate if γ7 protein was required for the suppression of $Ca_V2.2$ expression a construct was made which would produce a γ7 mRNA that would not be translated to γ7 protein. To make this construct primers were designed to generate γ7 in which the codon for cystine at position 4 was mutated to a stop codon (γ7_STOP).

tsA-201 cells were transiently transfected with γ7 or γ7_STOP. Three days post transfection total protein was harvested and separated by SDS PAGE. Expression of γ7 was determined by western blotting using the $\gamma7_{(Tail)}$ antibody. No γ7 protein was detected in cells transfected with γ7_STOP (Fig. 4.3.A). It is worth noting that the next possible start codon is in frame. If translation was starting from this start codon the protein produced would still be detected by the $\gamma7_{(Tail)}$ antibody. As there were no reactive lower molecular weight bands it would appear that this is not occurring.

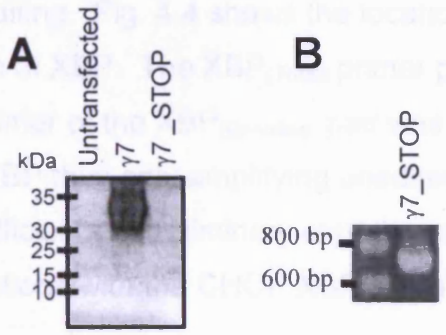

Fig. 4.3 Mutation of the codon for cysteine at position four of γ7 to a stop codon produces mRNA but not protein. Protein and mRNA were harvested from tsA-201 cells three days post transfection with either γ7 or γ7_STOP. A. Extracts of cells transfected with γ7 or γ7_STOP were western blotted with the $\gamma7_{(Tail)}$ antibody. B. RT-PCR of mRNA from tsA-201 cells transiently transfected with γ7_STOP gives the expected product (750 bp). First lane – molecular weight markers.

To confirm of transcription of γ7 RNA tsA-201 cells were transiently transfected with γ7_STOP and three days post transfection RNA was harvested and reverse transcribed. PCR was performed on the resulting cDNA with a primer pair to γ7 (Fig 4.3.B). A band of expected size (approximately 750 bp) was obtained confirming that γ7 mRNA was produced.

Experiments with this construct, performed by Dr J. Leroy, showed that it did not suppress N-type current through $Ca_V2.2$ channels in a tsA-201 cell expression system. These experiments are detailed in the Appendix (A.4.3. Fig. A.2.).

4.4.3. QPCR of the Markers of ER Stress, CHOP and Edited XBP

It has previously been reported that ER stress can lead to a suppression of protein expression. It was hypothesised that expression of γ7, or co-expression of $Ca_V2.2$ and γ7, would lead to ER stress. To test this hypothesis experiments were performed to quantify expression of CHOP and XBP editing, two markers of the activation of the ER stress pathway cells.

Primers were designed to allow QPCR of CHOP and XBP. Primers were also designed to quantify XBP editing. Fig. 4.4 shows the location of primers in relation to the edited section of XBP. The $XBP_{(Total)}$ primer pair will pick up all XBP cDNA. The reverse primer of the $XBP_{(Unedited)}$ pair was designed to be within the edited region of XBP thus only amplifying unedited XBP. QPCR is dependent upon the PCR efficiency. Preliminary experiments were performed to ensure that the PCR reactions with the CHOP $XBP_{(Total)}$ and $XBP_{(Unedited)}$ were sufficiently efficient.

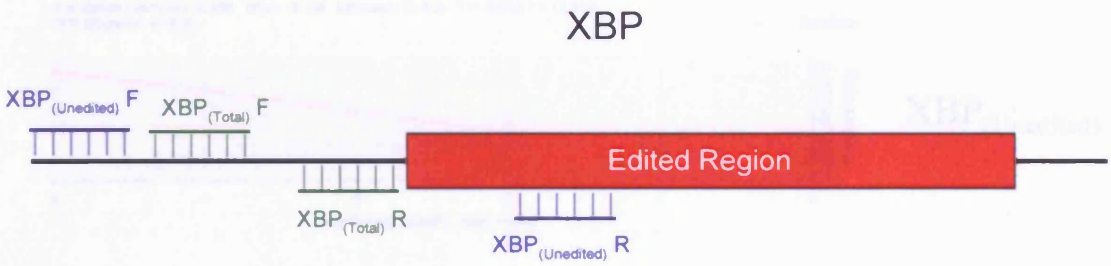

Fig. 4.4. Diagrammatic representation of the positions of the $XBP_{(Total)}$ and $XBP_{(Unedited)}$ primer pairs. The region edited out by IRE1 is shown as a red box. $XBP_{(Total)}$ primer pairs are shown in green and $XBP_{(Unedited)}$ primer pairs are shown in blue.

PCR efficiency is obtained by comparing the values obtained for the standard curve to that of an ideal PCR reaction in which a difference of 3.3 cycles would be equivalent to a 10 fold difference in the starting quantity of cDNA. Fig 4.5 shows the PCR efficiency using the (A) CHOP, (B) $XBP_{(Total)}$ and (C) $XBP_{(Unedited)}$ primer sets. All primer sets were of high efficiency (97.4%, 98.6% and 98.2% respectively), which is sufficient for use in QPCR. Fig. 4.6. shows the melt curves obtained for each construct. For each primer pair the PCR product obtained melts as a single, narrow peak. This suggests that only one PCR product was produced for each primer set.

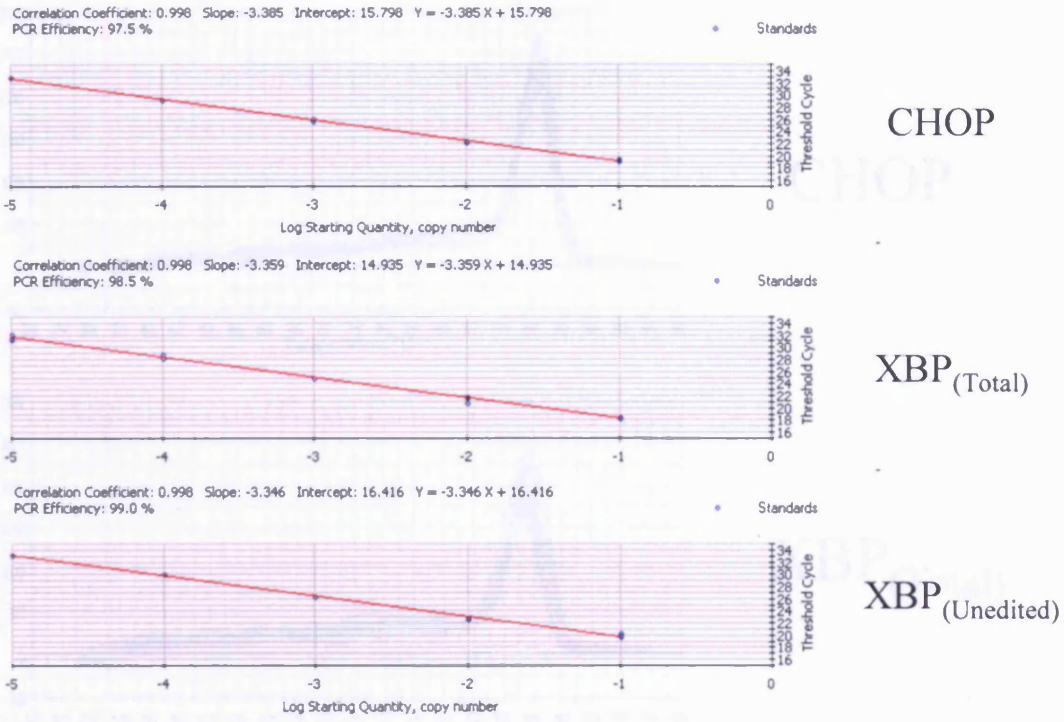

Fig. 4.5. PCR reactions using the CHOP XBP(Total) and XBP(Unedited) primer sets are of high efficiency and can be used for QPCR. A cDNA library derived from mRNA from tsA-201 cells treated with Tunicamycin was serially diluted and PCR performed using CHOP; $XBP_{(Total)}$ and $XBP_{(Unedited)}$ primer sets to obtain the PCR efficiency for each primer set.

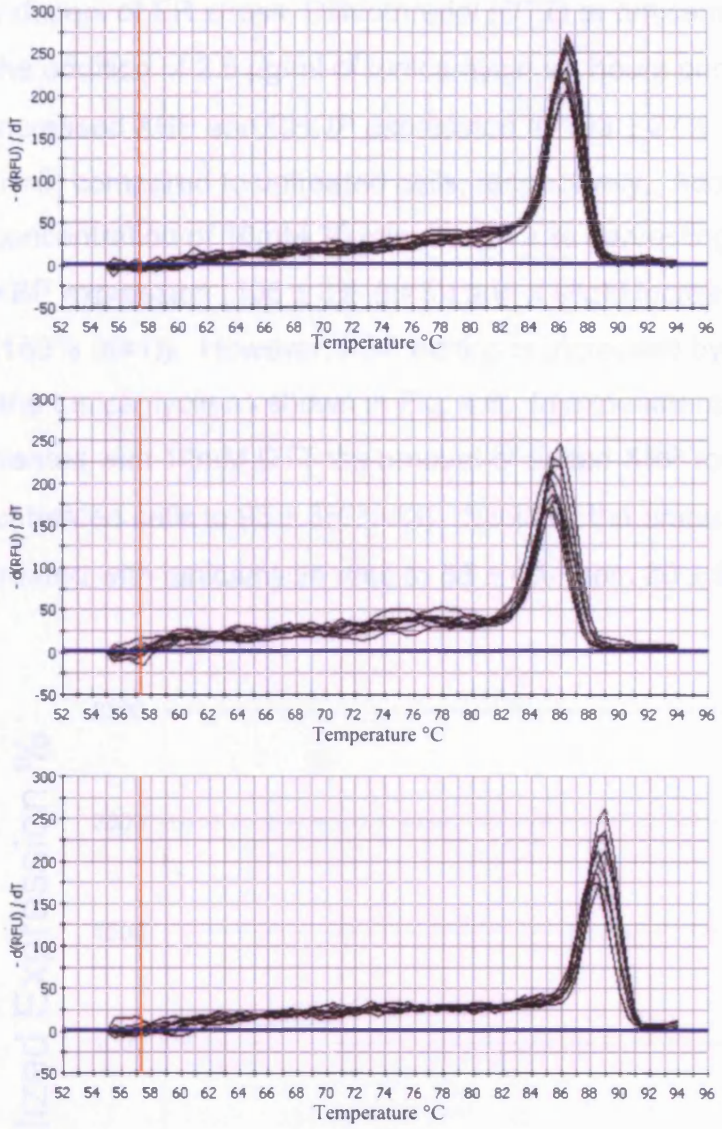

Fig. 4.6. Melt curves of the PCR products generated using the CHOP, $XBP_{(Total)}$ and $XBP_{(Unedited)}$ primer sets show specificity of the PCR products in each reaction. The PCR products obtained using the CHOP $XBP_{(Total)}$ and $XBP_{(Unedited)}$ primer pairs were heated from 54-94 °C in 80 steps increasing 0.5°C per step. The temperature at which there is the greatest change in fluorescence corresponds to the release of the SYBR dye and thus the melting of the PCR product.

4.4.4. Regulation of CHOP Expression and XBP Editing by the ER stress Inducers DTT and Tunicamycin

To confirm that the expression of CHOP and editing of XBP could be used as markers of ER stress in this system tsA-201 cells were treated with the

inducers of ER stress, Dithiothretiol (DTT) or tunicamycin. Fig. 4.7 shows that the addition of 2.5 μg/ml of tunicamycin six hours prior to harvesting RNA increased XBP and CHOP expression to 193 ± 27% (n=5) and 1620 ± 437% (n=5) compared to untreated cells, respectively. Addition of DTT to a final concentration of 10mM 30 minutes prior to harvesting produced no change in XBP expression (106 ± 3% (n=3)) and a slight increase in CHOP expression (163% (n=1)). However, XBP editing is increased by treatment with both DTT and tunicamycin as shown in Fig. 4.8. In experiments in which cells were treated with 10mM DTT the amount of edited XBP rose from 16 ± 6% in untreated cells to 95 ± 3% (n=3). Similarly the amount of edited XBP in cells treated with tunicamycin rose to 88 ± 4%, from 26 ± 9% in untreated cells (n=5).

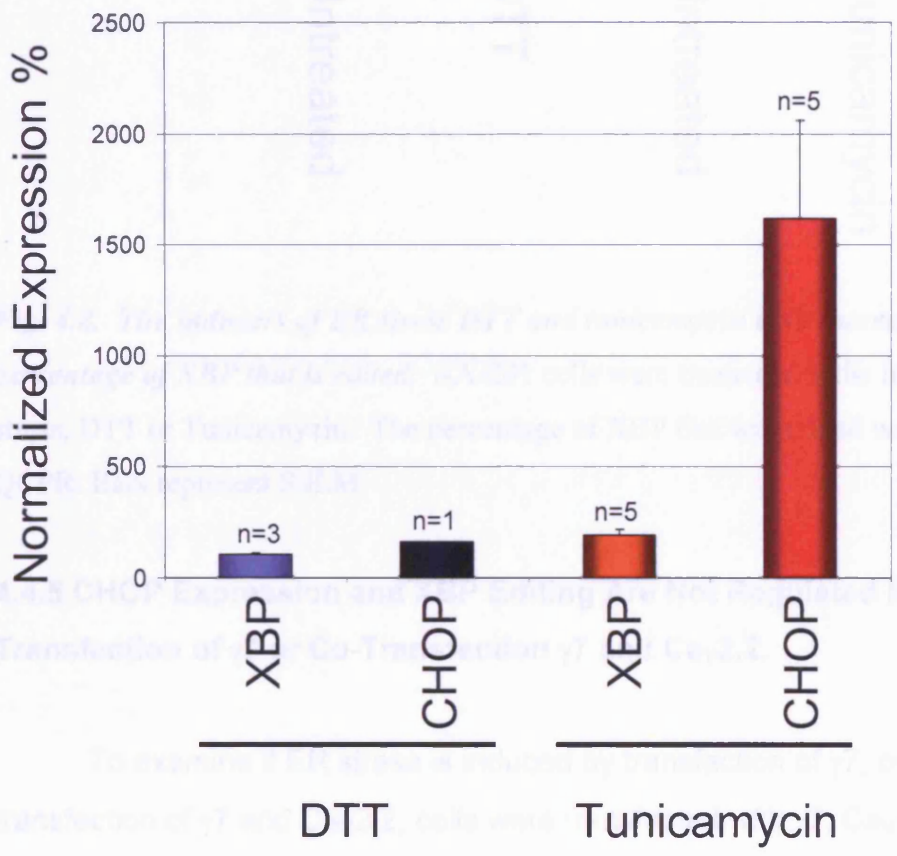

Fig. 4.7. XBP and CHOP levels during ER stress. tsA-201 cells were treated with the inducers of ER stress, DTT or Tunicamycin. The expression of XBP and CHOP were assessed by QPCR and normalized with respected to the expression measured in untreated cells. Where present bars represent S.E.M.

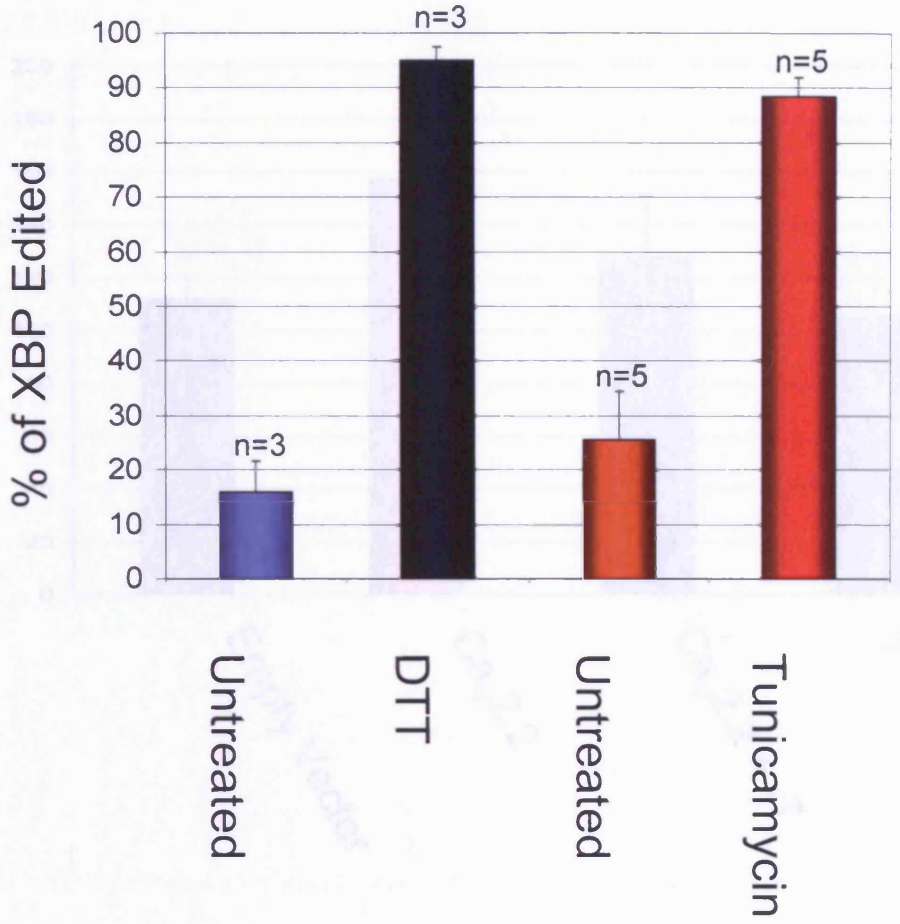

Fig. 4.8. The inducers of ER stress DTT and tunicamycin both increase the percentage of XBP that is edited. tsA-201 cells were treated with the inducers of ER stress, DTT or Tunicamycin. The percentage of XBP that was edited was assessed by QCPR. Bars represent S.E.M.

4.4.5 CHOP Expression and XBP Editing Are Not Regulated by Transfection of γ7 or Co-Transfection γ7 and $Ca_V2.2$.

To examine if ER stress is induced by transfection of γ7, or the co-transfection of γ7 and $Ca_V2.2$, cells were transfected with γ7, $Ca_V2.2$ (plus the auxiliary subunits β_1b and $\alpha_2\delta$-2), $Ca_V2.2$ (plus the auxiliary subunits β_1b and $\alpha_2\delta$-2) plus γ7, or as a control, empty pMT2 vector. After 24 hours mRNA was harvested from the cells and reverse transcribed. Expression of CHOP and XBP, were measured by QPCR. Fig 4.9 and Fig 4.10 show that neither CHOP nor XBP expression is regulated by the expression of $Ca_V2.2$, γ7 or $Ca_V2.2$ co-transfected with. γ7.

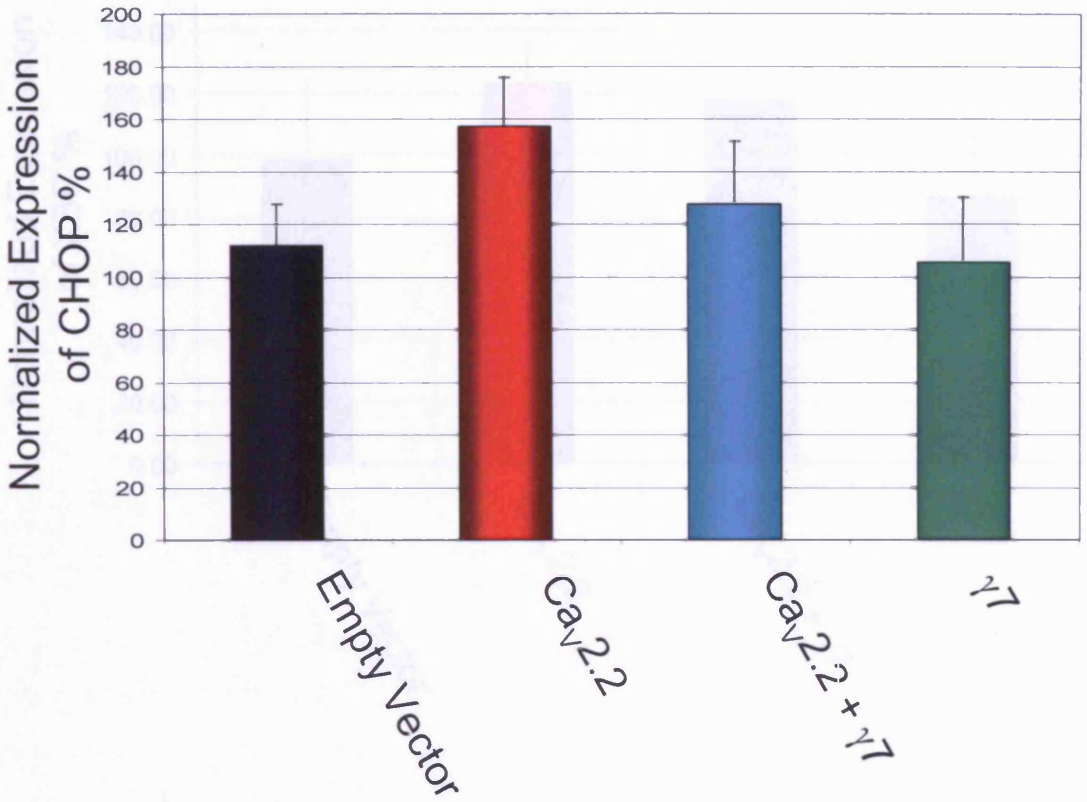

Fig. 4.9. CHOP expression is not increased by transient transfection of $Ca_V2.2$, γ7 or both $Ca_V2.2$ and γ7. tsA-201 cells were transiently transfected with $Ca_V2.2$, γ7 or $Ca_V2.2$ and γ7 co-transfected. Expression of the indicator of ER stress, CHOP, was assessed by QCPR and normalized by the expression measured in untreated cells. Bars represent S.E.M. (n = 5).

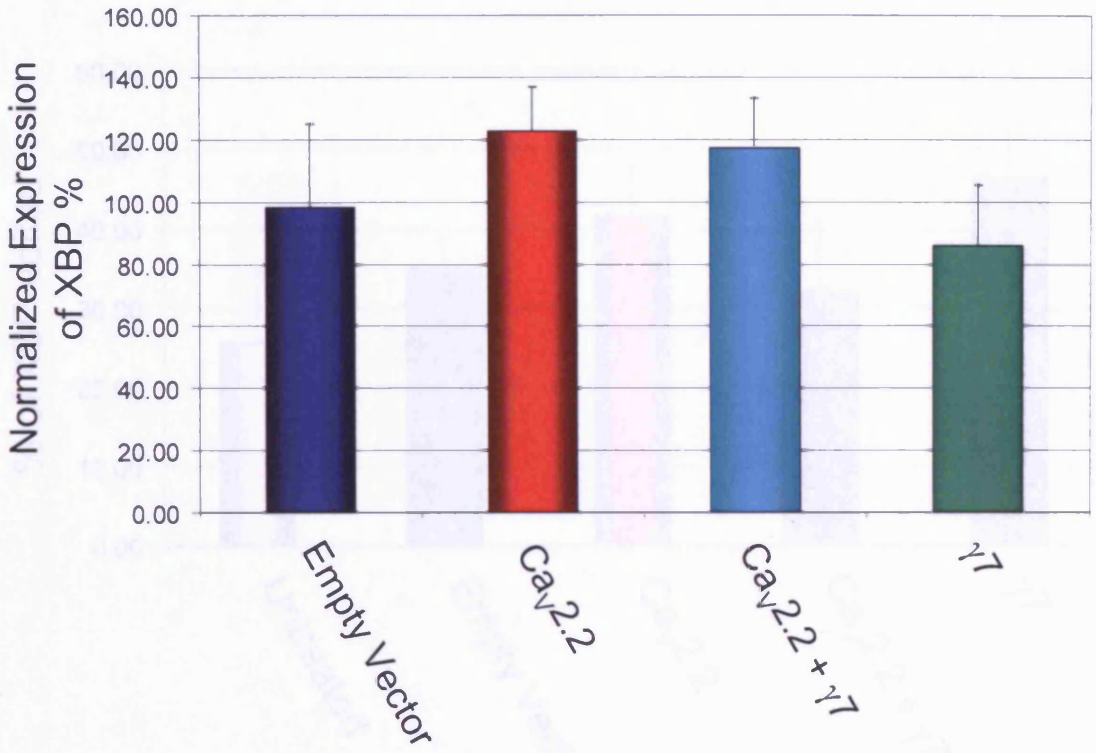

Fig. 4.10. XBP expression is not increased by transient transfection of $Ca_V2.2$, γ7 or both $Ca_V2.2$ and γ7. tsA-201 cells were transiently transfected with $Ca_V2.2$, γ7, or $Ca_V2.2$ and γ7 co-transfected. Expression of the indicator of ER stress, XBP, was assessed by QCPR and normalized by the expression measured in untreated cells. Bars represent S.E.M. (n =5)

A further indicator of ER stress, editing of XBP, was also examined using QPCR. XBP editing was not significantly increased when cells were transfected with $Ca_V2.2$ alone, or γ7 or with both $Ca_V2.2$ and γ7 (the highest p value obtained was 0.08 for untreated cells compared to γ7 transfected cells) (Fig 4.11).

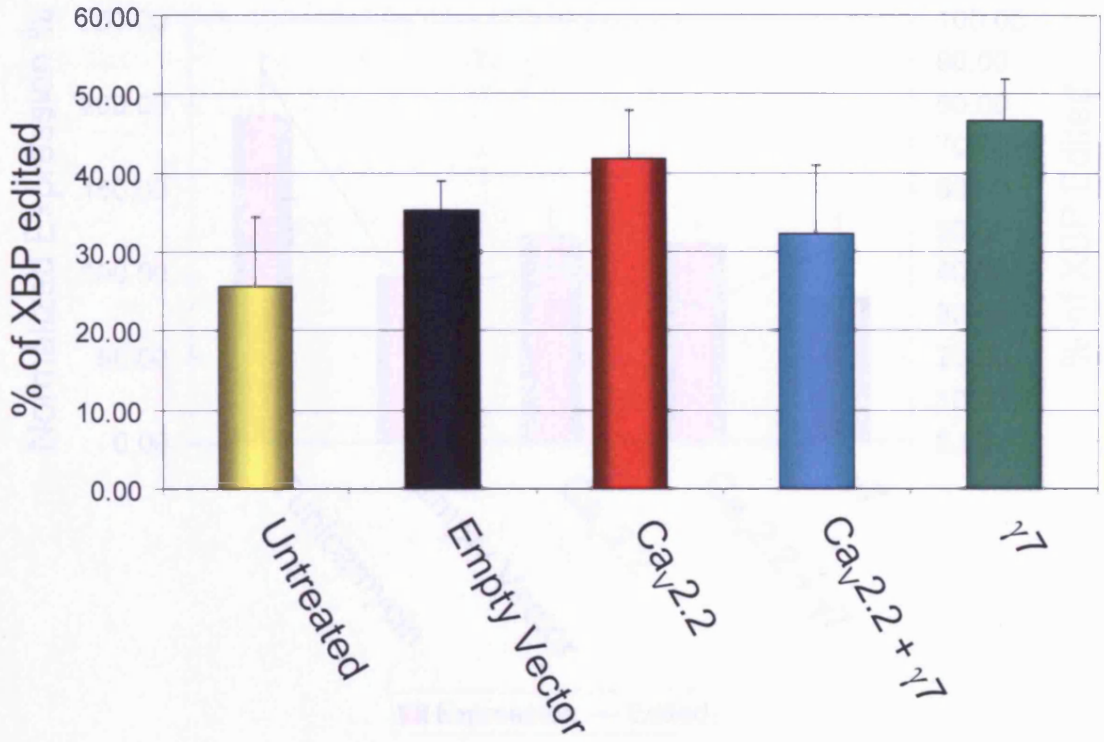

Fig. 4.11. XBP editing is not increased by transient transfection of $Ca_V2.2$, γ7 or both $Ca_V2.2$ and γ7 co-transfected. tsA-201 cells were transiently transfected with $Ca_V2.2$, γ7, or $Ca_V2.2$ and γ7. Editing of XBP, an indicator of ER stress, was assessed by QPCR. Bars represent S.E.M. (n = 5).

The level of XBP expression and the percentage of XBP editing are positively correlated with an R value of 0.84 in both transfected cells and cells treated with Tunicamycin, as a positive control (Fig. 4.12)

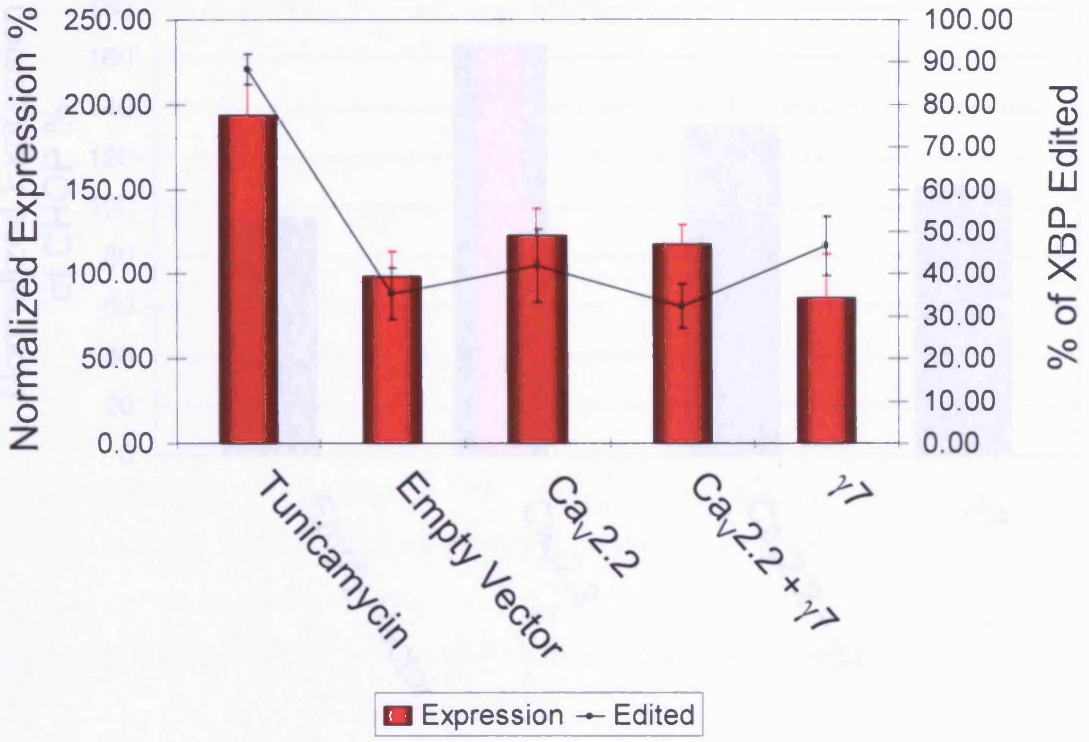

Fig. 4.12. Comparison of XBP expression and XBP Editing. XBP expression and XBP editing in cells transfected with $Ca_V2.2$, γ7, co-transfected with $Ca_V2.2$ and γ7, or treated with tunicamycin. Bars represent S.E.M. (n = 5).

It was possible that γ7 or γ7 co-transfected with $Ca_V2.2$ was inducing ER stress but that too few cells were transfected for the effect to be detected. To investigate this, the same experiment with the cells transfected using an Amaxa Nucleofector. Nucleofection gives a very high level of plasmid take up and protein expression. Once again, even with a very high rate of transfection, CHOP expression was not increased when transfected with γ7 or with $Ca_V2.2$ and γ7 (Fig 4.13). These values correlate well with the previous experiments with an R value of 0.95.

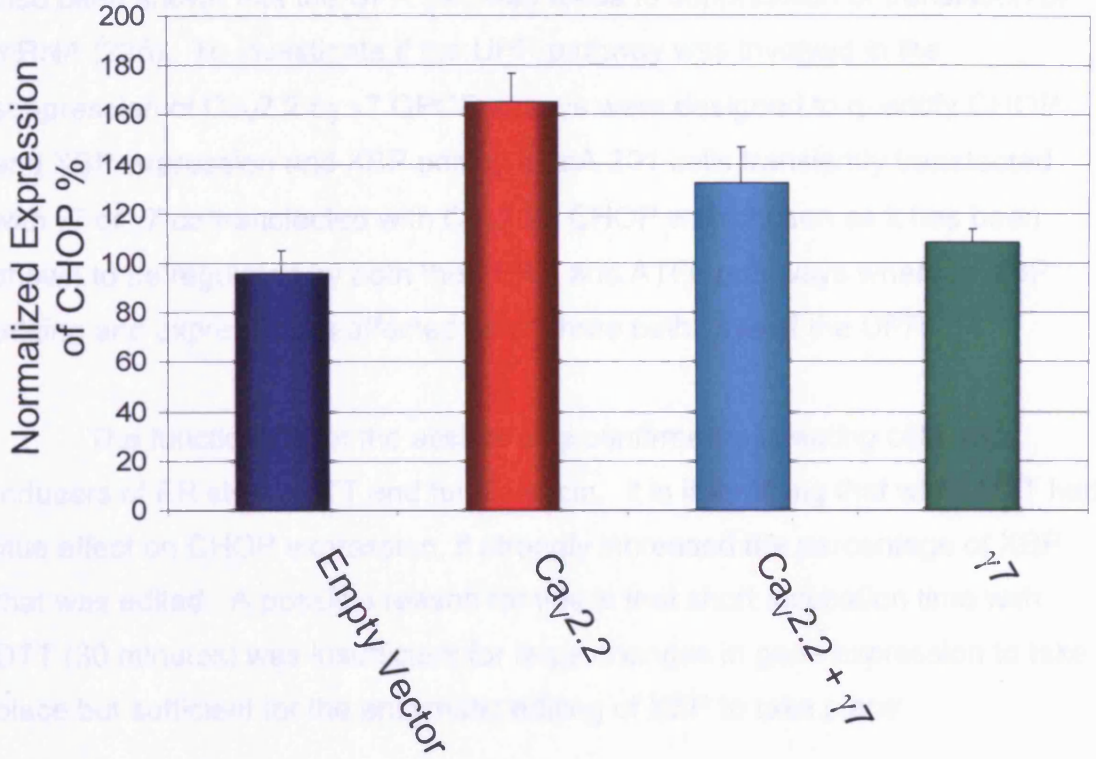

Fig. 4.13. CHOP expression is not increased in cells transfected by nucleofection of $Ca_V2.2$, γ7 or both $Ca_V2.2$ and γ7 co-nucleofected. tsA-201 cells were transiently transfected with $Ca_V2.2$, γ7 or $Ca_V2.2$ and γ7 co-transfected. Expression of the indicator of ER stress, CHOP, was assessed by QCPR. Bars represent range (n=2).

4.5. Discussion

The experiments using γ7_STOP, which produces γ7 mRNA that is not translated to γ7 protein, show that the production of γ7 mRNA alone is insufficient to cause a suppression of $Ca_V2.2$ expression. Therefore, the suppression of $Ca_V2.2$ expression by γ7 requires γ7 protein and is not due to an RNA-RNA interaction between $Ca_V2.2$ and γ7 mRNA. As promoter usage between γ7 and γ7_STOP should be identical these experiments also provide further evidence that the suppression of $Ca_V2.2$ is not due to promoter competition between plasmids.

Previous work by Page et al (238) has shown that suppression of $Ca_V2.2$ expression by truncated $Ca_V2.2$ expression involves the UPR pathway. It has

also been shown that the UPR pathway leads to suppression of translation of mRNA (225). To investigate if the UPR pathway was involved in the suppression of $Ca_V2.2$ by γ7 QPCR assays were designed to quantify CHOP and XBP expression and XBP editing in tsA-201 cells transiently transfected with γ7 or γ7 co-transfected with $Ca_V2.2$. CHOP was chosen as it has been shown to be regulated by both the PERK and ATF6 pathways whereas XBP editing and expression is affected by all three pathways of the UPR.

The functionality of the assays was confirmed by treating cells with inducers of ER stress DTT and tunicamycin. It is interesting that while DTT had little effect on CHOP expression, it strongly increased the percentage of XBP that was edited. A possible reason for this is that short incubation time with DTT (30 minutes) was insufficient for large changes in gene expression to take place but sufficient for the enzymatic editing of XBP to take place.

Transient transfection of tsA-201 cells with $Ca_V2.2$, plus auxiliary subunits, with or without γ7 or transfection with γ7 alone did not result in significant upregulation of expression of CHOP or XBP or increased editing of XBP. Despite the much higher rate of transfection, cells transfected by nucleofection also did not show a significant increase in CHOP expression with any of these combinations.

In both transiently transfected and nucleofected cells $Ca_V2.2$ expression resulted in a small, but not significant, increase in CHOP expression. While neither of these results was statistically significant when taken alone, together they suggest that overexpression of $Ca_V2.2$ cause significant stress upon the ER. This is perhaps to be expected as calcium channels are large multi-transmembrane, multi-subunits proteins. It may be that γ7, by reducing $Ca_V2.2$ expression, reduces the stress upon the ER, but in no case was there a significant reduction compared to $Ca_V2.2$ alone.

These results suggest that the UPR pathway is not induced and that this pathway is not involved in the suppression of $Ca_V2.2$ expression by γ7. Therefore, while the observed effects on $Ca_V2.2$ expression by the co-

transfection of γ7 are similar to those of co-transfection of truncated $Ca_V2.2$ constructs the mechanism of their action appears to be different.

Chapter 5 - γ7 and PC12 cells

5.1. Introduction

5.1.1. Generation of the PC12 Cell Line

The PC12 cell line was generated by Greene and Tischler from a transplantable rat adrenal pheochromocytoma (neuroendocrine tumours of adrenal chromaffin cells) line (241). It is a clonal line which upon treatment with NGF undergoes mitotic arrest and begins to put out branching processes similar to those seen in sympathetic neurons. This change in morphology is accompanied by a change in biochemistry to resemble neuronal cells. These properties have made PC12 cells a useful model system for the study of neural differentiation (242)

5.1.2. Voltage-Dependent Calcium Channels in PC12 Cells

PC12 cells have been shown to express N- L- P- and T-type currents (243-246). Differentiation induced by treatment with NGF leads to an increase in N-type current (243). This increase in N-type current has been shown to be accompanied by an increase in $Ca_V2.2$ mRNA (247;248).

5.2. Aims

The aims of the work described in this chapter were firstly to investigate if $\gamma7$ suppressed the expression of endogenous $Ca_V2.2$ in differentiating PC12 cells and secondly to investigate the endogenous expression of $\gamma7$ in PC12 cells.

5.3. Additional Methods

Experiments were performed as described in Chapter 2 with the following differences and additions.

5.3.1. QPCR

PC12 cells were cultured as described in Methods. NGF was applied at 100 ng/ml and every second day medium was removed and replaced with NGF containing media. RNA was harvested after seven days of treatment with NGF. Primer pairs $\gamma7_{(QPCR)}$, $Ca_V2.2_{(QPCR)}$ and $Ca_V1.2_{(QPCR)}$ are detailed in the Appendix (A.3.2.). Preliminary experiments were performed to define the optimum PCR conditions for each primer pair and accordingly step two of the second PCR cycle was set to temperatures of 56.7°C, 53°C and 53°C for primer pairs for $\gamma7_{(QPCR)}$, $Ca_V2.2_{(QPCR)}$ and $Ca_V1.2_{(QPCR)}$, respectively. Significance was determined using a one-sampled t-test.

5.3.2. RT-PCR

Primer pairs $\gamma1_{(Rat)}$, $\gamma2_{(Rat)}$, $\gamma4_{(Rat)}$, $\gamma6_{(Rat)}$, $\gamma7_{(Rat)}$, and $Actin_{(Rat)}$ are detailed in the Appendix (A.3.2). cDNA libraries were generated from undifferentiated PC12 cells.

5.3.3. Immunocytochemistry

In experiments with differentiated PC12 cells, actin was visualised by incubating the cells for 20 minutes at room temperature with 6.6 µM TexasRed–phalloidin. All cells were examined on a Leica TCS SP confocal laser scanning microscope. Photomultiplier settings were kept constant in each experiment. All images shown are single 0.5 µm sections through the cell. Anti-$\gamma7_{(Tail)}$ Anti- and $\gamma7_{(Loop)}$ antibodies were used at 0.8 µg/ml

5.3.4. Western Blotting

PC12 cells were taken up in PBS plus Complete™ protease inhibitors. Cells were lysed on ice by sonication for 3 x 10s second bursts. Unlysed cells and other material were removed by centrifugation at 3,000 x g for 3 minutes. The supernatant was decanted and spun at 50,000 x g for 4 hrs (4°C). The pellet was taken up in PBS plus Complete™ protease inhibitors and the protein

concentration determined by BCA assay. 200 μg of protein (along with 30 μg of whole cell lysate from γ7 transiently transfected tsA-201 cells) were run on NuPAGE 4-12% Bis-Tris gels. Western blotting was then performed with the anti-$\gamma7_{(Tail)}$ antibody at 0.4 μg/ml.

5.4. Results

5.4.1. Transient Transfection of γ7 into Undifferentiated PC12 Cells Does Not Suppress N-type Current Through $Ca_V2.2$ After Differentiation

NGF-induced differentiation of PC12 cells is accompanied by an increase of N-type current through $Ca_V2.2$ channels after about 3 days. It was hypothesised that transient transfection of γ7 into undifferentiated cells might inhibit $Ca_V2.2$ expression, thus preventing expression of N-type current in differentiated cells. To test this hypothesis PC12 cells were transiently transfected with γ7 and then differentiated by application of 100 ng/ml NGF. N-type current was recorded from cells five to seven days post transfection and subsequent treatment with NGF. These experiments were performed by Dr J. Leroy and are detailed are in Appendix (A.4.4. Fig. A.3.). Briefly, transient transfection with γ7 did not suppress the expression of N-type current in differentiated PC12 cells.

5.4.2. Suppression of $Ca_V2.2$ Expression by γ7 Still Occurs in Transiently Transfected PC12 cells.

As transient transfection of γ7 did not suppress endogenous N-type current in differentiated PC12 cells it was hypothesised that there may be a component which is endogenously expressed in PC12 cells, but not tsA-201 cells, COS7 cells or *Xenopus* oocytes, that prevented this effect of γ7. PC12 cells were transiently transfected with $Ca_V2.2$ and auxiliary subunits with or without γ7. Three days post transfection N-type current was recorded. These experiments were performed by Dr J. Leroy and are detailed in the Appendix (A.4.4. Fig. A.3.). Briefly, as in other cell types, N-type current through

transiently transfected $Ca_V2.2$ channels was suppressed by co-transfection with γ7.

5.4.3. γ7 is Endogenously Expressed in PC12 Cells

Previous work has shown that transient transfection of γ7 into SCG cells results in an altered morphology of the cell (174). Processes put out by SCG cells transiently transfected with γ7 were much finer than those of untransfected controls. Experiments were performed to examine if transient transfection with γ7 would also alter the morphology of PC12 cells. Although there were no obvious changes in morphology in PC12 transfected with γ7 compared to untransfected cells, it was observed that all PC12 cells were reactive to the $\gamma7_{(Tail)}$ antibody. γ7 was detected in both undifferentiated cells (Fig 5.1.A) and differentiated cells (Fig. 5.1.B).

In both differentiated and undifferentiated PC12 cells γ7 was found throughout the cell without the perinuclear concentration seen in transiently transfected cells. In differentiated cells γ7 was found along the process and appeared to localise with actin at the ends of the processes (Fig 5.1 B. Arrows). A similar spatial organization was observed when γ7 was detected with the $\gamma7_{(Loop)}$ antibody (Fig. 5.1 C).

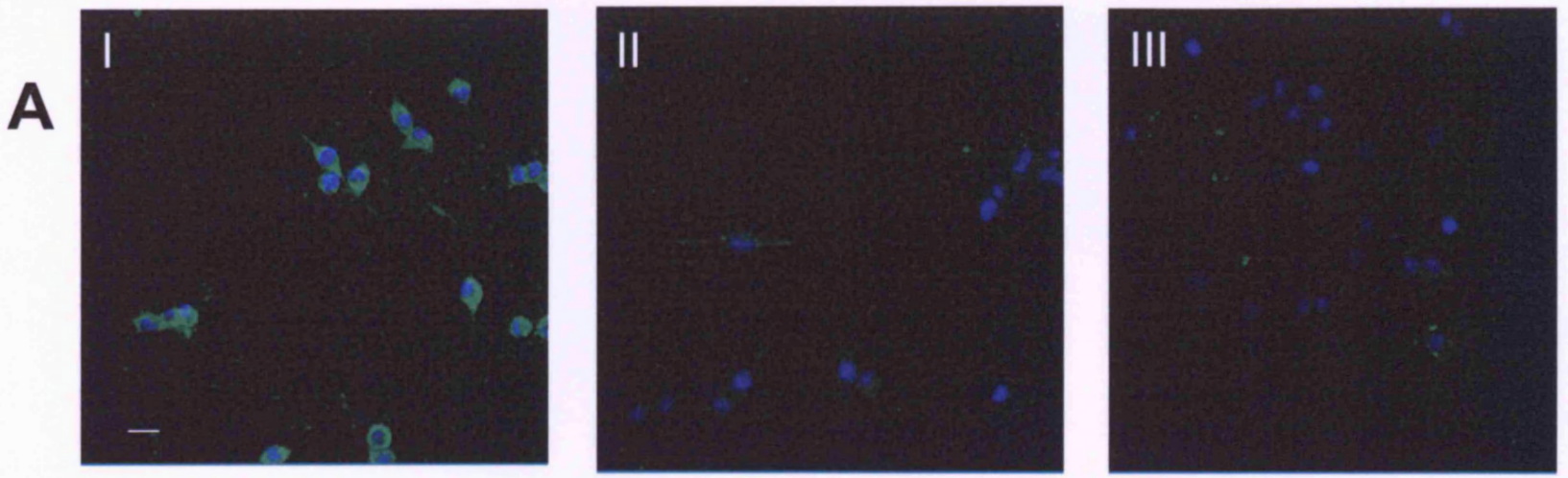
A
I
II
III

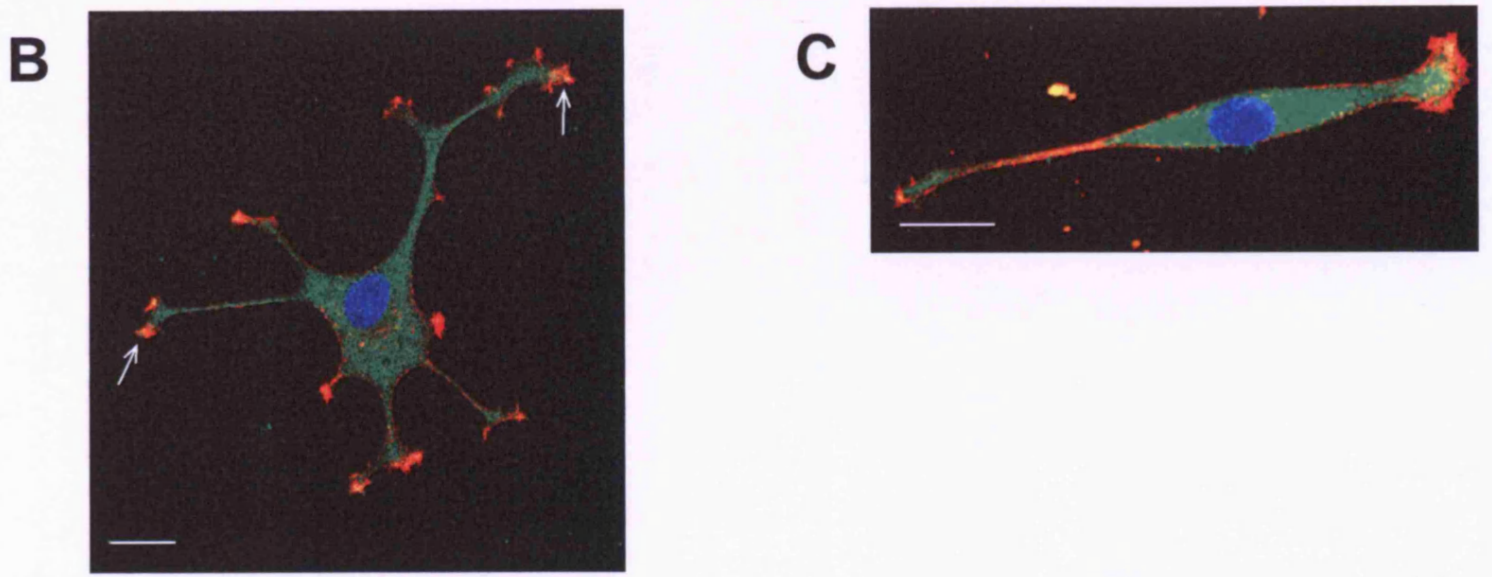

Fig. 5.1. γ7 is endogenously expressed in both undifferentiated and differentiated PC12 cells. Immunofluorescence for γ7 (green) was detected in undifferentiated (A I) and differentiated (B) PC12 cells. Immunofluorescence for γ7 was not detected if the γ7 antibody was pre-incubated with a 10-fold molar excess of the peptide it was raised against (A II) or when the γ7 antibody was omitted (A III). Co-location of γ7 and actin (red) at the ends of process is indicated by arrows. C) Expression was also detected with and antibody raised against a different epitope in γ7. The nuclear stain DAPI (blue) was used as a marker in all experiments. Texas-Red phalloidin was used to reveal F-actin in experiments B and C. Scale bar = 20 μm

To confirm expression of γ7 in PC12 cells RT-PCR with primer pairs for γ7 was performed on a cDNA library generated from undifferentiated PC12 cells (Fig. 5.2.A). A band of the expected size of 828 bp for γ7 was obtained. This band was confirmed to be γ7 by DNA sequencing. PC12 cells from an alternative source were also tested using RT-PCR and were found to express γ7. Western blotting with the $\gamma7_{(Tail)}$ with cell lysate from undifferentiated PC12 cells detected a faint band of the same molecular weight as γ7 transiently expressed in tsA-201 cells (Fig. 5.2 B).

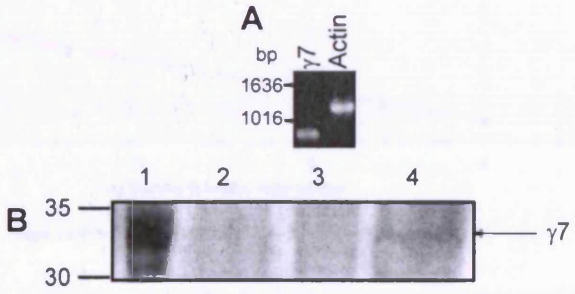

Fig. 5.2 RT-PCR and western blotting confirm endogenous expression of γ7 in undifferentiated PC12 cells. A) RTPCR of γ7 from a cDNA library generated from undifferentiated PC12 cells. Primers for actin were used as a positive control. B) Extracts from tsA-201 cells transiently transfected with γ7 (1) and undifferentiated PC12 cells. PC12 cells were sonicated and insoluble material (2) removed by centrifugation. The resulting supernatant was centrifuged at 50,000 x g for 4 hours and samples of the supernatant (3) and pellet (4) taken. All samples were western blotted with the $\gamma7_{(Tail)}$ antibody.

5.4.4. γ7 expression Does Not Significantly Change After Treatment of Cells with NGF

To examine if expression of γ7 in PC12 cells changed in response to NGF treatment, QPCR was performed using primer pairs to γ7. Expression of γ7 in PC12 cells after seven days treatment with NGF was compared to untreated cells. $Ca_V1.2$ and $Ca_V2.2$ expression were used as controls. Previous work by Colston *et al* (248) had shown a slight increase in $Ca_V2.2$ and a decrease in $Ca_V1.2$ expression in PC12 in response to NGF. Primer pairs for

$Ca_V1.2$, $Ca_V2.2$ and $\gamma7$ were tested to ensure that they were of sufficient efficiency for QPCR (Fig 5.3).

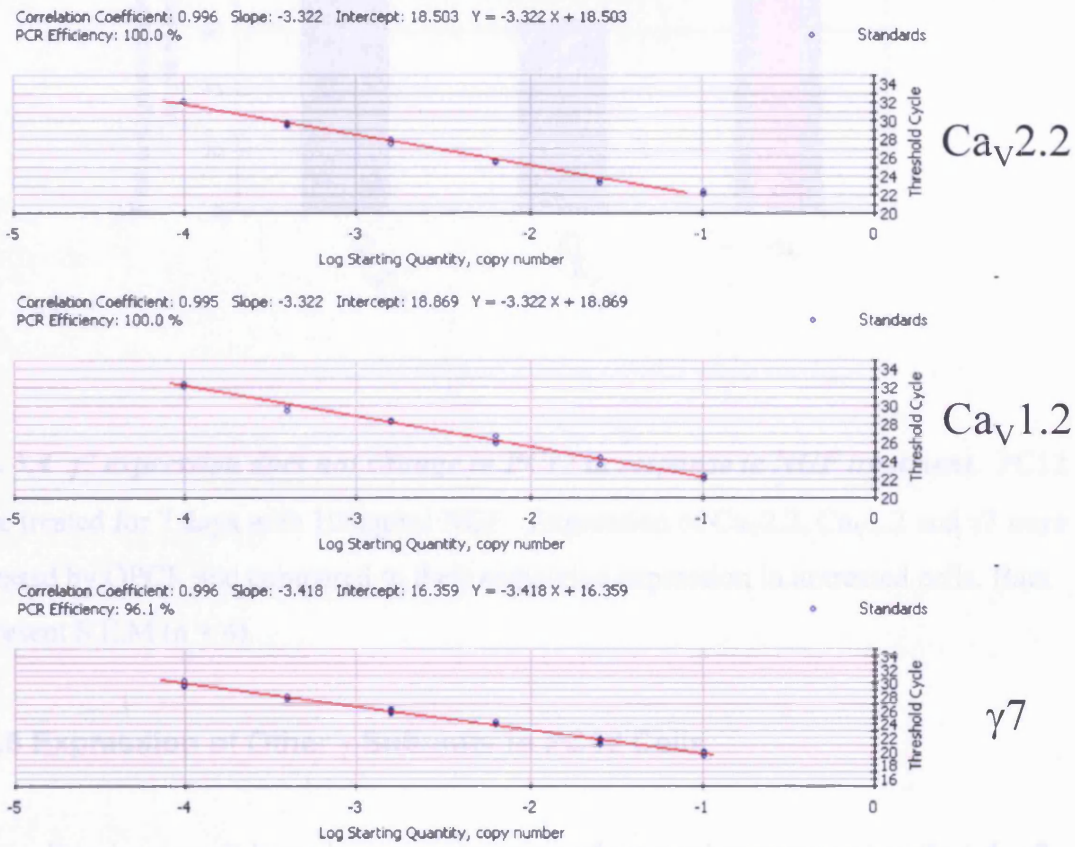

Fig. 5.3. PCR reactions using primer sets $Ca_V2.2_{(QPCR)}$, $Ca_V1.2_{(QPCR)}$ and $\gamma7_{(QPCR)}$ are of high efficiency and can be used for QPCR.. A cDNA library derived from mRNA from undifferentiated PC12 cells was serially diluted and PCR performed using the $Ca_V2.2_{(QPCR)}$, $Ca_V1.2_{(QPCR)}$ and $\gamma7_{(QPCR)}$ primer sets to obtain the PCR efficiency for each primer set.

As previously reported, exposure to NGF for seven days evoked a significant decrease of $Ca_V1.2$ expression (248). However, neither expression of $\gamma7$ nor $Ca_V2.2$ was affected.

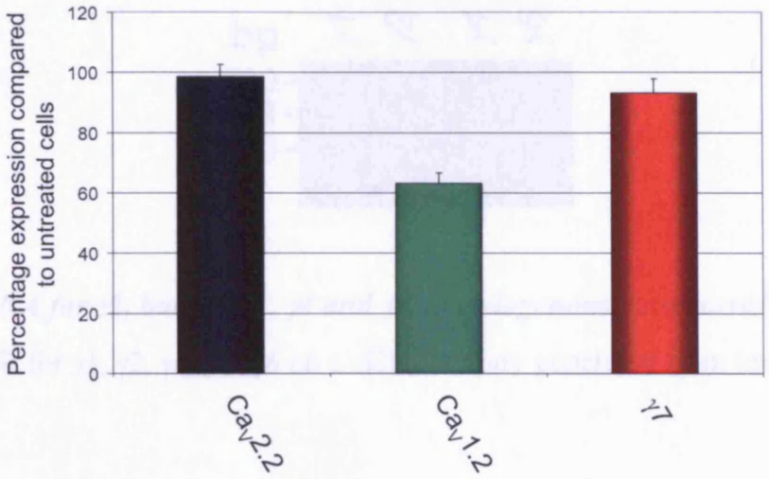

Fig. 5.4 γ7 expression does not change in PC12 in response to NGF treatment. PC12 were treated for 7 days with 100ng/ml NGF. Expression of $Ca_V2.2$, $Ca_V1.2$ and γ7 were assessed by QPCR and compared to their respective expression in untreated cells. Bars represent S.E.M (n = 4).

5.4.5 Expression of Other γ Subunits in PC12 Cells

Previous work has shown expression of several gamma subunits (γ1, γ2, γ4, γ6 and γ7) in the adrenal gland (173). RT-PCR was used to examine if any other γ subunits found in the adrenal gland, in addition to γ7, were expressed in PC12 cells. Primer pairs were designed to detect γ1, γ2, γ4 and γ6 giving bands of 95, 114, 131 and 76 bp respectively. RT-PCR using these primer pairs on a cDNA library generated from undifferentiated PC12 detected γ2 but not γ1, γ4 or γ6 (Fig 5.5).

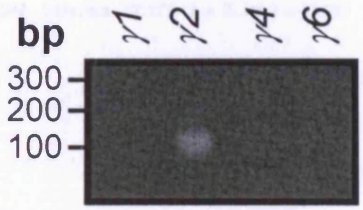

Fig. 5.5. mRNA for γ2, but not γ1, γ4 and γ6, is endogenously expressed in PC12 cells. RT-PCR for γ1, γ2, γ4 and γ6 on a cDNA library generated from undifferentiated PC12 cells.

To investigate if γ2 expression in PC12 cells changed upon treatment with NGF QPCR was performed on the cDNA libraries from undifferentiated and NGF treated cells generated previously. The primer pair for γ2 was tested and found to be suitable for QPCR (Fig. 5.6.A). Preliminary experiments showed a reduced expression of γ2 in NGF differentiated PC12 cells, but the effect was not statistically significantly ($p = 0.06$)(Fig. 5.6.B). Further experiments would need to be performed to confirm this result.

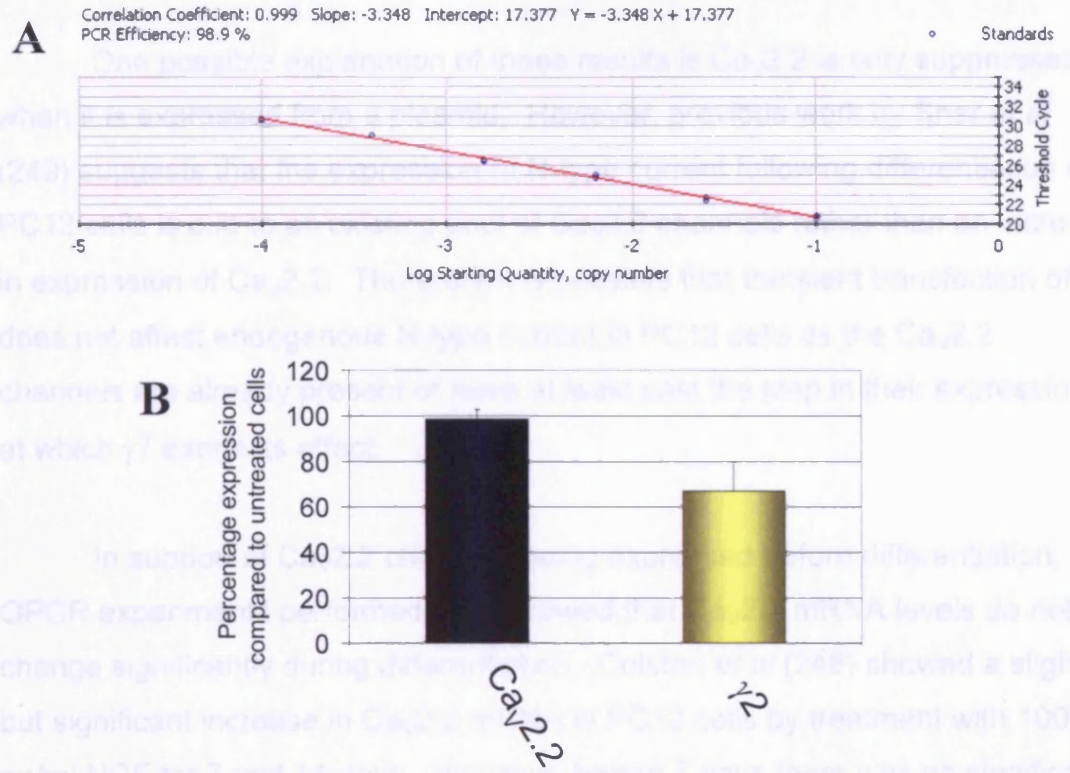

Fig. 5.6. Effect of NGF treatment on γ2 expression in PC12 cells A) Efficiency of PCR using the γ2 primer pair is sufficient for QPCR. B) PC12 were treated for 7 days with 100ng/ml NGF. Expression of γ2 was accessed by QPCR and compared to its expression in untreated cells. $Ca_V2.2$ expression obtained previously is shown as a comparison. Error bars represent S.E.M. (n = 4).

5.5. Discussion

Transient transfection of γ7 into undifferentiated PC12 cells did not suppress the expression of N-type current through $Ca_V2.2$ channels upon differentiation. However, in undifferentiated PC12 cells expression, of transiently transfected $Ca_V2.2$ was still suppressed by co-transfection of γ7. This would suggest that the failure of transfected γ7 to suppress expression of endogenous $Ca_V2.2$ is not due to another factor expressed in PC12 cells. A result similar to the present finding in differentiated PC12 cells was reported by Moss *et al* who showed that transient transfection of primary sympathetic neurons with γ7 did not suppress N-type current through $Ca_V2.2$ channels (174).

One possible explanation of these results is $Ca_V2.2$ is only suppressed when it is expressed from a plasmid. However, previous work by Sher *et al* (249) suggests that the expression of N-type current following differentiation of PC12 cells is due to an existing pool of $Ca_V2.2$ channels rather than an increase in expression of $Ca_V2.2$. Therefore it is possible that transient transfection of γ7 does not affect endogenous N-type current in PC12 cells as the $Ca_V2.2$ channels are already present or have at least past the step in their expression at which γ7 exerts its effect.

In support of $Ca_V2.2$ channels being expressed before differentiation, QPCR experiments performed here showed that $Ca_V2.2$ mRNA levels do not change significantly during differentiation. Colston *et al* (248) showed a slight but significant increase in $Ca_V2.2$ mRNA in PC12 cells by treatment with 100 ng/ml NGF for 7 and 14 days. However, before 7 days there was no significant difference in $Ca_V2.2$ mRNA. The differences seen between those experiments and those performed here could be explained by the sensitivity of using real time QPCR compared to measuring ethidium bromide binding used by Colston *et al* or due to the differences between PC12 cells from different sources. The larger and more significant decrease of $Ca_V1.2$ expression was detected in both sets of experiments.

If γ7 acts as a regulator of $Ca_V2.2$ expression then it would be expected that NGF treatment would reduce γ7 expression as N-type current through $Ca_V2.2$ channels increased. However, there was no significant change in the mRNA level of endogenous γ7 in NGF-treated cells compared to untreated cells.

γ7 is endogenously expressed in PC12 cells. It was detected at a mRNA level by RTPCR and at protein level by immunocytochemistry and western blotting. γ7 has been shown to be mainly neuronal (174) but has also been found at the mRNA level in a range of tissues (171;173). The adrenal gland, from which PC12 cells are derived, has been to shown express γ1, γ2, γ4, γ6 and γ7 (173). In addition to γ7, γ2 was also found in PC12 cells. The presence

of γ2, shown to be a TARP, in PC12 is surprising as PC12 cells have been shown not to express glutamate receptors of the AMPA type, although they do express NMDA type glutamate receptors (250).

Chapter 6 – The C-terminus of γ7

6.1. Introduction

Multi-subunit proteins require the correct folding and stoichiometry of the individual subunits to function correctly. One of the ways in which the cell prevents individual subunits from leaving the ER before they assemble correctly is by the use of RXR motifs. RXR motifs were first discovered by Zerangue *et al* (251). They showed that an RXR motif was involved at multiple stages of the assembly of the ion channel K_{ATP} and restricted surface expression to fully assembled and correctly regulated channels.

The presence of a RXR motif in the subunit resulted in the immature K_{ATP} subunits being retained within the ER in the absence an auxiliary subunit. Mutation of the RXR motif to alanines resulted in surface expression of the subunit even in the absence of an auxiliary subunit. Furthermore, addition of the RXR motif to IRK1, another potassium channel that is normally trafficked to the cell surface, resulted in this protein being retained within the ER. Further work by Ma *et al* went on to confirm the importance of RXR motifs in the regulation of surface potassium channel numbers (252;253).

RXR motifs are located cytoplasmically and it is believed that when they are exposed the protein is retained within the ER. Upon the correct assembly of the multi-subunit complex the RXR motif is masked allowing the protein complex to leave the ER.

RXR motifs have also been shown to be important in the regulation of trafficking of other proteins to the plasma membrane including GABA(B), kainite, $5HT_3$ and NMDA receptors (253;254).

6.2. Aims

The aims of this study were to investigate if RXR motifs, present in the C-terminal tail of γ7, are involved in the knockdown of $Ca_V2.2$ expression. To do this a series of truncated γ7 mutations were made and their effect on $Ca_V2.2$

expression measured by western blotting. The effect of the C-terminal tail of γ7 alone on $Ca_V2.2$ expression was also investigated.

6.3. Additional Methods

Experiments were performed as described in Chapter 2 with the following differences and additions.

6.3.1. Generation of Constructs

$\gamma7_{(1-217)}$, $\gamma7_{(1-238)}$, $\gamma7_{(1-271)}$, $\gamma7_{(201-275)}$, $\gamma7_{(201-275)}$ _HA, γ2TM γ7Tail and γ7_PDZ were made by standard molecular biological techniques using the primer pairs detailed in the Appendix (A.3.1). All constructs used in these experiments were subcloned into the pMT2 expression vector.

6.3.2. Western blotting

To determine the level of expression of the truncated γ7 constructs they were transfected into tsA-201 cells and three days post transfection cells were harvested and taken up in 200 µl of SDS buffer. Samples were then sonicated briefly (3 10 second pulses, on ice) and heated to 70°C for 10 minutes. A 15 µl aliquot of each sample was separated on 4-12% Bis-Tris gels using MES running buffer. Using MES as a running buffer provides better resolution of lower molecular weight proteins. SigmaMarker™LowRange makers were used. Anti-$\gamma7_{(Loop)}$ and anti- $\gamma7_{(Tail)}$ antibodies were both used at 1 µg/ml.

In quantification of $Ca_V2.2$ expression by western blotting experiments, 4-12% Tris-Glycine gels, which provide better resolution and more favourable transfer conditions, were used instead of 4-12% Bis-Tris gels. Transfer conditions of 25V and 400 mA (current limiting) for 1 hour were used. An antibody to $Ca_V2.2$ was used as the primary antibody at a concentration of 1.2µg/ml. Quantitative analysis of western blots was performed using ImageQuant software. The intensity of the $Ca_V2.2$ band from cells co-transfected with a γ7 construct was measured and given as a percentage of the

intensity of the band obtained for cells transfected with $Ca_V2.2$ and empty vector. Significance was determined by a one sample t-test.

6.3.3. Imaging

In sub-cellular localisation experiments cells were examined on a Leica TCS SP confocal scanning laser microscope. Photomultiplier settings were kept constant in each experiment and all images were scanned sequentially. All images shown are single 0.5 μm optical sections through the cell. Anti-$\gamma7_{(Loop)}$ was used at 0.8 μg/ml.

6.4. Results

6.4.1. Expression of Truncated γ7 Subunits

The C-terminal region of γ7 contains two putative ER retention motifs RPR (218-220) and RGR (239-241). To investigate if these were involved in the knockdown of $Ca_V2.2$ expression, two truncated γ7 constructs were made. Primers were designed to replace either R218 or R239 with a stop codon to give $\gamma7_{(1-217)}$ and $\gamma7_{(1-238)}$ respectively. A third truncated γ7 construct $\gamma7_{(1-271)}$ was also made in which the last four amino acids were deleted. It has been hypothesised that these four amino acids may be similar to a PDZ binding motif shown to be important in TARPs (177). These three constructs are shown diagrammatically in Fig. 6.1. and their expression confirmed by western blotting (Fig. 6.2.) using antibodies raised against epitopes in either the predicted extracellular loop ($\gamma7_{(Loop)}$) or the C-terminal tail ($\gamma7_{(Tail)}$) as appropriate.

1 MSHCSSRALT LLSSVFGACG LLLVGIAVST DYWLYMEEGT VLPQNQTTEV

51 KMALHAGLWR VCFFAGREKG RCVASEYFLE PEINLVTENT ENILKTVRTA

101 TPFPMVSLFL VFTAFVISNI GHIRPQRTIL AFVSGIFFIL SGLSLVVGLV

151 LYISSINDEV MNRPSSSEQY FHYRYGWSFA FAASSFLLKE GAGVMSVYLF

201 TKRYAEEEMY RPHPAFY**RPR** LSDCSDYSGQ FLQPEAWR**RG R**SPSDISSDV

251 SIQMTQNYPP AIKYPDHLHI STSPC

Fig. 6.1. Diagrammatic representation of truncated γ7 constructs. Putative RXR motifs are highlighted in bold. $\gamma7_{(1\text{-}217)}$ is underlined in green, $\gamma7_{(1\text{-}238)}$ underlined in yellow and $\gamma7_{(1\text{-}271)}$ underlined in orange. $\gamma7_{(201\text{-}275)}$ is underlined in light blue. In γ7_PDZ the last 4 amino acids were mutated from TSPC to TTPV.

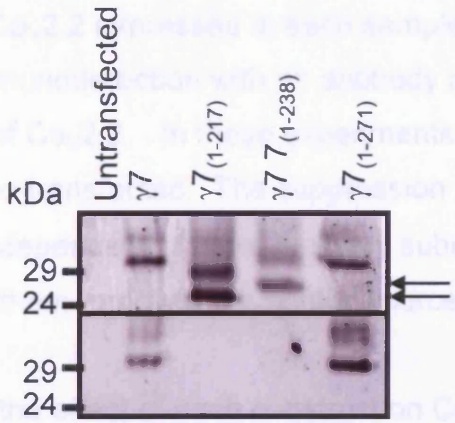

Fig. 6.2. Western blotting and immunodetection of truncated γ7 constructs. γ7 and truncated γ7 constructs were expressed in tsA-201 cells. Three days post transfection cells were harvested and whole cell lysate separated by SDS PAGE. Upper panel: Immunodetection using the $\gamma7_{(Loop)}$ antibody. The upper arrow indicates $\gamma7_{(1\text{-}238)}$ and the lower arrow indicates $\gamma7_{(1\text{-}217)}$. Lower panel: Immunodetection using the $\gamma7_{(Tail)}$ antibody.

All constructs appear as doublets with the majority of the protein being found in the lower of the two bands. This band corresponds to the expected molecular weight of each protein, assuming the protein is unmodified (γ7, $\gamma7_{(1\text{-}}$

$_{217)}$, $\gamma7_{(1\text{-}238)}$ and $\gamma7_{(1\text{-}271)}$ are 31kDa, 24 kDa, 27 kDa and 31kDa respectively). The upper band seen may be the glycosylated form of each protein. $\gamma7_{(1\text{-}217)}$ and $\gamma7_{(1\text{-}238)}$ lack the epitope to which the C-terminal antibody was raised and are consequently not detected with the $\gamma7_{(Tail)}$ antibody.

6.4.2. Removal of the C-terminal Region of γ7 Negates the Knockdown of $Ca_V2.2$ Expression

COS7 cells were transiently transfected with $Ca_V2.2$, co-transfected with either empty pMT2 or full length γ7 or one of the truncated γ7 constructs. In control experiments the non-related six transmembrane domain voltage-dependant potassium channel ($K_V3.1b$) replaced a γ7 construct. Three days post transfection the cells were harvested, total protein concentration was measured by BCA assay and all samples were standardised to a protein concentration of 1.67 µg/µl. 30 µg of each sample was separated by SDS PAGE. The amount of $Ca_V2.2$ expressed in each sample was estimated by Western blotting and immunodetection with an antibody raised against an epitope in the II-III loop of $Ca_V2.2$. In these experiments no auxiliary calcium channel subunits were co-transfected. The suppression of $Ca_V2.2$ expression by γ7 was found to be independent of other auxiliary subunits (as shown in Chapter 3) and omitting them removes a potential source of variation.

Example blots of the effect of each construct on $Ca_V2.2$ expression are shown in Fig. 6.3. A. $Ca_V2.2$ was detected as a discrete band just above the 205 kDa marker ($Ca_V2.2$ expected molecular weight 261 kDa). The intensities of the bands representing $Ca_V2.2$ in both control and experimental lanes were measured using ImageQuant. In each experiment $Ca_V2.2$ co-transfected with empty pMT2 was designated as100% and $Ca_V2.2$ co-transfected with other constructs given as a corresponding percentage. The mean data from 5 to 12 experiments is given in Fig. 6.3.B.

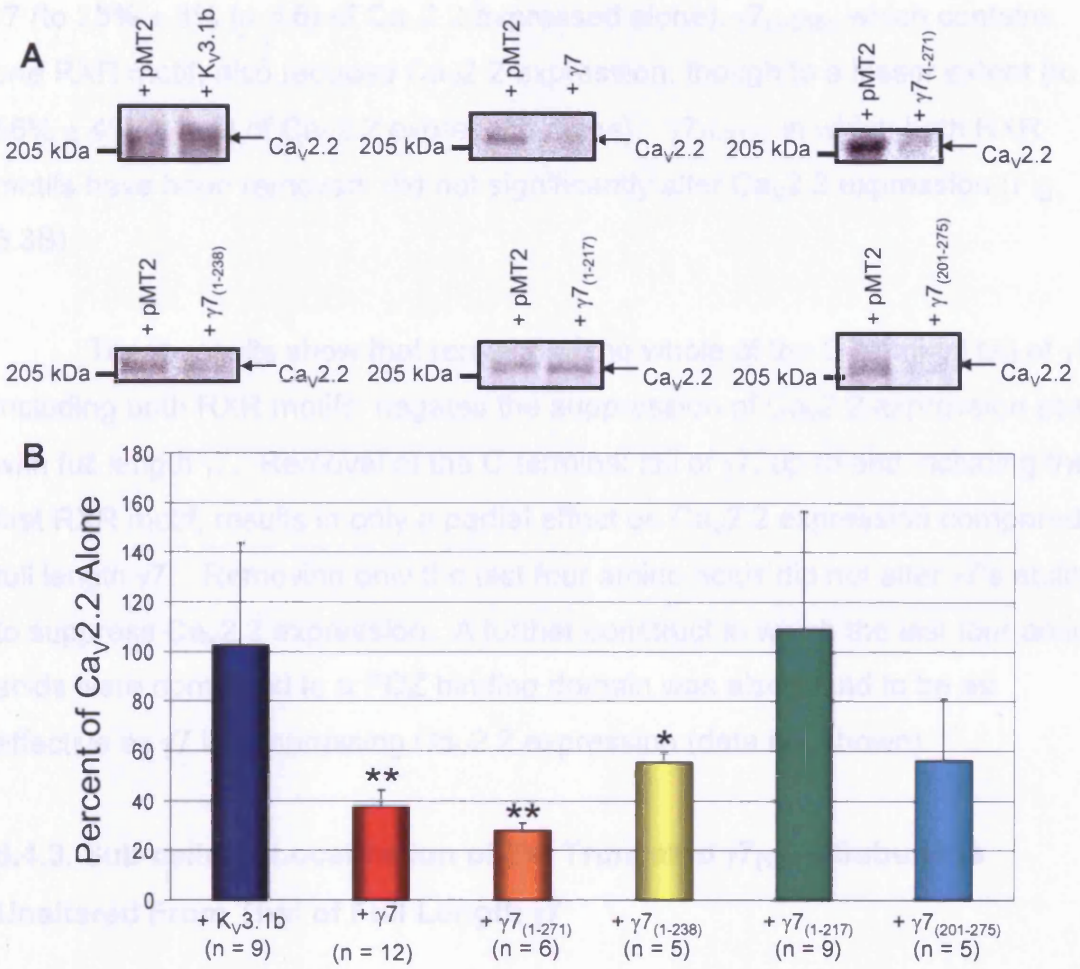

Fig. 6.3. The effect of γ7, the truncated γ7 constructs and K_V3.1b on the co-expression of Ca_V2.2. A) COS7 cells were transfected with Ca_V2.2 plus γ7, one of the truncated γ7 constructs, K_V3.1b or empty pMT2 vector. The expression of Ca_V2.2 was measured by western blotting and immunodetection using an antibody raised against Ca_V2.2. Ca_V2.2 is indicated by an arrow in each blot. B) Quantitative analysis of suppression of expression of Ca_V2.2 by γ7 and truncated γ7 constructs. Ca_V2.2 co-transfected with pMT2 alone was designated to be 100% and other co-transfected constructs are given as corresponding percentages. Bars represent S.E.M. ** $p<0.01$, * $p<0.05$.

Ca_V2.2 expression was reduced to 38% ± 7% (n = 12) when co-transfected with γ7 compared to Ca_V2.2 co-transfected with control empty pMT2 vector. Co-transfection of K_V3.1b with Ca_V2.2 did not significantly alter Ca_V2.2 expression. The effect of co-transfecting the truncated γ7 constructs was also examined. $\gamma7_{(1\text{-}271)}$ reduced Ca_V2.2 expression to the same extent as full-length

γ7 (to 28% ± 3% (n = 6) of $Ca_V2.2$ expressed alone). $\gamma7_{(1-238)}$, which contains one RXR motif, also reduced $Ca_V2.2$ expression, though to a lesser extent (to 56% ± 4% (n = 5) of $Ca_V2.2$ expressed alone). $\gamma7_{(1-217)}$, in which both RXR motifs have been removed, did not significantly alter $Ca_V2.2$ expression (Fig. 6.3B).

These results show that removal of the whole of the C-terminal tail of γ7, including both RXR motifs, negates the suppression of $Ca_V2.2$ expression seen with full length γ7. Removal of the C-terminal tail of γ7, up to and including the first RXR motif, results in only a partial effect on $Ca_V2.2$ expression compared to full length γ7. Removing only the last four amino acids did not alter γ7's ability to suppress $Ca_V2.2$ expression. A further construct in which the last four amino acids were converted to a PDZ binding domain was also found to be as effective as γ7 in suppressing $Ca_V2.2$ expression (data not shown).

6.4.3. Sub-cellular Localisation of the Truncated $\gamma7_{(1-217)}$ Subunit is Unaltered From That of Full Length γ7

It was hypothesised that removal of the RXR motifs in γ7 would result in a change in its location to the plasma membrane, as is common in other γ subunits (177;187). To investigate this γ7 and the truncated $\gamma7_{(1-217)}$ construct were transiently expressed in COS7 cells. Three days post transfection cells were fixed, permeablised and stained with the nuclear marker DAPI. The cellular distribution of the γ7 and $\gamma7_{(1-217)}$ was detected using an antibody raised against the predicted first extracellular loop of γ7 ($\gamma7_{(Loop)}$) and imaged by confocal microscopy (Fig. 6.4 A).

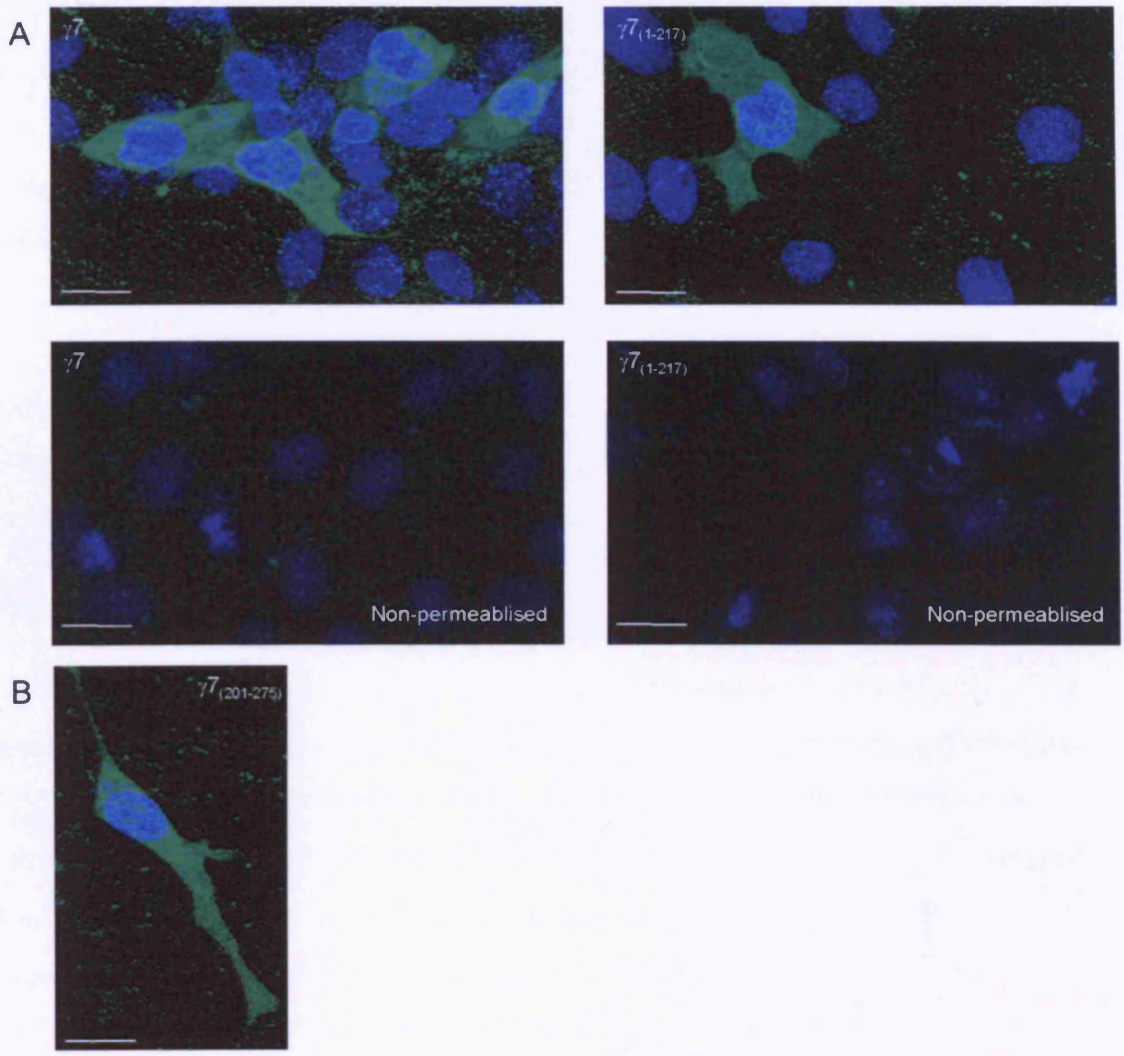

Fig. 6.4. Removal of the C-terminal tail of γ7 does not alter its sub-cellular location.
A. Immunofluoresence for γ7 or $\gamma7_{(1\text{-}217)}$ with an antibody raised against an epitope in the predicted first extracellular loop of γ7 (green). γ7 was only detectable if the cells were permeablised by treatment with 0.02 % Triton for 15mins at room temperature following fixation. B. Immunofluoresence for $\gamma7_{(201\text{-}275)}$ with an antibody raised against an epitope in the C-terminal tail of γ7 (green). In both experiments the nuclear stain DAPI (blue) was used as a marker. Bars = 50 μm.

γ7 was found to be present throughout the cytoplasm and often showed mainly perinuclear location, characteristic of it being present in the ER. $\gamma7_{(1\text{-}217)}$ was all also located throughout the cytoplasm with the strongest staining often being perinuclear. Neither γ7 nor $\gamma7_{(1\text{-}217)}$ localised to the plasma membrane. This is supported by the observation that no γ7 could be detected if the cells

were not permeablised. Similar patterns of location were seen for the $\gamma7_{(1-238)}$ and $\gamma7_{(1-271)}$ constructs.

6.4.4. The C-terminal Region of γ7 is Sufficient to Cause a Knockdown of $Ca_V2.2$ Expression

As removal of the C-terminal tail of γ7 negated the suppression of expression of $Ca_V2.2$ it was decided to investigate the effect of the C-terminal tail alone. Primers were designed to generate a construct that would express the C-terminal region of γ7 (amino acids 201-275) ($\gamma7_{(201-275)}$).

Three days post-transfection into COS7 cells $\gamma7_{(201-275)}$ was not detectable by Western blot and immunodetection with the $\gamma7_{(Tail)}$ antibody. This was shown not to be a cell-type specific effect as $\gamma7_{(201-275)}$ transfected into tsA-201 cells was also undetectable. To examine if this lack of detection was a problem, such as low affinity, with the $\gamma7_{(Tail)}$ antibody, a C-terminally HA tagged construct was also made. This construct was also not detectable with either the $\gamma7_{(Tail)}$ antibody or an antibody raised against the HA epitope. However, expression of this construct was observed after concentration by immunoprecipitation with an anti-HA antibody and a band of expected size (11 kDa) was detected (Fig. 6.5).

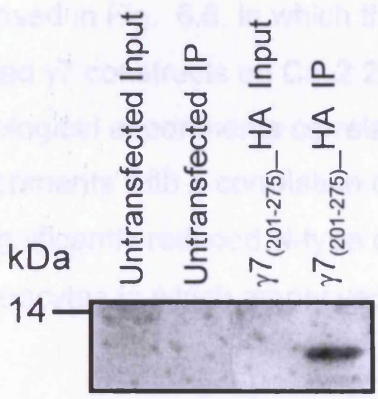

Fig. 6.5. $\gamma7_{(201-275)}$_HA is only observable after concentration by immunoprecipitation. Extracts of tsA-201 cells transfected with $\gamma7_{(201-275)}$_HA or untransfected controls were immunoprecipitated and expression of $\gamma7_{(201-275)}$_HA detected with an anti-HA antibody.

Despite not being detectable by western blotting, when transiently transfected into COS7 cells and imaged by confocal microscopy $\gamma7_{(201-275)}$ is detectable. $\gamma7_{(201-275)}$ appears throughout the cytoplasm and occasionally also in the nucleus (Fig. 6.4.B). $\gamma7_{(201-275)}$ does not show the perinuclear localisation seen with $\gamma7$ or the truncated $\gamma7$ constructs.

Quantitative Western blotting experiments, as detailed above (Fig 6.3), were performed to investigate the effect of $\gamma7_{(201-275)}$ on expression of $Ca_V2.2$ protein. Co-expression of $\gamma7_{(201-275)}$ with $Ca_V2.2$ resulted in a knockdown of $Ca_V2.2$ expression to 56% ± 25% (n=5) of $Ca_V2.2$ expressed with empty vector.

Electrophysiological studies were performed in collaboration to examine the effect of $\gamma7$ on N-type current through $Ca_V2.2$ channels. To examine if removal of the C-terminal tail of $\gamma7$ resulted in a reduction in N-type current $\gamma7$ and the truncated $\gamma7$ constructs were used in a *Xenopus* oocyte expression system. These experiments were performed by Prof. A. Dolphin. Briefly, $Ca_V2.2$, the auxiliary subunits $\alpha_2\delta$-2 and β1b, and either $\gamma7$, one of the truncated $\gamma7$ constructs or empty pMT2 vector were injected into *Xenopus* oocytes. Three days post injection N-type current was recorded by two electrode voltage clamp.

The results are summarised in Fig. 6.6. in which they are compared to the effect of γ7 and the truncated γ7 constructs on $Ca_V2.2$ protein expression in COS7 cells. The electrophysiological experiments correlate well with the previous Western blotting experiments with a correlation coefficient of 0.919. In these experiments $\gamma7_{(201\text{-}275)}$ significantly reduced N-type current though $Ca_V2.2$ channels compared to control oocytes in which empty vector replaced a γ7 construct.

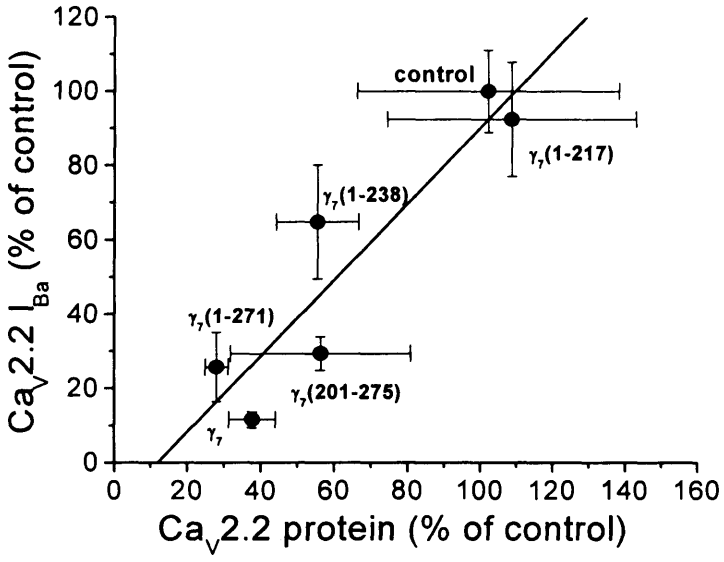

Fig. 6.6. Correlation between the effect of γ7 and the truncated γ7 constructs on $Ca_V2.2$ expression in COS7 cells and on their reduction of $Ca_V2.2$ Ba^{2+} currents in Xenopus oocytes. Quantitative western blotting experiments were compared to the effect of γ7 and the truncated γ7 on N-type Ba^{2+} currents through $Ca_V2.2$ in *Xenopus* oocytes. Bars represent S.E.M. The straight line was obtained by linear regression, r = 0.919.

Further to these experiments the effect of $\gamma7_{(1\text{-}217)}$ and $\gamma7_{(201\text{-}275)}$ on N-type current through $Ca_V2.2$ was tested in the mammalian tsA-201 cell line. These experiments were performed by Dr J. Leroy. Briefly, γ7 reduced N-type current through $Ca_V2.2$ channels and $\gamma7_{(1\text{-}217)}$ did not. $\gamma7_{(201\text{-}275)}$ did not reduce N-type current. This was likely to be due to the low level of $\gamma7_{(201\text{-}275)}$ expression in tsA-201 cells.

To investigate if the C-terminal tail of γ7 would be able to suppress $Ca_V2.2$ expression when attached to another protein a further construct was made which contained the transmembrane domains of γ2 and the C- terminal tail of γ7 (γ2TM γ7Tail). Expression was confirmed by western blotting and immunodetection with the $\gamma7_{(Tail)}$ antibody resulting in a band of the expected size (32 kDa) (Fig. 6.7). The effect of γ2TMγ7Tail, γ2 and γ7 on N-type current through $Ca_V2.2$ in tsA-201 cells was investigated by Dr J Leroy. Briefly γ7 once again was shown to reduce N-type current. However, γ2 and γ2TM γ7Tail did not.

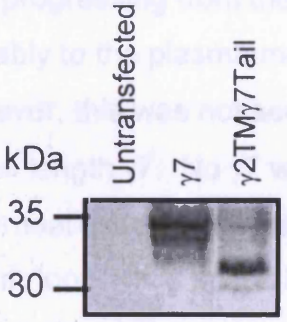

Fig. 6.7. Detection of γ2TMγ7Tail in tsA-201 cells. Extracts of tsA-201 cells transfected with γ7 or γ2TMγ7Tail or untransfected controls were western blotted with the $\gamma7_{(Tail)}$ antibody.

6.5. Discussion

The results described here are in agreement with those published by Moss *et al* (174) in which suppression of expression by γ7of GFP tagged-$Ca_V2.2$, but not Kv3.1b, was observed. The present results extend this finding by showing that the C-terminal tail of γ7 plays a critical role in the suppression of $Ca_V2.2$ currents and expression. Removal of the C-terminal tail of γ7 negates γ7 suppression of $Ca_V2.2$ and expression of the C-terminal tail alone is enough to partially suppress $Ca_V2.2$ expression. This has been shown in both a mammalian cell line and in *Xenopus* oocytes by western blotting and electrophysiology respectively.

It is possible that removal of the C-terminal tail of γ7 results in a protein that is misfolded and non-functional. However, from the evidence that the C-terminal tail expressed alone is sufficient to suppress $Ca_V2.2$ expression, this would seem unlikely.

Although it is possible that the RXR domains in the C-terminal tail of γ7 are critical in the suppression of $Ca_V2.2$ expression by γ7, this is not demonstrated by these experiments. Site-directed mutagenesis of the RXR domains would be required to determine if mutation of the RXR domains was sufficient to negate the suppression of $Ca_V2.2$ expression by γ7. If the RXR domains were preventing γ7 from progressing from the ER then one would expect a change in location, probably to the plasma membrane, for the truncated $\gamma7_{(1\text{-}217)}$ construct. However, this was not seen. $\gamma7_{(1\text{-}217)}$ showed the same subcellular distribution as full length γ7. No γ7 was localised to the plasma membrane and in non-permeablised cells it was not detectable with an antibody to a predicted extracellular loop. It is possible that the epitope for the extracellular antibody is somehow masked in non-permeablised cells. It is also possible that the four transmembrane structure, with intracellular N and C-termini and two extracellular loops, for γ7 is incorrect. Alternative structures for PMP22, to which family γ7 belongs, have been put forward (255). However, these structures would still put the γ7 loop epitope on the extracellular side of the plasma membrane.

These experiments show that the last four amino acids, TSPC which are similar to the TTPV found in the TARPs, are unimportant in the suppression of $Ca_V2.2$ expression. The removal of these four amino acids did not prevent the suppression by γ7 of $Ca_V2.2$ expression in COS7 cells or the reduced N-type current through $Ca_V2.2$ channels n *Xenopus* oocyte expression systems. Mutation from TSPC to TTPV also resulted in suppression of $Ca_V2.2$ expression in COS7 cells. This however does not rule out that these four amino acids are important in another aspect of the function of γ7. Indeed, they may well form a motif with similar functionality to the PDZ binding motif formed by TTPV in TARPS.

Immunocytochemistry experiments showed that there were few cells that were strongly expressing $\gamma7_{(201-275)}$, suggesting that the problem was due to poor expression of $\gamma7_{(201-275)}$. As $\gamma7_{(201-275)}$ is in the same vector as the other truncated constructs it would consequently have the same promoter. It was also ensured that there was a Kozak sequence (256) incorporated into the construct. The poor expression of $\gamma7_{(201-275)}$ could be due to the composition of the C-terminal tail of $\gamma7$. The C-terminal tail of $\gamma7$ contains 29% proline, glutamate, serine and threonine. Proteins high in these amino acids have been shown to be rapidly degraded (257) and certain sequences of these amino acids are known as PEST sequences. Although prediction programmes do not pick a specific PEST sequence in the C-terminal tail it possible that the high percentage of these amino acids of $\gamma7_{(201-275)}$ leads to $\gamma7_{(201-275)}$ being quickly degraded. This is further supported by the observation that purified His-tagged $\gamma7_{(201-275)}$ was found to be very quickly degraded. Also, after concentration by immunoprecipitation HA tagged $\gamma7_{(201-275)}$ was detectable by western blotting with an anti-HA antibody.

It is unknown why γ2TMγ7Tail did not reduce N-type current through $Ca_V2.2$ in tsA-201 cells. A possible explanation for this result could be that the construct may not fold in a way in which the C-terminus is available to or may be localised to a different cellular location where the C-terminus can not exert its effect.

In conclusion it would appear the C-terminal tail of $\gamma7$ is necessary and sufficient for the suppression of CaV2.2 in overexpression systems.

Chapter 7 – γ7 and its Association With RNPs

7.1. Introduction

7.1.1 Identification of Protein-Protein Interactions by Co-immunoprecipitation and Peptide Mass Fingerprinting

Identification of protein-protein interactions by proteomics methods is becoming increasingly popular. One method that has successfully identified novel protein interactions is by identification of proteins that co-immunoprecipitate with the protein of interest by peptide mass fingerprinting (258). Briefly the mix of proteins that have been immunoprecipitated are separated by 1D (SDS PAGE) or 2D electrophoresis (SDS PAGE followed by iso-electrofocusing).

A detailed description of the methodology of peptide mass fingerprinting will not be discussed here. Briefly, the proteins of interest are excised from the gel, washed and the cystine residues reduced and alkylated. The protein is then digested with trypsin and the resulting peptides are analysed by MALDI (Matrix-assisted Laser Desorption/Ionization) mass spectrometry. The masses of the tryptic peptides are determined and the resulting peptide map is queried against a non redundant sequence database containing all known protein sequences. The significance of the match between the peptide map obtained and the protein it is predicted to represent is then determined. One method of doing this is to assign a Mowse (molecular weight score) value using the Mowse algorithm (259).

7.2. Aims

The aims of the work described in this chapter were firstly try to and identify potential binding partners of γ7 through co-immunoprecipitation and secondly to examine if one identified potential binding partner, hnRNP A2, interacts with a putative A2RE in $Ca_V2.2$ mRNA.

7.3. Additional Methods

Experiments were performed as described in Chapter 2 with the following differences and additions.

7.3.1. Staining and Preparation of Proteins for Identification by Peptide Mass Fingerprinting

7.3.1.1. Silver Staining

Gels were stained using Silver Express® Silver Staining kit following the manufactures guidelines. Briefly, after running the gel proteins were fixed and sensitised to staining using the respective solutions from the kit. The gel was then thoroughly washed with ultra pure water before being incubated in developing solution until the desired intensity was achieved. The reaction was stopped by the addition of stopping solution and the gel was then once again thoroughly washed with ultra pure water. An image of the gel was then scanned and edited using Photoshop.

7.3.1.2 Coomassie Staining

Gels were stained using SimplyBlue™ SafeStain following the manufactures guidelines. Briefly, after running gels, they were thoroughly washed with ultra pure water. 20 ml of stain was then added and the gels were left to incubate at room temperature for one hour with constant shaking. The stain was then removed and replaced with 100 ml of water and incubated for a further hour. An additional 20 ml of a 20% NaCl (w/v) solution was added and incubated overnight at room temperature with gentle shaking. A second one hour wash with ultra pure water was performed before scanning or excision of bands.

Samples that were sent for identification were run on 4-12% Bis-Tris gels and then stained with SimplyBlue™ SafeStain. To reduce possible contamination gel tanks were extensively washed before running gels and fresh buffers and containers were used throughout. Bands of interest were excised from the gel using a clean scalpel blade for each band. Gels were run, stained and bands excised in a laminar flow hood. Peptide mass fingerprinting was performed by the Proteomics and Peptide Facility at the MRC Clinical Science Centre, Imperial College. Details of the Mascot search engine can be found at http://matrixscience.com (260). Briefly, a high score represents a low probability that the match between the experimental data and the matched protein is random.

7.3.2. hnRNP A2 Binding Experiments

Experiments to investigate if the potential A2RE site in $Ca_V2.2$ mRNA bound hnRNP A2 were performed as described previously (261) with the exception that mouse brain, rather than rat brain, was used as a source of hnRNP A2. These experiments are briefly described below.

7.3.2.1. Biotinylated Oligonucleotides

5'-Biotinylated RNA oligonucleotides were purchased from Invitrogen and are detailed in the Appendix. A2RE and non-specific are identical in base composition as used previously (261). $Ca_V2.2$ corresponds to bases 1096-1116 of mouse $Ca_V2.2$.

7.3.2.2. Protein Extraction

Brains were removed from adult male mice and washed extensively in ice cold PBS prior to homogenisation in extract buffer (20 mM HEPES, 0.65 M KCl, 2 mM EDTA, 1 mM $MgCl_2$ 2M glycerol 14.3 mM β-mercaptoethanol 8.7 mM Nonidet-p40, 12.1 mM deoxycholic acid and Complete™ protease inhibitors pH

7.4). Samples were then centrifuged at 13,000xg for 15 minutes at 4°C. The supernatant was extracted and protein concentration estimated by BCA assay.

7.3.2.3. hnRNP A2 Binding Assay

0.5 mg of streptavidin-coated magnetic particles were incubated with 2 μg of biotinylated RNA oligonucleotide in a solution of 10 mM Tris-HCl, 1mM EDTA and 100 mM NaCl, pH 7.5 for 10 minutes on ice. Beads were then washed twice for 5 minutes with 10 mM Tris-HCl to remove unbound RNA. 1 ml of binding buffer (10 mM HEPES, 3 mM $MgCl_2$, 40 mM NaCl, 5% (v/v) glycerol and 10 g/L Heparin, pH 7.5) containing 5 mg of mouse brain homogenate was added and left to incubate with constant shaking for 30 minutes at 4°C. The supernatant was then removed and three five minute washes performed with binding buffer.

Proteins were released by the addition of 200 μl of SDS sample buffer and heating to 65° C for 10 minutes. Beads were then removed before separation by SDS PAGE. 20 μl of each sample was run on a 4-12% Bis-Tris gel and western blotting and immunodetection with Anti-hnRNP A2 (1:200 dilution) performed.

7.3.3. Co-Immunoprecipitation of γ7_HA From Transiently Transfected tsA-201 Cells.

γ7_HA was co-immunoprecipitated from transiently transfected tsA-201 cells as previously described for stably transfected PC12 cells. Immunoprecipitated proteins were taken up in SDS buffer. Western blotting was performed with the Anti-hnRNP A/B at 1:1000 dilution.

7.4. Results

7.4.1. The RNA Interacting Proteins, hnRNP A2, hnRNP A3 and the Rat Homologue of Pigpen Co-immunoprecipitate With γ7_HA from Stably Transfected PC12 Cells

In an attempt to further understand the role of γ7 it was decided to identify proteins with which it interacts endogenously. For this a PC12 cell line was generated that stably expressed γ7_HA (as detailed in Chapter 3). PC12 cells were chosen as they had previously been shown to endogenously express γ7 and thus would be expected to also express the proteins with which γ7 interacts.

PC12 cells stably transfected with γ7_HA and untransfected PC12 cells were harvested and proteins were immunoprecipitated with an anti-HA antibody. Immunoprecipitated proteins were taken up in loading buffer and separated by SDS PAGE. Proteins then were visualised by silver or coomassie staining. Proteins that were present in the γ7_HA sample but not the untransfected control were considered to represent proteins which potentially interact with γ7.

Fig.7.1. shows preliminary results in which low amounts of cells were used and the resulting gel silver stained gel. A number of additional proteins were immunoprecipitated from γ7-HA expressing cells compared to untransfected cells. A diffuse band (red arrow) at around 34 kDa was thought to be γ7_HA.

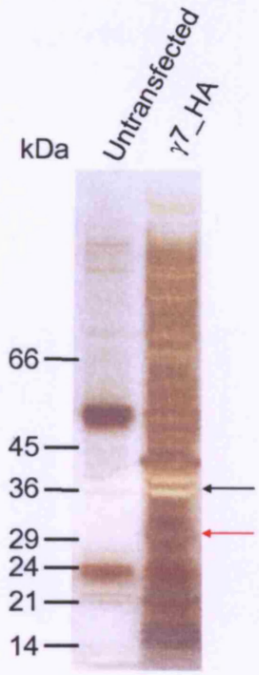

Fig. 7.1. γ7_HA and additional proteins can be immunoprecipitated from γ7_HA stably transfected PC12 cells. Immunoprecipitated proteins from γ7_HA stably transfected and control untransfected PC12 cells were separated by SDS PAGE and identified by silver staining. Red arrow indicates expected γ7_HA. Black arrow indicates the doublet of bands thought to correspond to hnRNP A2 and hnRNP A3 later identified by peptide mass fingerprinting.

However, the sensitivity of silver staining makes individual bands hard to distinguish. Furthermore, although MS protein analysis can be performed on very low levels of protein, which are only detectable by silver staining the use of a larger amount of protein reduces problems with potential contaminating proteins. Additionally silver staining that is compatible with peptide mass fingerprinting analysis is equally sensitive but results in higher background levels.

Repeating the above experiment but scaling up the amount of starting material increased the amount of immunoprecipitated protein to a level that could be detected by Coomassie staining (Fig 7.2). Bands corresponding to proteins which were present in the γ7_HA transfected cells, but not in the

untransfected cells, were excised under sterile conditions and taken for identification by peptide mass fingerprinting.

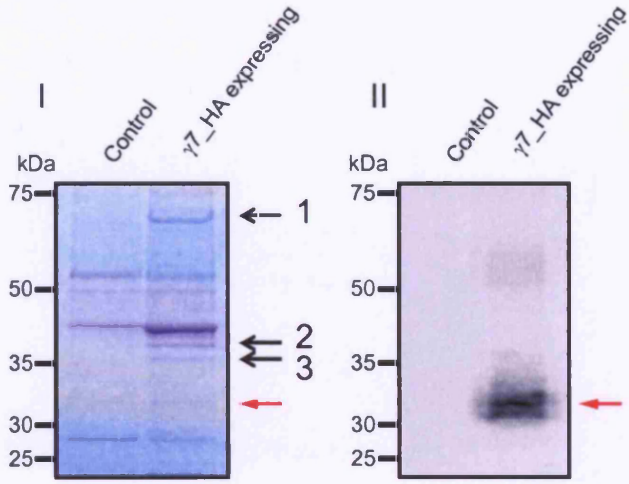

Fig. 7.2. Immunoprecipitation of γ7_HA and additional proteins from γ7_HA stably transfected PC12 cells. Immunoprecipitated proteins from γ7_HA stably transfected and untransfected PC12 cells (Control) were separated by SDS PAGE. I. Coomassie blue staining II. Western blotting with Anti-HA antibody. Red arrows indicate γ7_HA. Black arrows labelled 1,2 and 3 indicate bands excised from gel and identified by peptide mass fingerprinting. Representative of two independent experiments.

Fig. 7.3., Fig. 7.4. and Fig. 7.5. show the results of peptide mass fingerprinting. Bands 3, 2 and 1 correspond to hnRNPA2, a mixture of hnRNP A2/B1 and hnRNP A3 and Pigpen, respectively.

Peptide mass fingerprinting identified the protein corresponding to the band of approximately 36 kDa (Band 3) to most likely be the RNA binding protein hnRNP A2/B1 (Fig 7.3). 12 peptides were successfully matched with 34% of the protein covered. From this data it is not possible to determine if it is the A2 or B1 isoform of hnRNP. The apparent molecular weight of 36 kDa would suggest that it is the A2 isoform (predicted molecular weight 36 kDa) rather than the B1 isoform (predicted molecular weight 38 kDa). Also, none of the matched peptides falls within the addition 12 amino acids present in the B1 isoform.

I

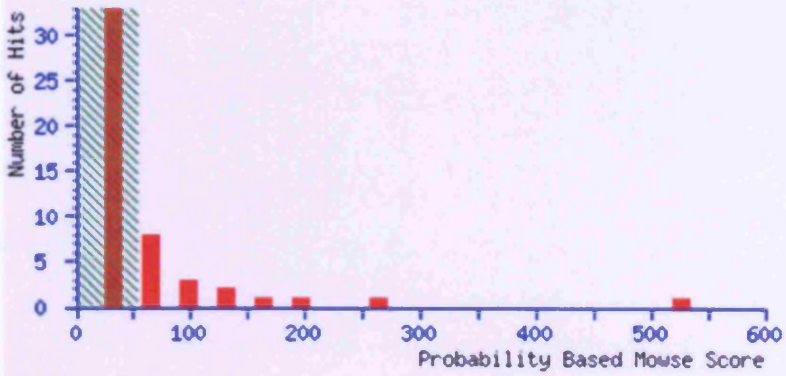

II

Q91ZR9 **Mass:** 35957 **Total score:** 527 **Peptides matched:** 12
Heterogeneous nuclear ribonucleoprotein A2/B1.- Mus musculus (Mouse).

III

Sequence Coverage: **34%**

```
  1 MEREKEQFRK LFIGGLSFET TEESLRNYYE QWGKLTDCVV MRDPASKRSR
 51 GFGFVTFSSM AEVDAAMAAR PHSIDGRVVE PKRAVAREES GKPGAHVTVK
101 KLFVGGIKED TEEHHLRDYF EEYGKIDTIE IITDRQSGKK RGFGFVTFDD
151 HDPVDKIVLQ KYHTINGHNA EVRKALSRQE MQEVQSSRSG RGGNFGFGDS
201 RGGGGNFGPG PGSNFRGGSD GYGSGRGFGD GYNGYGGGPG GGNFGGSPGY
251 GGGRGGYGGG GPGYGNQGGG YGGGYDNYGG GNYGSGSYND FGNYNQQPSN
301 YGPMKSGNFG GSRNMGGPYG GGNYGPGGSG GSGGYGGRSR Y
```

Fig. 7.3. 36 kDa protein (Band 3) identified as hnRNP A2/B1. I. Probability based Mowse Score. Score is -10*Log(P), where P is the probability that the observed match is a random event. Individual ions scores > 52 (to the right of the green hatched region) indicate identity or extensive homology ($p<0.05$). II. hnRNP A2 identified as the most probable match. III. Sequence coverage of hnRNP A2. Matched peptides shown in bold red.

I

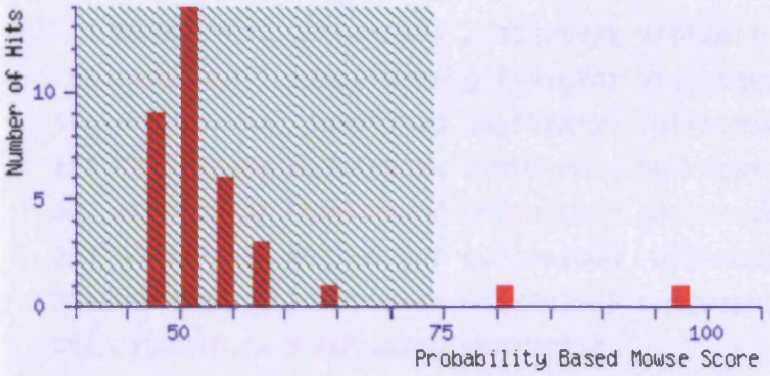

II

Mixture Total score: 172 Peptides matched: 24

Components (only one family member shown for each component):

AAN76992 **Mass:** 37063 **Total score:** 97 **Peptides matched:** 14

AF463524 NID: - Mus musculus

Q91ZR9 **Mass:** 35957 **Total score:** 76 **Peptides matched:** 11

Heterogeneous nuclear ribonucleoprotein A2/B1.- Mus musculus (Mouse).

III

Sequence Coverage of hnRNP A3: **38%**

```
   1 MEVKPPPGRP QPDSGRRRRR RGEEGHDPKE PEQLRKLFIG GLSFETTDDS
  51 LREHFEKWGT LTDCVVMRDP QTKRSRGFGF VTYSCVEEVD AAMCARPHKV
 101 DGRVVEPKRA VSREDSVKPG AHLTVKKIFV GGIKEDTEEY NLRDYFEKYG
 151 KIETIEVMED RQSGKKRGFA FVTFDDHDTV DKIVVQKYHT INGHNCEVKK
 201 ALSKQEMQSA GSQRGRGGGS GNFMGRGGNF GGGGGNFGRG GNFGGRGGYG
 251 GGGGGSRGSY GGGDGGYNGF GGDGGNYGGG PGYSSRGGYG GGGPGYGNQG
 301 GGYGGGGGGY DGYNEGGNFG GGNYGGGGNY NDFGNYSGQQ QSNYGPMKGG
 351 SFGGRSSGSP YGGGYGSGGG SGGYGSRRF
```

Sequence Coverage of hnRNP A2/B1: **38%**

```
   1 MEREKEQFRK LFIGGLSFET TEESLRNYYE QWGKLTDCVV MRDPASKRSR
  51 GFGFVTFSSM AEVDAAMAAR PHSIDGRVVE PKRAVAREES GKPGAHVTVK
 101 KLFVGGIKED TEEHHLRDYF EEYGKIDTIE IITDRQSGKK RGFGFVTFDD
 151 HDPVDKIVLQ KYHTINGHNA EVRKALSRQE MQEVQSSRSG RGGNFGFGDS
 201 RGGGGNFGPG PGSNFRGGSD GYGSGRGFGD GYNGYGGGPG GGNFGGSPGY
 251 GGGRGGYGGG GPGYGNQGGG YGGGYDNYGG GNYGSGSYND FGNYNQQPSN
 301 YGPMKSGNFG GSRNMGGPYG GGNYGPGGSG GSGGYGGRSR Y
```

Fig. 7.4. 37 kDa protein (Band 2) identified as mixture hnRNP A2/B1 and hnRNP A3. I. Probability based Mowse Score. Score is -10*Log(P), where P is the probability that the observed match is a random event. Protein scores greater than 74 (to the right of the green hatched region) are significant ($p<0.05$). II. A mixture of hnRNP A2/B1 and hnRNP A3 are identified as the most probable matches. III. Sequence coverage of hnRNP A2/B1 and hnRNP A3. Matched peptides shown in bold red.

I

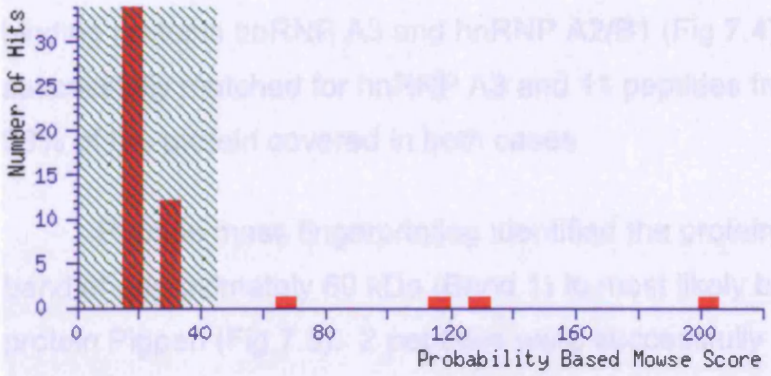

II

Q8CFQ9 **Mass:** 52570 **Total score:** 72 **Peptides matched:** 2

Similar to pigpen.- Mus musculus (Mouse).

III

Sequence Coverage: **3%**

```
  1 MASNDYTQQA TQSYGAYPTQ PGQGYSQQSS QPYGQQSYSG YGQSADTSGY
 51 GQSSYGSSYG QTQNSYGTQS APQGYGSTGG YGSSQSSQSS YGQQSSYPGY
101 GQQPAPSSTS GSYGGSSQSS SYGQPQSGGY GQQSGYGGQQ QSYGQQQSSY
151 NPPQGYGQQN QYNSSSGGGG GGGGGNYGQD QSSMSGGGGG GGYGNQDQSG
201 GGGGGYGGGQ QDRGGRGRGG GGGYNRSSGG YEPRGRGGGR GGRGGMGGSD
251 RGGFNKFGGP RDQGSRHDSE QDNSDNNTIF VQGLGENVTI ESVADYFKQI
301 GIIKTNKKTG QPMINLYTDR ETGKLKGEAT VSFDDPPSAK AAIDWFDGKE
351 FSGNPIKVSF ATRRADFNRG GGNGRGGRGR GGPMGRGGYG GGGSGGGGRG
401 GFPSGGGGGG GQQRAGDWKC PNPTCENMNF SWRNECNQCK APKPDGPGGG
451 PGGSHMGGNY GDDRRGRGGY DRGGYRGRGG DRGGFRGGRG GGDRGGFGPG
501 KMDSRGEHRQ DRRERPY
```

Fig. 7.5. 60 kDa protein (Band 1) identified as Pigpen. I. Probability based Mowse Score. Score is -10*Log(P), where P is the probability that the observed match is a random event. Individual ions scores > 45 indicate identity or extensive homology

($p<0.05$). II. Pigpen identified as the most probable match. III. Sequence coverage of Pigpen. Matched peptides shown in bold red.

Peptide mass fingerprinting identified the protein corresponding to the band of approximately 37 kDa (Band 2) to most likely be a mixture to two RNA binding proteins hnRNP A3 and hnRNP A2/B1 (Fig 7.4). 14 peptides were successfully matched for hnRNP A3 and 11 peptides fro hnRNP A2/B1 with 38% of the protein covered in both cases

Peptide mass fingerprinting identified the protein corresponding to the band of approximately 60 kDa (Band 1) to most likely be the RNA binding protein Pigpen (Fig 7.5). 2 peptides were successfully matched covering 3% of the protein.

7.4.2. Endogenous hnRNP A2 Co-Immunoprecipitate with γ7_HA in Transiently Transfected tsA-201 cells

To confirm co-immunoprecipitation of hnRNP A2 tsA-201 cells were transiently transfected with γ7_HA. Three days post transfection cells were harvested and γ7_HA immunoprecipitated using an anti-HA antibody. Co-immunoprecipitation of hnRNP A2 was confirmed by western blotting with an anti-hnRNP A/B antibody (Fig. 7.6).

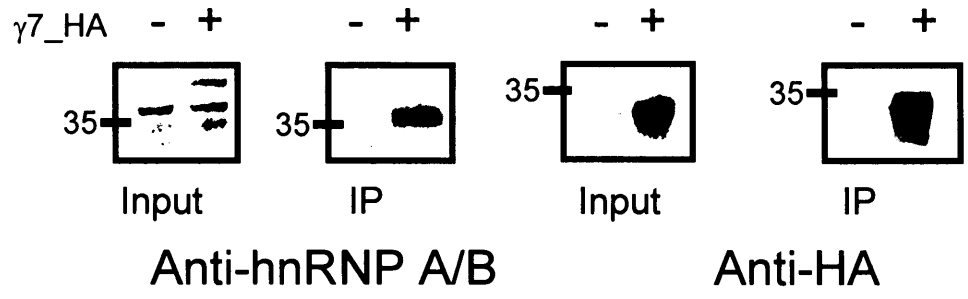

Fig. 7.6. Endogenous hnRNP A2 co-immunoprecipitates with γ7_HA in transiently transfected tsA-201 cells. tsA-201 cells were transiently transfected with γ7_HA. Three days post transfection γ7_HA was immunoprecipitated using an anti-HA antibody. Proteins were separated by SDS PAGE and hnRNP A2 and γ7_HA identified by western blotting with anti-hnRNP A/B and anti-HA antibodies, respectively. Representative of four experiments.

Western blotting with an anti-hnRNP A/B antibody identified a single band of approximately 36 kDa from immunoprecipitated material from γ7_HA transfected cells. From the apparent molecular weight it was thought to be hnRNP A2. No additional bands were seen in the γ7_HA sample compared to the control untransfected sample in the input blots suggesting that there was no non-specific binding of the anti-hnRNP A/B antibody to γ7_HA. A faint higher molecular weight band of approximately 37-38 kDa, which could correspond to the B1 isoform of hnRNP or hnRNP A3, was detectable in the input blot but not detected in the immunoprecipitated blot. No bands were detected in the immunoprecipitated blot from control, untransfected, tsA-201 cells, suggesting that hnRNP A2 does not bind non-specifically to the beads alone.

7.4.3. $Ca_V2.2$ mRNA Contains an A2RE element

Previous work by Ainger *et al* (262) had identified a potential A2RE site in $Ca_V2.2$ mRNA. To examine if this A2RE site could indeed bind hnRNP A2 a

repeat of the original experiment performed by Hoek *et al* (261), to identify the A2RE, was performed using a ribonucleotide oligonucleotide corresponding to the potential A2RE in $Ca_V2.2$.

Mouse brain homogenate was incubated with biotinylated ribonucleotide oligonucleotides corresponding to the consensus A2RE site from MBP, the potential A2RE site in $Ca_V2.2$ and a scrambled non-specific sequence (identical to the non-specific sequence used by Hoek et al (261)). Streptavidin-coated magnetic beads were added and ribonucleotides and any bound proteins were separated using magnetic separators. As a further control a beads alone sample was used. Bound proteins were taken up in SDS sample buffer, separated by SDS PAGE and hnRNP A2 detected by western blotting with an anti-hnRNP A2 antibody (Fig 7.7).

Fig. 7.7. $Ca_V2.2$ contains an A2RE site. Biotinylated ribonucleotides corresponding to the consensus A2RE, the potential A2Re in $Ca_V2.2$ mRNA and a scrambled non-specific sequence were incubated with mouse brain extract and bound proteins isolated using streptavidin coated paramagnetic beads. Proteins were separated by SDS PAGE and hnRNP A2 identified by western blotting with an anti-hnRNPA2 antibody.

A strong band of approximately 36 kDa was pulled down with the biotinylated ribonucleotides corresponding to the A2RE site and the potential A2RE site in $Ca_V2.2$ mRNA, but not with the non-specific scrambled sequences or beads alone. A slightly higher molecular weight band was also pulled down, which could correspond to the B1 isoform of hnRNP A2/B1 or to hnRNP A3.

7.5. Discussion

7.5.1. Ribonucleoprotein Complexes and RNA Trafficking

To function correctly eukaryotic mRNA requires the association of RNA-binding proteins. These are collectively referred to as mRNA-protein complex proteins (mRNP proteins) or heterogeneous ribonucleoproteins (hnRNP proteins). These proteins have a range of roles including splicing, mRNA export, localisation, translation and stability (213). mRNPs bind to nascent transcripts and many remain bound until they reach the ribosomes, shuttling between the nucleus and the cytoplasm (263;264).

The mRNA for a range of proteins has been shown to be trafficked to discrete locations within the cell before translation takes place (265-268). This allows the cell to achieve high levels of protein expression at the site of mRNA localisation and allows the exclusion of protein from certain cellular domains. It is thought that the mRNAs are assembled into trafficking intermediates termed 'RNA granules' (269). These granules contain multiple RNA molecules, trafficking factors and translation machinery components (270). Granules containing mRNAs that encode soluble proteins are retained within the cytoplasm, whereas those encoding membrane proteins are targeted to the ER. Other granules, such as those containing mRNA encoding myelin basic protein (MBP), are trafficked within the cell to where the protein is required. In the case of MBP in oligodendrocytes the mRNA granules are trafficked to the myelin compartment (271;272). The trafficking pathway of each granule is determined

by specific *cis*-acting elements in the RNA cargo and cognate *trans*-acting factors in the cell (273).

7.5.2. Heterogeneous Nuclear Ribonucleoproteins

Heterogeneous nuclear ribonucleoproteins (hnRNPs) were first described as a group of chromatin-associated RNA-binding proteins (263). There are now more than 20 proteins that have been shown to be part of the hnRNP complex. These proteins have been shown to be involved in multiple functions including transcriptional regulation, telomere length maintenance, mRNA trafficking, splicing and mRNA stability (265;274-278).

hnRNP A2 was first identified by Brayer et al (279). It is a 36 kDa protein consisting of an N-terminal domain containing two RNA-binding domains and a C-terminal domain containing an RGG arginine/glycine rich motif (280;281). Tissue distribution analysis shows high levels of expression in the brain and testes with lower levels of expression in the liver, lung and heart. Within the cells it is located within the cell nucleus, but is also found in the cell body (261). The human orthologue was cloned by Biamonti et al (282) who showed it is encoded by 11 exons. An alternatively spliced variant, hnRNP B1, was also found which contained a 36 nucleotide mini-exon. This results in the addition of twelve amino acids near the N-terminus present in hnRNP B1 but not hnRNP A2 (280). The hnRNP B1 variant ranges between 2 to 5% of total hnRNP A2/B1 transcripts depending upon the tissue (283;284).

hnRNP A2 has been shown to be involved in the trafficking to mRNA. A 21 nucleotide *cis*-acting sequence within the 3'-untranslated region of MBP mRNA was shown to be necessary and sufficient for mRNA trafficking in oligodendrocytes. Hoek *et al* showed that the cognate *trans*-acting factor to this *cis*-acting sequence was hnRNP A2 (261). This sequence was named the hnRNP A2 response element (A2RE). Munro *et al* went on to show that degenerate A2REs are present in other trafficked mRNAs, including activity-related cytoskeleton-associated protein (ARC) and the GABA receptor α subunit, also bound hnRNP A2 (285). Shan *et al* proposed that mRNA trafficking involving A2RE and hnRNP A2 takes place not only within

oligodendrocytes but is also responsible for dendritic RNA localisation in neurons (286). They also showed trafficking by this mechanism involves microtubules. Potential A2REs have been found in a range of proteins that have been shown or are thought to be localised, among these is $Ca_V2.2$ (262;268).

Proteomic techniques are becoming increasingly popular to find novel interactions between proteins. Using co-immunoprecipitation and subsequent identification by peptide mass fingerprinting three proteins were found that potentially interact with γ7. All three of these proteins, hnRNP A2, hnRNP A3 and Pigpen, are RNA interacting proteins.

The co-immunoprecipitation of hnRNP A2 was confirmed by its co-immunoprecipitation with γ7_HA from tsA-201. Endogenous hnRNP A2 could be detected in tsA-201 cells and could also be detected in the immunoprecipitate of γ7_HA transfected cells. However, no hnRNP A2 was detected in the immunoprecipitate of untransfected control cells. No additional bands were seen in lysate from γ7_HA transfected tsA-201 cells compared to untransfected cells showing that the hnRNP A/B antibody does not non-specifically detect γ7.

As the name would suggest hnRNP A3 is similar to hnRNP A2. It shows similar tissue distribution as hnRNP A2 and is also is mostly localised to the nucleus but can also be found in cytoplasmic granules. hnRNP A3 is a *trans*-acting factor to the A2RE element. Furthermore it has been shown to interact directly with the A2RE and not just through association with hnRNP A2. It has been suggested that it may serve a similar role in RNA trafficking as hnRNP A2 (287).

Pigpen is another putative RNA-binding protein (288). The human orthologue TLS (translocated in liposarcomas) is a 53 kDa protein which is also found in heterogeneous nuclear ribonucleoprotein complexes (289;290). It has been shown to interact with RNA polymerase II (291) and is involved in transcriptional activation (292).

These three proteins can be found together in RNP complexes and it is possible that co-immunoprecipitation of one these proteins will result in the other proteins being co-immunoprecipitated also. It is also possible that γ7 could interact with a further unidentified protein or indeed RNA itself. Treatment with RNase would help to identify if there is direct interaction between these proteins and γ7. In addition a yeast two-hybrid system could be used to confirm these results and find other proteins that interact with γ7. However, interactions between transmembrane proteins are difficult to determine by this method. Also, yeast two-hybrid is known to give many false positive results.

In the peptide mass fingerprinting experiments it is possible that the hnRNP A2, detected in band 2 was actually due to contamination of the sample from the lower hnRNP A2 band below. To overcome this better separation of proteins could have been achieved by using a higher percentage acrylamide gel or using MES instead of MOPS as the running buffer. Ideally 2D electrophoresis, in which proteins are separated by iso-electrofocusing prior to separation by SDS PAGE could have been used. This may have identified further proteins that had co-immunoprecipitated.

The experiments performed here show that the potential A2RE site in $Ca_V2.2$ does indeed bind hnRNP A2. As hnRNP A2 has previously been shown to be involved in the trafficking of mRNA in neurons (286) and $Ca_V2.2$ mRNA is trafficked in neurons (268) it is possible that the A2RE element and hnRNP A2 are the *cis*-acting element and cognate *trans*-acting factors that result in $Ca_V2.2$ mRNA localisation.

Chapter 8 – Discussion and Future Work

This study attempts to deduce more information about the role of the recently identified stargazin-like protein γ7. It has been shown that the expression of the neuronal VDCC α_1 subunit $Ca_V2.2$ is suppressed by the co-transfection of γ7 in both *Xenopus* oocyte and mammalian cell overexpression systems. The work presented here attempts to further characterise γ7. It identifies the region of γ7 that is responsible for the suppression of $Ca_V2.2$ expression and further investigates the mechanism by which this takes place. It also identifies a possible interaction between γ7 and proteins involved in the trafficking of RNA.

8.1. γ7 as a Auxiliary Subunit of Voltage-Dependent Calcium Channels

By homology the family of γ subunits can be subdivided into three sub-families. The first is comprised of γ1 and γ6; the second comprises γ2, γ3, γ4 and γ8; and the third comprises γ5 and γ7. All of these proteins are part of the larger tetraspannin PMP-22/EMP/MP20/Claudin family.

It remains controversial if all, or indeed any, of the γ subunits form part of a functional VDCC. The effects of γ7 upon VDCC kinetics and voltage dependant properties are slight compared to $\alpha_2\delta$ and β subunits. In general γ subunits downregulate calcium channel activity (293), although there is conflict between results from different groups. Other roles for γ subunits have been elucidated (177;210) and it remains uncertain what physiological roles γ subunits play. It could be argued that each of the sub-families, while sharing a degree of similarity to one another, serve different physiological roles.

Evidence for γ subunits being involved in VDCC function is strongest for the first sub-family. γ1 was initially identified by co-purification with $Ca_V1.1$ from skeletal muscle. In addition to this biochemical evidence several studies have shown γ1 to have an effect on VDCC kinetics and voltage dependant properties (293). Recently both the long and short isoforms of γ6 have been shown to modulate $Ca_V3.1$ currents (187). Co-expression of the long isoform of γ6 with

$Ca_V3.1$ was shown to significantly decrease current density. However, this decrease must be due to a different mechanism than the suppression of $Ca_V2.2$ by γ7 as γ6 expression did not affect the level of $Ca_V3.1$ mRNA or the amount of total Cav3.1 protein.

The second sub-family (γ2, γ3, γ4 and γ8) have been clearly shown to have a role in the trafficking of AMPA receptors. These have now been designated as TARPs (160;177). In addition to their role in trafficking they have also recently been shown to be involved in the modulation of AMPA receptors. Along with their roles in AMPA receptor trafficking and function it remains possible that they may also interact with VDCCs. Several studies have found changes in VDCC kinetics when co-expressed with TARP's. Also, $Ca_V2.2$ was found to co-precipitate with GluR1 and γ2 and it has been proposed that they may form a complex *in vivo* (117).

Of the three families the third (γ5, γ7) is the least well categorised. Overall there is little similarity between these proteins and the TARPs. The C-terminal regions of these proteins are much shorter (especially compared to γ8) and lack a type I PDZ-binding motif important for TARP functionality. Tomita *et al* have showed that γ5 is not a TARP and does not traffic AMPA receptors (177). γ7, has been shown to suppress Ba^{2+} current through $Ca_V2.2$, and to a lesser extent $Ca_V1.2$ and $Ca_V2.1$ (174). However, this reduction in current is due to reduction in channel expression rather than modulation of the channel. $Ca_V3.1$ current and expression was shown to be unaffected by γ7 expression (187). No work presented here supports the view that γ7 is a subunit of VDCCs.

8.2. Structure and Cellular Distribution of γ7

A shared motif between all γ subunits is a predicted glycosylation site present in the 1st extracellular loop of the protein. Here it is shown that γ7 is glycosylated at this site when expressed in tsA-201 cells. Mutation of the predicted site of glycosylation, asparagine at position 45 to alanine, resulted in γ7 running on SDS-PAGE at the predicted molecular mass of 32 kDa. It

remains to be ascertained if γ7 is endogenously glycosylated and, if so, the composition of the carbohydrate residues. Also, the observation that a HA tag placed at the N-terminus of γ7 was not detectable using a Anti-HA antibody despite the expression of the rest of the protein suggests there may be some modification of the N-terminus of the protein.

γ7 does not share the same cellular distribution as the rest of the examined γ subunits. Both the data presented here, and the experiments performed by Hansen *et al* (187), found γ7 to be located intracellularly with no expression at the plasma membrane. Here we show that a CFP tagged γ7 construct in part co-localises with PDI, a marker of ER when stably transfected into PC12 cells. However, co-localisation is incomplete suggesting expression in intracellular membranes other than those of ER. Removal of RXR domains, shown to be involved in ER retention of proteins and present in the C-terminus of γ7, did not lead to it reaching the plasma membrane, suggesting that there must be other sequences within γ7 that keep it intracellular.

Cell adhesion is one of the functions of the claudin family of proteins. γ2 has been shown to have retained the ability to induce cell aggregation when expressed in mouse L-fibroblasts, suggesting a role in cell adhesion (294). The lack of plasma membrane localisation would preclude such a role for γ7.

In both this study and that of Hansen *et al* (187) the subcellular distribution of γ7 was examined using mammalian cell over expression systems. The endogenous distribution of γ7 in PC12 cells was more diffuse, but once again γ7 was not detectable in the plasma membrane. In PC12 cells that were undergoing differentiation and had put out processes, γ7 was often found at the end of these processes.

8.3. Suppression of $Ca_V2.2$ Expression by the Co-expression of γ7

Moss *et al* (174) had previously shown that the reduction of N-type current through $Ca_V2.2$ caused by the co-expression of γ7 was not due to

modulation of the channel but rather by a reduction in the expression of the channel. One of the aims of this study was to try to elucidate the mechanism by which the suppression of $Ca_V2.2$ expression occurs.

One hypothesis would be that the suppression of $Ca_V2.2$ expression by γ7 was non-specific. Thus, the expression of any protein would also result in a reduction of $Ca_V2.2$ expression. Moss *et al* (174) used confocal microscopy to show that contrary to this hypothesis co-expression of γ7, but not $K_V3.1b$ reduced the expression of a GFP tagged $Ca_V2.2$ construct. This result was confirmed here by western blotting. γ7 significantly reduced $Ca_V2.2$ expression when co-transfected in a mammalian cell expression system. However, co-transfection of $K_V3.1b$ had no significant effect on $Ca_V2.2$ expression.

To confirm that the suppression of $Ca_V2.2$ expression by γ7 co-transfection was not due to promoter competition a construct was designed that would produce γ7 mRNA which would not be translated. Co-transfection of this construct with $Ca_V2.2$ did not affect N-type current through $Ca_V2.2$ channels.

Combined with the work performed by Moss *et al* (174) these experiments would suggest that the suppression of $Ca_V2.2$ by γ7 is specific and not due to promoter competition. The suppression of $Ca_V2.2$ is also somewhat specific to γ7 as co-transfection $K_V3.1b$, another transmembrane protein, does not suppress $Ca_V2.2$ expression. Furthermore, the lack of suppression of $Ca_V2.2$ by non-translated γ7 mRNA suggests that it is not RNA-RNA interaction between γ7 and $Ca_V2.2$ mRNA that is responsible for $Ca_V2.2$ expression.

An alternative hypothesis would be that γ7 expression would suppress the expression of any protein that was co-transfected with it. Moss *et al* (174) had used western blotting to show that another VDCC subunit, β1b was unaffected by γ7 co-transfection. They also used confocal microscopy to show that $K_V3.1b$ expression was unaltered by γ7 co-transfection. Here, western blotting was used to confirm that co-expression of γ7 did not alter $K_V3.1b$ expression. Thus, γ7 does not non-specifically suppress the expression of all proteins with which it is co-transfected.

Previous work by Wei *et al* (180) indicated a possible interaction between β and γ subunits. They found that the modulation of L-type current through $Ca_V1.2$ by γ1 was β dependent. β subunits have also been shown to increase the expression α_1 subunits (109). Moss *et al* showed previously that γ7 does not suppress β1b subunit expression. However, γ7 may have prevented interaction between the β1b and $Ca_V2.2$ and thus prevented the increase in $Ca_V2.2$ expression due to β1b co-expression. This could not be examined electrophysiologically as the small size of the currents produced by $Ca_V2.2$ when transfected into mammalian cells without β subunits would make the identification of a reduction, due to γ7 co-transfection, difficult to determine. Changes in the amount of $Ca_V2.2$ protein could still be detected by western blotting even in the absence of β or $\alpha_2\delta$. These experiments showed that $Ca_V2.2$ expression was still suppressed by γ7 co-transfection and did not depend upon the presence of β or $\alpha_2\delta$ subunits.

Raghib *et al* (237) reported that $Ca_V2.2$ expression could be suppressed by the co-transfection of truncated $Ca_V2.2$ constructs. Recently the mechanism of this suppression was shown to involve the ER stress pathways (238). ER stress has been shown to activate a series of pathways that result in the suppression of protein expression, giving the cell time to recover. In this study three markers of ER stress, the upregulation of CHOP, the upregulation of XBP and the editing of XBP, were examined. Using QPCR none of these markers was found to be upregulated by the expression of γ7, or γ7 and $Ca_V2.2$. This would suggest that ER stress is not involved in the suppression of $Ca_V2.2$ expression. Furthermore it suggests that the mechanism of the suppression of $Ca_V2.2$ expression by γ7 is different to the mechanism of the suppression of $Ca_V2.2$ by truncated $Ca_V2.2$ constructs.

During this study work performed by Dr K. Page showed that $Ca_V2.2$ mRNA was reduced by the co-expression of γ7 in mammalian cell expression system. In addition experiments performed by Prof A. Dolphin showed that in *Xenopus* oocytes, if synthetically synthesised $Ca_V2.2$ mRNA was used, rather than expressing $Ca_V2.2$ from a vector, γ7 failed to suppress $Ca_V2.2$ expression

and there was no significant difference in N-type current between control and γ7 co-injected oocytes. Furthermore, injection of RNasin, an inhibitor of RNases, was found to attenuate the suppression of $Ca_V2.2$ expression. These experiments would suggest that the suppression of $Ca_V2.2$ expression by γ7 is due to a reduction in $Ca_V2.2$ mRNA. There are several possibilities as to why $Ca_V2.2$ mRNA is reduced including reduced synthesis and increased degradation of $Ca_V2.2$ mRNA.

Thus far suppression of $Ca_V2.2$ protein by γ7 has only been identified in overexpression systems. Endogenous N-type current through $Ca_V2.2$ channels are unchanged when γ7 is transfected in both SCG's and PC12 cells. This may be due to insufficient turnover of the endogenous channels to give an observable result. Investigation of endogenous mRNA level, rather than currents, may reveal a change there. It is also possible that $Ca_V2.2$ expression is only suppressed by co-expression of γ7 when $Ca_V2.2$ is expressed from cDNA in a vector.

Here it is shown that the C-terminus of γ7 is necessary and sufficient for the suppression of $Ca_V2.2$ expression. Both biochemically and biophysically expression of γ7 without the C-terminus was shown to have no significant effect upon $Ca_V2.2$ expression. Additionally expression of the C-terminus alone was sufficient to cause suppression of $Ca_V2.2$ expression. The last four amino acids (TSPC), which resembles the type I PDZ binding motif which was found to be important in the function of TARPs, were found not to be involved in the suppression of $Ca_V2.2$ expression by γ7. Also, removal of the glycosylation site present in γ7 did not attenuate the suppression of $Ca_V2.2$ expression.

8.3. Interaction Between hnRNP A2 and γ7

Immunoprecipitation of a HA tagged γ7 construct from a stably transfected PC12 cell line identified several proteins that potentially interact with γ7. Subsequently three of these proteins were identified by peptide mass fingerprinting to be hnRNP A2, hnRNP A3 and Pigpen. Interestingly all three of these proteins are RNA binding proteins. Endogenous hnRNP A2 also co-

immunoprecipitated the HA tagged γ7 construct when it was transiently transfected into tsA-201 cells. This would suggest that the interaction between γ7 and hnRNP A2 was not an artefact generated during the generation of the stable cell line.

It cannot be excluded that the interaction between γ7 and hnRNP A2 is an artefact due to the use of an overexpression system. Ideally co-immunoprecipitation of endogenous γ7 and hnRNP A2 could be obtained. Unfortunately however the antibodies for γ7 and hnRNP A2 where found to be unsuitable for immunoprecipitation. It also has not yet been determined if there is a direct interaction between γ7 and hnRNP A2. It is possible that the interaction was through either of the two other identified proteins or through some as yet unidentified protein. It is also possible that these proteins interact with each other through RNA. Incubation of the immunoprecipitated proteins with RNase would answer this question.

Of these three proteins, hnRNP A2, has been the most extensively studied. It is a 36 kDa protein that is found within the nucleus and also throughout the cell body (261). hnRNP A2 shares a similar tissue distribution with γ7 (as identified by Chu *et al* (171)) with high levels of expression in the brain and testes (Fig 8.1).

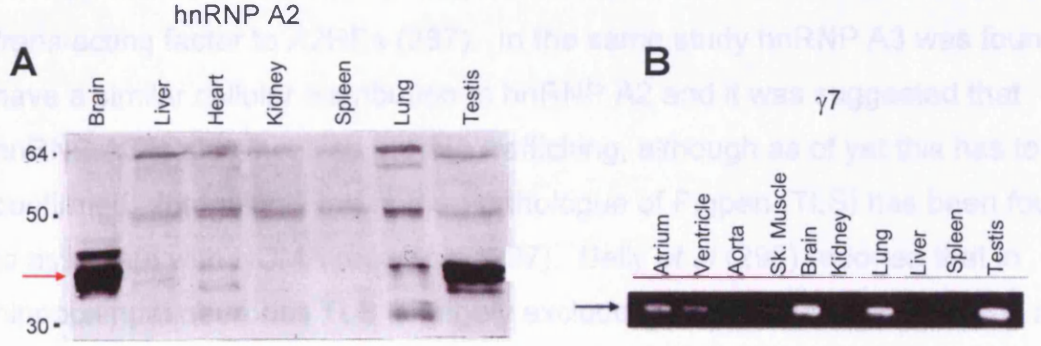

Fig. 8.1 hnRNP A2 and γ7 have similar expression profiles. Tissue distribution of A) hnRNP A2 protein (red arrow) and B) γ7 mRNA (blue arrow). Adapted from A. Hoek *et al* (261). B. Chu *et al* (171)

hnRNP A2 has been shown to be a *trans*-acting factor that has a role in the trafficking of mRNA (261). The cognate *cis*-acting sequence is a 21 nucleotide sequence known as the A2RE. In oligodendrocytes, A2RE/hnRNP A2 determinants are involved in at least four steps in the RNA trafficking pathway: (1) export from the nucleus to the cytoplasm, (2) granule assembly in the perikaryon, (3) transport along microtubules in the processes, and (4) translation activation in the myelin compartment (295). They have also been proposed to be responsible for dendritic RNA localisation in neurons of several mRNAs, including calcium-calmodulin-dependent protein kinase II alpha subunit and neurogranin mRNA (286;296).

$Ca_V2.2$ mRNA has previously been shown to be trafficked to the dendritic growth cones of cultured hippocampal neurons (268) and potential A2RE sites have been identified within it (262). Here it is shown that a potential A2RE site corresponding to bases 1096-1116 in mouse $Ca_V2.2$ mRNA is confirmed to bind hnRNP A2. Other potential A2REs are also present within $Ca_V2.2$ mRNA, however these have yet to be confirmed to bind hnRNP A2. These finding would suggest that the trafficking of $Ca_V2.2$ mRNA involves the A2RE/hnRNP A2 trafficking mechanism.

As mentioned previously the other two proteins identified were also RNA binding proteins. It is also possible that both these proteins are involved in the localisation of mRNA. hnRNP A3, like hnRNP A2 has been shown to be a *trans*-acting factor to A2REs (287). In the same study hnRNP A3 was found to have a similar cellular distribution to hnRNP A2 and it was suggested that hnRNP A3 is also involved in RNA trafficking, although as of yet this has to be confirmed. Intriguingly the human orthologue of Pigpen (TLS) has been found to associate with NDMA receptors (297). Belly *et al* (298) reported that in hippocampal neurones TLS is largely excluded from the neuronal nucleus and is found in the cytosol and in somatodendritic particles with some co-localisation with NMDA receptor clusters. They proposed that TLS may contribute to steering, anchoring or regulating mRNAs at synaptic sites.

Members of the hnRNP family of proteins have been shown to be involved in RNA stability. hnRNP D acts to stabilise c-fos,

granulocyte/macrophage colony-stimulating factor and β-adrenergic receptor mRNA (299-301). It has also been shown to destabilise c-myc mRNA (302). It has been proposed that the regulation of RNA metabolism is likely to involve a complex interplay between multiple RNA elements and trans-acting factors, including hnRNP A2.

Given the role of RNPs in RNA stability, the interaction between γ7 and three RNP's and that $Ca_V2.2$ mRNA is reduced by the co-expression of γ7, it is tempting to hypothesise that the mechanism of suppression of $Ca_V2.2$ expression by γ7 involves one of the three RNPs identified. A simple hypothesis would be that overexpression of γ7 sequesters the RNP which leads to $Ca_V2.2$ mRNA being destabilised. Alternatively overexpression of γ7 may lead to upregulation of one of the RNPs which leads to $Ca_V2.2$ mRNA destabilisation. It is possible that the RNPs bound to $Ca_V2.2$ mRNA expressed from a vector are different from endogenous $Ca_V2.2$ mRNA, as many RNPs bind during the splicing process. This may in part explain the lack of effect of γ7 upon endogenous channels.

The TARPs have been shown to be involved in the trafficking of AMPA receptor. From homology it is possible that γ7 would also be involved in trafficking. Here it is shown that γ7 co-immunoprecipitates with three RNPs that have been proposed to be involved in the trafficking of mRNA. It is an intriguing possibility that γ7 acts in a similar method to the TARPs, and is involved with guiding trafficked mRNA to its correct location within the cell.

As was described previously the C-terminus of γ7 alone is sufficient to suppress expression of $Ca_V2.2$. Interestingly a BLASTp search found that there is homology between the C-terminus of γ7 and the APOBEC-1 (Fig.8.2). While this is a low significance match, the protein it identifies is interesting. APOBEC1 is the catalytic subunit of the apoB RNA-editing enzyme which edits apolipoprotein B mRNA. This protein has previously been shown to interact with hnRNP A2 (303) and another member of the hnRNP family hnRNP C1 (304).

```
Score = 32.0 bits (68), Expect = 4.1
Identities = 16/40 (40%), Positives = 20/40 (50%), Gaps = 18/40 (45%)

          ISSDVSIQ-MTQ----------NYPPAI-----KYPDHL γ7
          ISS V+IQ MT+          NYPP+      +YP HL
          ISSGVTIQIMTEQEYCYCWRNFVNYPPSNEAYWPRYP-HL APOBEC-1
```

Fig. 8.2. There is homology between the C-terminus of γ7 and APOBEC-1. A BLASTp search for short, nearly exact matches to the C-terminus of γ7 identified a region in APOBEC-1 as have the highest similarity (excluding other γ subunits).

APOBEC-1 is a cytidine deaminase converting cytidine to uridine. Related to APOBEC-1 (and sharing some similarity to the C-terminus of γ7) are the adenosine deaminases acting on RNA (ADAR) family of proteins. These proteins convert adenosine residues into inosine (A to I) in mRNA. Interestingly one member of the ADAR family has been shown to be involved in the editing of GluR2 receptor mRNA (305). This results in the replacement of glutamine with arginine at position 607. Unedited Gln containing subunits readily tetramerize and traffic to synapses, whereas edited Arg containing subunits are largely unassembled and ER retained. Also, mRNA editing by ADARs has been suggested to be involved in mRNA stability (306).

While γ7 is unlikely to directly involved in A to I editing (as it doesn't not contain the catalytic site conserved in the ADAR family of proteins) it could be involved in recruiting ADARs or another RNA editing protein. There is already evidence of Ca_V α1 subunit mRNA being edited (307;308) and it is possible that γ7 may recruit a protein that edits $Ca_V2.2$ mRNA, resulting in the $Ca_V2.2$ mRNA or protein being more unstable.

8.4. Future Work

8.4.1. Cellular Distribution of γ7

The cellular distribution of γ7 could be further investigated using electron microscopy and gold immunolabelling. This would identify if any γ7 is present at

the plasma membrane and also if it is present within any intracellular organelles. The endogenous expression of γ7 in Purkinje cells would make them suitable to be used in these experiments.

8.4.2. Phosphorylation Sites of γ7

In addition to the N-glycosylation site present in γ7 there are also several potential phosphorylation sites. Phosphorylation of γ2 has been shown to be important in its role as a TARP (203-205) and the phosphorylation of γ7 may prove to be important also. Mutation of these sites to alanine, to mimic the non-phosphorylated site, and glutamate, to mimic the phosphorylated site, may reveal the importance of these site to the function of γ7.

8.4.3. The Structure of γ7

It is unlikely that a high-resolution structure of γ7, or any of the γ subunits, will be obtained soon. Members of the PMP family have thus far proved hard to purify and crystallise (309). If a model of any of the PMP family is identified then a model for the structure of γ7 may be obtained by comparison.

8.4.4. γ5

γ5 has high similarity to γ7 and is likely to serve similar functions. It would be interesting to examine if γ5 has similar effects on $Ca_V2.2$ expression. Furthermore, γ5 may interact with hnRNP A2, hnRNP A3 and Pigpen.

8.4.5. Interaction of γ7 and RNPs

It is essential to further confirm the interaction between γ7 and hnRNP A2, hnRNP A3 and Pigpen. One system that could be used is the yeast 2-hybrid system. This would require sub-cloning of the γ7, hnRNP A2, hnRNP A3 and Pigpen into vectors with a portion of a transcriptional activator of a reporter gene (e.g. β-Gal or Lex A). This method will only identify a direct interaction between γ7 and one of the RNPs. If the interaction between γ7 and the RNPs

requires a yet undetected protein then it will not be picked up by this system. A search for proteins that interact with γ7 could be performed by using a library of proteins rather than testing direct interactions. Unfortunately previous attempts to use γ7 for the yeast 2-hybrid system were unsuccessful as the vector autoactivated (Dr. F. Moss personal communication).

Endogenous interaction between γ7 and hnRNP A2, hnRNP A3 and Pigpen could be identified by co-immunoprecipitation from mouse brain. Thus far however, the antibodies for γ7, and hnRNP A2 were found to be unsuitable for this. It would also be interesting to investigate if γ7 and any of the RNPs co-localise within the cells. This was attempted for hnRNP A2 and γ7 in PC12. However, once again the antibodies for hnRNP A2 were unsuitable (hnRNP A2 was not detectable above background). Antibodies for hnRNP A3 and Pigpen have yet to be tested.

It is hypothesised that the C-terminus of γ7 is required for the interaction with the RNPs and it may be sufficient by itself to form these interactions. Co-immunoprecipitation could once again be used. However, the C-terminus of γ7 was found to express poorly in mammalian cells. Using a large amount of starting material may overcome this problem. In addition a His-tagged γ7 construct has been generated to express the C-terminus of γ7 in a bacterial system. This can then be used to attempt to pull down interacting proteins from mouse brain. In addition, if purified hnRNP A2, hnRNP A3 and Pigpen can be obtained, then direct *in vitro* interaction between them and the C-terminus of γ7 can be tested.

8.4.6 γ7 and RNA editing

It would be interesting to see if $Ca_V2.2$ mRNA is edited and, if so, if γ7 is involved in this process. Traditionally RNA editing has been identified by sequencing genomic DNA and comparing the sequence to cDNA. This can be a time consuming process. However, improved, quicker methods of identifying RNA editing are now being used (310).

8.4.7 γ7 and RNA Trafficking

The interaction of γ7 with proteins that have been shown to be involved in the trafficking of RNA points towards the intriguing possibility that γ7 may also be involved in this process. As mentioned above, it would be interesting to perform experiments to see if γ7 and any of the three RNPs co-localise in cells that have been shown to traffic RNA. In addition it would be interesting to see if suppression of γ7 expression, using RNAi, alters RNA trafficking within these cells.

8.4.8. The Effect of γ7 on $Ca_V2.2$ mRNA

It has been determined that the suppression of $Ca_V2.2$ by the co-expression of γ7 takes place at the level of RNA. The reduced amount of $Ca_V2.2$ mRNA could be due to a reduced level of expression or due to an increased rate of degradation. To examine this QPCR could be used to determine $Ca_V2.2$ mRNA half life of $Ca_V2.2$ in the presence and absence of γ7. A decreased half life would suggest that the co-expression of γ7 leads to destabilisation of $Ca_V2.2$ mRNA. This has now been performed by Dr L. Ferron in our laboratory with the result that γ7 doubles the rate of degradation of $Ca_V2.2$ mRNA.

As $Ca_V2.2$ mRNA has been found to be destabilised by γ7 co-expression then it would be interesting to see if this effect could be attenuated by the further co-expression of one of the RNPs. Additionally, it would be interesting to investigate whether expression of any of the RNPs leads to a stabilisation or destabilisation of $Ca_V2.2$ mRNA. Furthermore, it would be interesting to see if there was a difference between $Ca_V2.2$ mRNA expressed from a vector and endogenously expressed $Ca_V2.2$ mRNA in the presence and absence of γ7.

In summary there is little evidence that γ7 forms part of a VDCC complex. However, it does affect $Ca_V2.2$ mRNA. Further work examining the relationship between γ7 and $Ca_V2.2$ mRNA will hopefully elucidate γ7 physiological roles.

Appendix

A.1. Materials Used

A.1.1. Chemicals

4',6-diamidino-2-phenylindole (DAPI)	Molecular Probes
Agarose	Sigma
Amplicillin	Sigma
Cholic Acid	Sigma
Complete™ protease inhibitor cocktail	Roche Diagnostics
dNTPs	Invitrogen
EDTA	Sigma
Ethidium bromide	Sigma
FITC	Invitrogen
Igepal	Sigma
NaCl	Sigma
Phosphate buffered saline (PBS)	Sigma
Protein G Agarose	Sigma
Sodium dodecyl sulphate (SDS)	Sigma
TexasRed–phalloidin	Invitrogen
Tris 7-9	Sigma
Triton-X 100	Sigma
Tween	Sigma
VectorShield	Vector Laboratories

A.1.2. Kits

BCA assay	Pierce
Big Dye Kit	Applied Biosystems
Gel extraction kit	Invitrogen
ECLPlus	APB
Maxiprep kit	Invitrogen
Miniprep kit	Invitrogen
PCR clean up kit	Invitrogen
RNeasy kit	Qiagen

SilverExpress Silver Stain	Invitrogen

A.1.3. Tissue Culture Reagents

1% non-essential amino acids	Invitrogen
Cell Line Nucleofector™ Kit V (Solution V)	Amaxa GmbH
Collagen (Type IV) Rat Tail	Sigma
Dulbecco's Modified Eagle's Medium	Invitrogen
Fetal bovine serum	Invitrogen
FuGENE 6 transfection reagent	Roche Diagnostics
Geneporter transfection reagent	Gene Therapy Systems
Geneticin	Invitrogen
Horse Serum	Invitrogen
Minimum Essential Medium	Invitrogen
Nerve Growth Factor 7S fragment (murine, natural)	Invitrogen
Poly-L-lysine	Sigma
Roswell Park Memorial Institute 1640 medium	Invitrogen

A.1.4. Equipment

Avant-3100 Sequencer	Applied Biosystems
DU 800 Spectrophotometer	Beckman Coulter
iCylcer	BioRad
LSM 510 Microscope	Zeiss
Nucleofector device	Amaxa GmbH
PCR machine	Techne
Semi-dry transfer system	BioRad
TCS SP confocal scanning laser microscope	Leica
Typhoon phosphoimager	APB

A.1.5. Enzymes

Calf Intestinal Alkaline Phosphatase (CIAP)	Promega
EcoRI	Invitrogen
Moloney Murine Leukemia Virus Reverse Transcriptase (MMLVRT)	Promega
NcoI	Invitrogen
Pfu	Stratgene
PvuI	Invitrogen
RNase-free DNase	Quigen
T4 ligase	Promega

A.1.6. Miscellaneous

Library efficiency DH5a competent cells	Invitrogen
iQ SYBR supermix	BioRad
QIAshredder columns	Qiagen
RNasin	Promega
Random hexamer primers	Promega
Polyvinylidene fluoride membrane (PVDF)	BioRad
Bovine serum albumin (BSA)	Sigma
Rainbow markers	APB
Sigma high markers	Sigma
Sigma low markers	Sigma
4-12% Bis-Tris gels	Invitrogen

A.1.6. Software

Beacon Designer	Premier Biosoft
Chromas	Technelysium Pty Ltd
ImageQuant	Molecular Dynamics
Omiga	Accelrys
Photoshop	Adobe

A.2. Antibodies

Anti-γ7 (Loop). Rabbit polyclonal antibody. Raised against the peptide YPPAIKYPDHLHIS, which is in the expected extracellular loop of γ7. Affinity purified against the peptide.

Anti-γ7 Tail). Rabbit polyclonal antibody. Raised against the peptide VASEYFLEPEINLVTEN, which is in the expected cytoplasmic C-terminal tail of γ7. Affinity purified against the peptide.

Anti-Ca_V2.2. Rabbit polyclonal antibody. Raised against the peptide identical to residues 846-861 within the II-III loop of rabbit brain Ca_V2.2 which is in the expected cytoplasmic II/III loop of Ca_V2.2. Affinity purified against the peptide.

Anti-K_V3.1b. Rabbit polyclonal antibody. Raised against the CKESPVIAKY MPTEAVRVT, corresponding to residues 567-585 of rat K_V3.1b. Purchased from Alomone labs.

High Affinity Anti-HA (Clone 3F10). Rat monoclonal antibody. Recognizes the HA peptide sequence (YPYDVDYA) derived from the hemagglutinin protein of human influenza virus. Purchased from Roche Diagnostics.

Anti-HA. Rabbit polyclonal antibody. Recognizes the HA peptide sequence (YPYDVDYA) derived from the hemagglutinin protein of human influenza virus. Purchased from Sigma.

Anti-Rabbit-HRP. Goat polyclonal antibody raised against rabbit IgG. Conjugated to horseradish peroxidase. Purchased from BioRad.

Anti-hnRNP A2/B1 (F16) Goat polyclonal antibody. Raised against a peptide mapping within an internal region of hnRNP A2/B1 of human origin. Purchased from Autogen Bioclear.

Anti-hnRNP A/B (H200). Rabbit polyclonal antibody. Raised against amino acids 1-200 mapping at the N-terminus of hnRNP A1 of human origin. Purchased from Autogen Bioclear.

Anti-PDI (ab2792) Mouse monoclonal antibody. Raised against full length native protein (purified from rat). Purchased from Abcam

Anti-Rabbit IgG (Whole Molecule) Biotin Conjugate Goat polyclonal antibody. Raised against rabbit IgG. Purchased from Sigma.

Anti-Mouse IgG (Whole Molecule) Biotin Conjugate Goat polyclonal antibody. Raised against mouse IgG. Purchased from Sigma.

A.3. Primers Used

All primers used were purchased from Invitrogen.

A.3.1. Primers Used for the Generation of Constructs

$\gamma 7_{(1\text{-}238)}$

Forward 5'-GACGAATTCACCATGAGTCACTGCAG-3
Reverse 5'-ATAGAATTCCTCAGCGCCACGCCTCGGGCT-3'

$\gamma 7_{(1\text{-}271)}$

Forward 5'-GACGAATTCACCATGAGTCACTGCAG-3'
Reverse 5'-AGCGAATTCTCAGGAGATGTGCAGGTGGT-3'

$\gamma 7_{(201\text{-}275)}$

Forward 5'-ACGAATTCATGACCAAGCGCTACG-3'
Reverse 5'-ACGAATTCAGCAGGGCGAGGTG-3'

$\gamma 7$_CFP

Forward 5'-GACGAATTCACCATGAGTCACTGCAG-3'
Reverse 5'-ATAGGATCCGAGCAGGGCGAGGTGGAGA-3'

$\gamma 7$_HA

Forward 5'-ATAGGACGGTACCAGCATGAGTCACTGCAGCA-3'
Reverse 5'-ATAGAATTCAAGCGTAGTCTGGGACGTCGTATGGGTAGC
AGGGCGAGGTGGAGA-3'

HA_γ7

Forward 5'-TATGGTACCATGTACCCATACGACGTCCCAGACTACGCTAGT
CACT GCAGCAGCCG-3'
Reverse 5'-TATGAATTCAGCAGGGCGAGGTGG-3'

$\gamma 7_{(201\text{-}275)}$ _HA

Forward 5'-ACGGTACCATGACCAAGCGCTACG-3'
Reverse 5'-ATAGAATTCAAGCGTAGTCTGGGACGTCGTATGGGTAGCAG
GGCGAGGTGGAGA-3'

γ7_STOP

Forward 5'-TACGGTACCAGCATGAGTCACTGAAGCA-3'
Reverse 5'-TATGAATTCAGCAGGGCGAGGTGG-3'

γ2TM γ7Tail

Forward_1 5'-TATGGTACCATGGGGCTGTTTGATCGAG-3'
Reverse_1 5'-GCGTAGCGCTTGGTGATAAACATGTGCAC-3'

Forward_2 5'-GTGCACATGTTTATCACCAAGCGCTACGC-3'
Reverse_2 5'-TATGAATTCAGCAGGGCGAGGTGG-3'

γ7_PDZ

Forward 5'-ATAGGACGGTACCAGCATGAGTCACTGCAGCA-3'
Reverse 5'-TAAGTAGAATTCATACGGGGGTGGTGGAGATGTGCAGGT-3'

γ7N45A

Forward 5'-ATAGGACGGTACCAGCATGAGTCACTGCAGCA
ACCGCAGGCCCAGACCAC-3'
Reverse 5'-GTGGTCTGGGCCTGCGGT-3'

A.3.2. RT-PCR and QPCR Primers

A.3.2.1. QPCR primers

$Ca_V2.2_{(QPCR)}$

Forward 5'-GGCAAGAAGGAGGCAGAG-3'
Reverse 5'-GCAGAAGCGACGGAGTAG-3'

Annealing temperature used: 53°C

$Ca_V1.2_{(QPCR)}$

Forward 5'-TCGCTCTGCCTCTCCATT-3'
Reverse 5'-TTCCACTACCGCCTCCTT-3'

Annealing temperature used: 53°C

$\gamma 7_{(QPCR)}$

Forward 5'-GAGAGTCTGCTTCTTTGC-3'
Reverse 5'-CACCAAGTTGATCTCTGG-3'

Annealing temperature used: 56.7°C

CHOP

Forward 5'-GAAAGCAGCGCATGAAGG-3'
Reverse 5'-CCATTCGGTCAATCAGAGC-3'

Annealing temperature used: 61°C

XBP edited

Forward 5'-GCCTTGTAGTTGAGAACCAG-3'
Reverse 5'-GAGGTGCACGTAGTCTGAG-3'

Annealing temperature used: 56.7°C

XBP unedited

Forward 5'-GTAGTTGAGAACCAGGAG-3'
Reverse 5'-CTGGCCTCACTTCATTC-3'

Annealing temperature used: 61.1°C

A.3.2.2. RT-PCR primers

$\gamma 1_{(Rat)}$

Forward 5'-CACTCAGAAGGAGTACAGC-3'
Reverse 5'-CCGAAGGACAGAAAGG-3'

$\gamma 2_{(Rat)}$

Forward 5'-CACTTTCCCGAAGACG-3'
Reverse 5'-GACCACCCATGAAGAGC-3'

This primer pair was also used for QPCR. Annealing temperature used: 54°C

$\gamma 4_{(Rat)}$

Forward 5'-GTGAGCTGTCCATGTACACG-3'
Reverse 5'-GGAAACCCTCCTTTAGGTCC-3'

$\gamma 6_{(Rat)}$

Forward 5'-GAATCTCGGCTTGACTCC-3'
Reverse 5'-GAATCTCGGCTTGACTCC-3'

$\gamma 7_{(Rat)}$

Forward 5'-ATGAGTCACTGCAGCAGC-3'
Reverse 5'-TCAGCAGGGTGAAGTGGA-3'

$Actin_{(Rat)}$

Forward 5'-ATGGATGACGATATCGCTGC-3'
Reverse 5'-CTAGAAGCATTTGCGGTGCA-3'

$\gamma 7\_STOP_{(RT)}$

Forward 5'-TGAGTCACTGAAGCA-3'
Reverse 5'-AACTGGCCCGAGTAGT-3'

A.3.3. Biotinylated RNA Oligos

A2RE

5'-Biotin-GCCAAGGAGCCAGAGAGCAUG-3'

$Ca_V2.2$

5'-Biotin-GCCAAGGAGCGGGAGCGAGUC-3'

Non-specific

5'-Biotin-CAAGCACCGAACCCGCAACUG-3'

A.4. Companies

Accelrys, Cambridge, UK

Adobe, CA, USA

Alomone labs, Jerusalem, Israel

Amaxa GmbH, Koeln, Germany

Amersham Pharmacia Biotech (APB), Little Chalfont, UK

Applied Biosystems, CA, USA

Beckman Coulter, Bucks, UK

BioRad, Hercules, CA, USA

Carl Zeiss Ltd, Harts, UK

Clontech, CA, USA

ECACC, Salisbury, UK

Gene Therapy Systems, San Diego, CA, USA

Invitrogen Carlsbas CA, USA

Leica, Bucks, UK

Molecular Dynamics, Bucks, UK

Pierce, Northumberland, UK

Premier Biosoft, CA, USA

Qbiogene, Harefield, UK

Qiagen, Crawley, UK

Roche Diagnostics, Mannheim, Germany

Sigma, UK

Stratgene La Jolla, CA, USA

Techne, Staffs, UK

Technelysium Pty Ltd, Tewantin, Australia

Vector Laboratories, Burlingame, USA

A.4. Additional Experiments

A.4.1 Additional Methods

A.4.1.1. Immunohistochemistry

For detection of $\gamma 7_{(Loop)}$ antibody was used. Free-floating brain coronal sections (40µm thick) from adult mice perfused with 4% paraformaldehyde were blocked for 1 hour at room temperature with PBS, 0.1% Triton X-100 and 10% goat serum. Sections were incubated overnight at 4°C with the affinity purified γ7 loop antibody (0.8 $\mu g.ml^{-1}$), the antibody adsorbed with its peptide (0.8 and 17.5 $\mu g.ml^{-1}$ respectively), or no primary antibody. The secondary antibody used was biotin-conjugated goat anti-rabbit followed by streptavidin-Horse Radish Peroxidase and reaction with diaminobenzidine for 15 min. Sections were mounted on poly-L-lysine-coated slides, dehydrated, cleared and mounted in DPX.

A.4.1.2. In situ Hybridization

Adult male mice were killed by cervical dislocation and the brains removed and frozen on dry ice. Sagittal sections (14 µm thick) were cut with a cryostat and mounted on poly-L-lysine-coated slides, fixed in 4% paraformaldehyde for 5 min. at 4°C, washed for 1 min. in PBS, then treated for 5 minutes in 70% ethanol and stored in 90% ethanol at 4°C. An antisense probe for γ7 was prepared from the oligonucleotide 5'-CGTCACCAAGTTGATCTCTGGTTCAAGAAAGTACTCAGAAGC CAC-3' by 3' end labelling with [^{35S}]dATP. A sense probe was also generated from the complementary sequence. For *in situ* hybridization, after drying at room temperature each slide was incubated with 1µl of the radiolabelled probe (~1.5 x 108 d.p.m.) and 2µl of DTT in 100 µl of hybridization solution containing 50% formamide, 4 x SSC, 25 mM Sodium phosphate (pH 7.0), 1 mM Sodium pyrophosphate, 5 x Denhardt's solution, 200 $mg.ml^{-1}$ denatured herring sperm

DNA, 100 µg.ml-1 polyadenylic acid and 10% (w/v) dextran sulphate in a humid chamber overnight at 42°C. Control slides with adjacent sections were labelled with the sense probe. The following day the slides were washed two times in 1 x SSC at 55°C for 30 minutes followed by a sequence of 0.1 x SSC, 70% and 95% ethanol at room temperature for 1 minute each. Slides were left to dry at room temperature for up to 2 hours and exposed to a X-ray film for about two weeks. For examination at higher power, slides were developed by immersion in photographic emulsion K5. After development, slides were viewed by dark field illumination.

A.4.1.3 Electrophysiology

Xenopus oocytes were prepared, injected and utilized for electrophysiology as previously described (311), with the following exceptions. Plasmid cDNAs for the different VDCC subunits α_1, $\alpha_2\delta$-2, β_{1b} and other constructs such as γ7 were mixed in equivalent weight ratios at 1 $\mu g.\mu l^{-1}$, unless otherwise stated, and 9 nl injected intranuclearly. The corresponding cRNAs were made by mMessage mMachine, diluted to 0.5 $\mu g.\mu l^{-1}$, and 60 nl of the mixture injected intracytoplasmically.

When used, (~0.25 U in 30 nl) of recombinant RNAsin or its vehicle, was injected intracytoplasmically 2 hours before cDNA injection. The recording solution for $Ca_V2.2$ injected oocytes contained: 5 mM $Ba(OH)_2$; 80 mM TEA-OH ; 2 mM CsOH ; 5 mM HEPES (pH 7.4 with methanesulfonic acid). The $Ba(OH)_2$ concentration was raised isotonically to 10 or 40 mM where stated.

Whole-cell patch-clamp recording using tsA-201 and PC12 cells was performed and analyzed as described (238;312), with 1 - 20 mM Ba^{2+} as charge carrier and a holding potential of –100mV. Currents were measured 10 ms after the onset of the test pulse and the average over a 2 ms period was calculated and used for analysis. *Xenopus* oocyte recordings were performed as described (313). The Ba^{2+} concentration was 5 mM, unless stated. Data are expressed as mean ± S.E.M. and I-V plots were fit with a modified Boltzmann equation as described (313).

A.4.1.1. Measurement of mRNA Levels

COS-7 cells were transfected with cDNA encoding γ7 alone, γ7 with $Ca_V2.2$ (ratio 1:2), or $Ca_V2.2$ alone using GenePorter. Cells were harvested after 48 hours. Total RNA was purified using the RNeasy kit. mRNA was then purified from 30 µg total RNA using Dynabeads. Samples were denatured, run on a 1% formaldehyde gel and transferred onto positively-charged membranes by downward capillary action. RNA was cross-linked onto the membrane using UV.

DNA fragments were made using the following primers: $Ca_V2.2$, 5'ACT TCG TGG TAG TCC TCA and 5'GTC GCT TCT GCT CTT CTT GG; γ7, 5'TTC TGA AGA CAG TGC GCA CG and 5'TCA TTT GGA TGG ACA CGT CG. The probes were labelled with psoralen-biotin using the BrightStar labelling kit, stored at -80°C and denatured at 90°C for 10 min immediately before use. Membranes were prehybridized in UltraHyb buffer at 42°C for 6h. and then hybridized with the biotinylated probe at 50°C overnight. After washing membranes in 0.5 x SSC (1 x SSC is 150 mM NaCl, 15 mM Na citrate pH 7) , 0.1% SDS at 65°C, the BrightStar assay was carried out following kit instructions. Bands were detected using autoradiography. Data were analysed using ImageQuant after scanning autoradiographs.

For QPCR, plasmid cDNAs for CaV2.2, β_{1b}, $\alpha_2\delta$-2, Kir2.1-AAA plus γ7 or blank vector were injected intranuclearly into oocytes in the ratio 6 : 2 : 2 : 1 :3. After 72 h, individual oocytes were harvested following electrophysiological recording. RT and QPCR were performed as describe in general methods. The following primers were used:

$Ca_V2.2$, 5'CTC TGC GCT TAC TGA GAA TC-3' and 5'AAC AGG AAG AGC AGG AAG AG-3'

Kir2.1-AAA, 5'TGG GTG AGA AGG GAC AGA GGT A and 5'AGG AGA GCA CGA AGG CAA GAC-3'

β_{1b}, 5'CTT AAG GAA GGA GGC AGA GC-3' and 5'GGA GAC GGA TTG TAG CCA AC-3'

18S, 5'TGA CTC AAC ACG GGA AAC CT-3' and 5'AAT CGC TCC ACC AAC TAA GAA C-3'

Data were normalized for expression of 18S ribosomal RNA.

A.4.2. γ7 Localisation

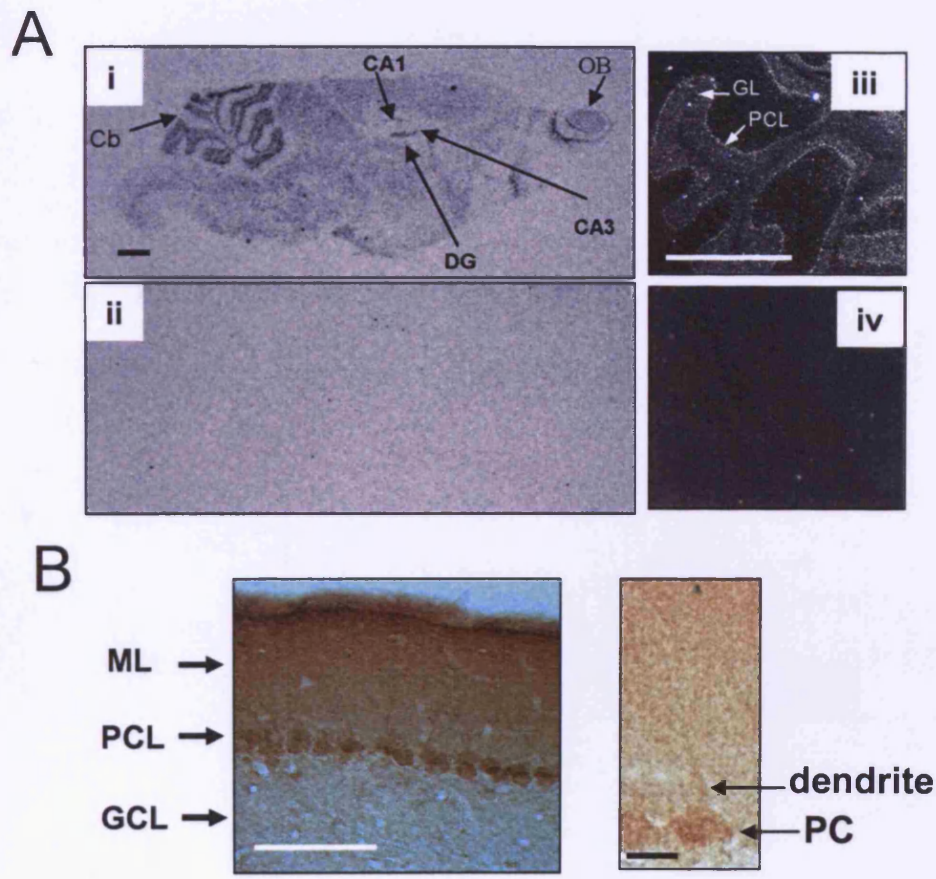

Fig.A.1. Localisation of γ7 mRNA and protein. A) *In situ* hybridization for γ_7 mRNA in a sagittal section of mouse brain, using a ^{35}S-γ7 antisense oligonucleotide probe (i, iii) and a γ7 sense control probe (ii, iv). Expression of γ7 mRNA is widespread (i), with stronger expression in olfactory bulb (OB), cerebellum (Cb) and CA1, CA3 and dentate gyrus (DG) regions of the hippocampus. The localisation of γ7 mRNA in the cerebellum was examined at higher power (iii) and showed strong expression in the Purkinje cell layer (PCL)

and also in the granule cell layer (GL). Scale bars represent 1mm. B) Immunohistochemical localisation for γ7 in mouse cerebellum, showing presence in individual Purkinje cells (left) and their dendrites (right), using the $\gamma7_{(Loop)}$ antibody. Staining was lost with no primary antibody or with antibody preabsorbed to immunizing peptide (data not shown). Scale bar represents 50 μm (left) and 10 μm (right).

A.4.3. Electrophysiological Data for γ7 Constructs

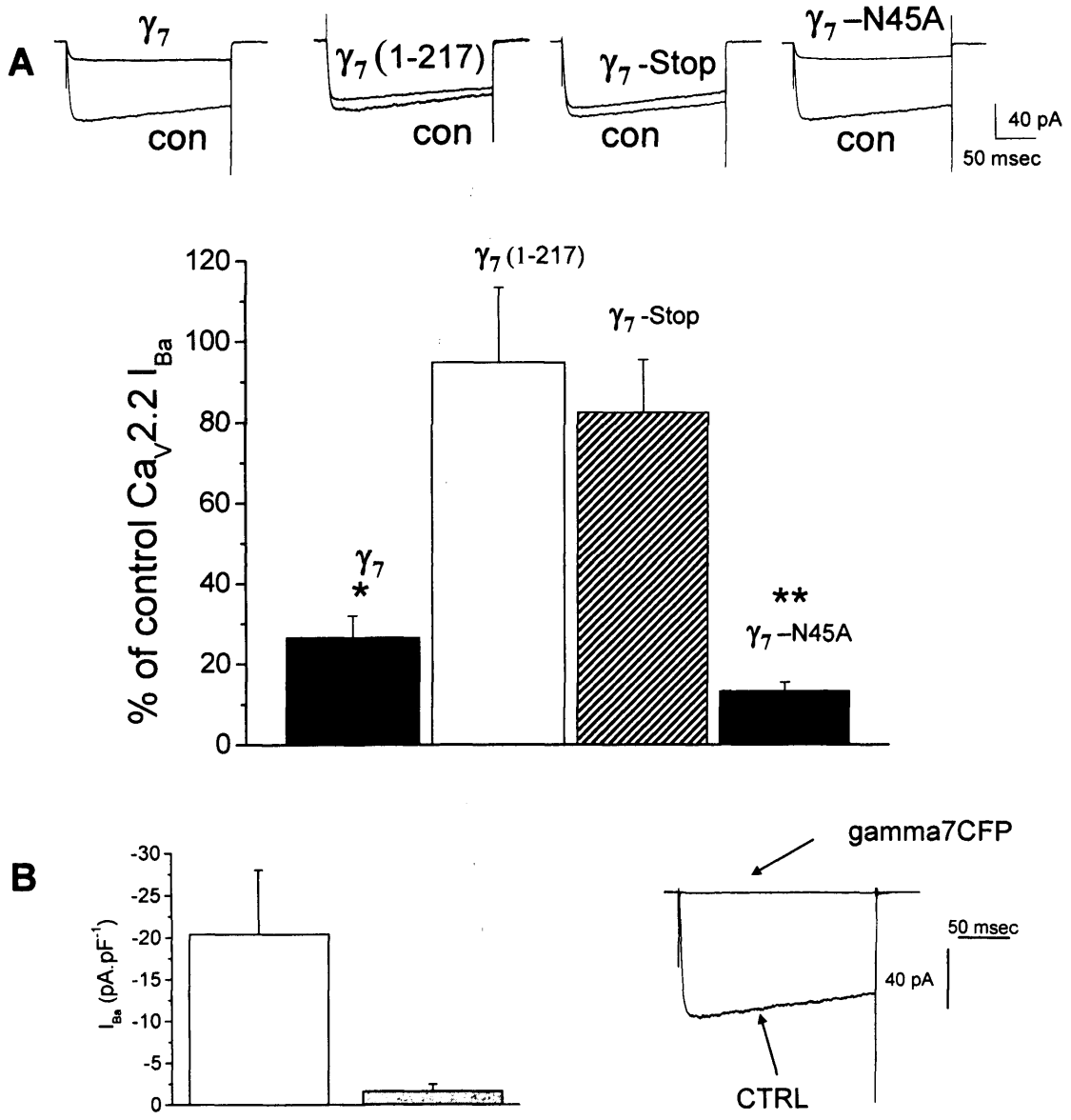

Fig.A.2. The effect of γ7constructs on $Ca_V2.2$ current expressed in tsA-201 cells.
A)Upper panel: representative traces of Ba^{2+} currents induced by co-

transfection of $Ca_V2.2$, β1b and $\alpha_2\delta$-2with pMT2 as control (con), compared to γ7 (left), $\gamma7_{(1\text{-}217)}$ (center left), γ7_STOP (center right) and γ7(N45A) (right). Currents were elicited by depolarisation to +5 mV from a holding potential of –100 mV. Calibration bars refer to all traces. Lower panel: mean inhibition of Ba^{2+} currents (expressed as % of control ± S.E.M.) induced by co-expression of $Ca_V2.2$ with γ7 (black bar, n=21), $\gamma7_{(1\text{-}217)}$ (white bar, n=15), γ7_STOP (hatched bar, n=28) or γ7(N45A) (grey bar, n=10). Statistical significance ** $p<0.01$ Student's t test. B) Left. Value of the peak of barium current recorded at 0 mV for $Ca_V2.2$ (white bar n=10) and for $Ca_V2.2$ + γ7 (grey n=12). Right: Representative traces of Ba^{2+} currents induced by co-transfection of $Ca_V2.2$, β1b and $\alpha_2\delta$-2with pMT2 as control (CTRL), compared to γ7_CFP.

A.4.4. Electrophysiological Data for PC12 Cells

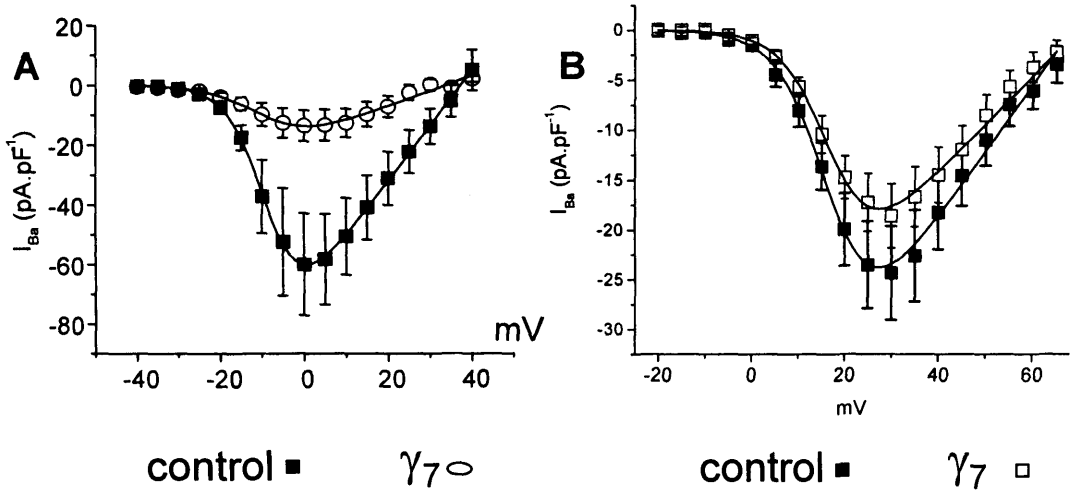

Fig.A.3. Effect of γ7 expression on endogenous and transient transfection induced N-type calcium current in PC12 cells. A) I-V relationship of N-type Ba_{2+} currents induced by transfection of $Ca_V2.2$ cDNA (control, ■, n=44) or $Ca_V2.2$ plus γ_7 (γ_7, ○, n=21).into undifferentiated PC12 cells. B) I-V relationship of endogenous N-type Ba^{2+} currents in differentiated PC12 cells. (control, ■, n = 18) or γ_7 (γ_7,□, n = 12)

A.4.5. Suppression of $Ca_V2.2$ Expression by γ7 Takes Place at the RNA Level

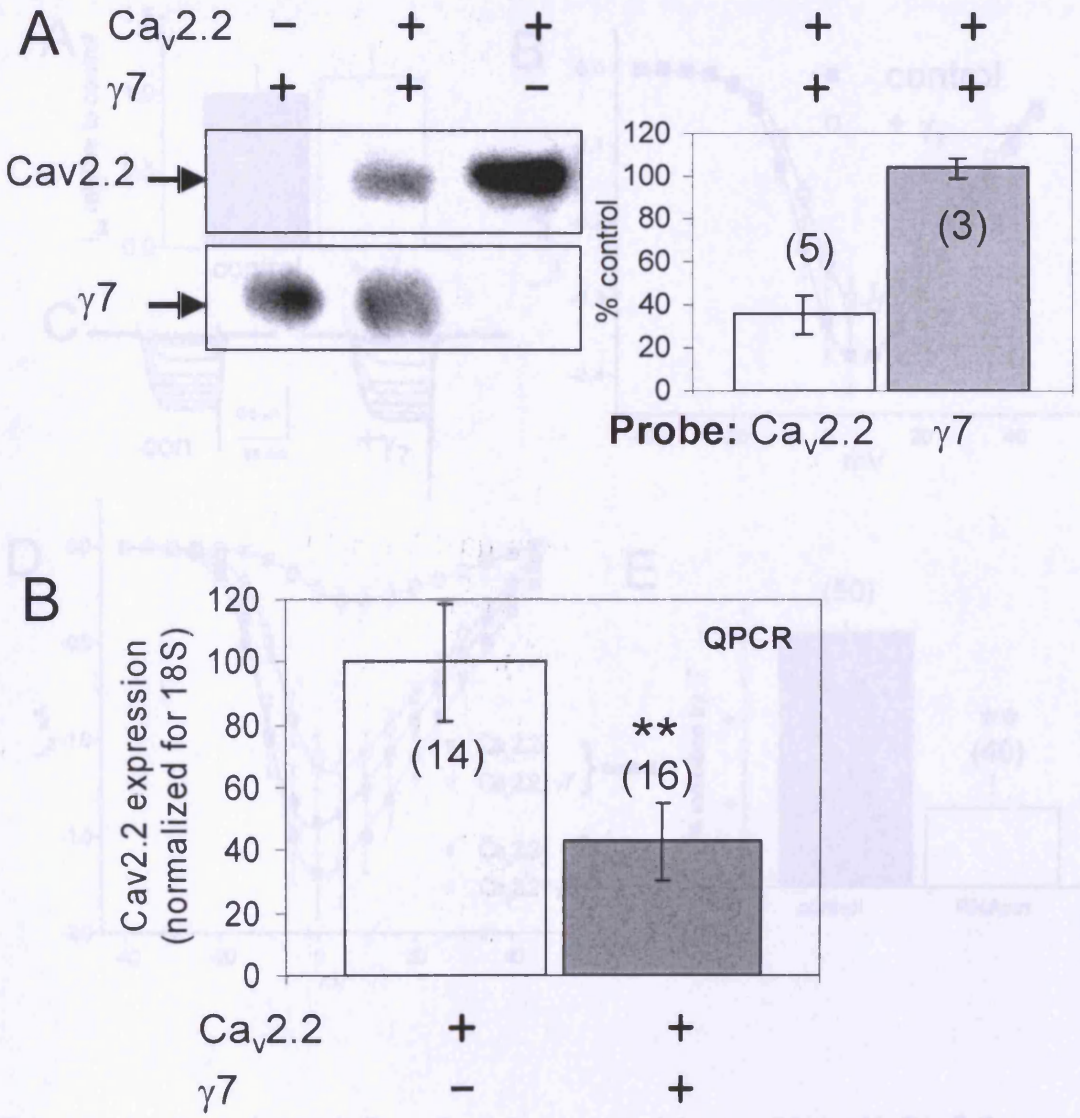

Fig. A.4. Effect of γ7 on $Ca_V2.2$ mRNA levels. A: Northern blots were prepared using mRNA isolated from COS-7 cells expressing γ7 alone (left), γ7 plus $Ca_V2.2$ (middle) or $Ca_V2.2$ alone (right) and hybridized with a biotinylated probe against the I-II loop of $Ca_V2.2$ (top). The blot was stripped and re-probed for γ7 (bottom). Right, histogram showing data analysed using ImageQuant. Amount of $Ca_V2.2$ (open bar) or γ7 (grey bar) is shown as a percentage of control, either $Ca_V2.2$ or γ7 alone. Numbers of separate experiments are given in parentheses. ** $p < 0.01$ B: $Ca_V2.2$, β1b, $\alpha_2\delta$-2were expressed in oocytes in the absence (open bar) or presence (grey bar) of γ7. QPCR was used to detect

$Ca_V2.2$ in individual oocytes. Numbers of samples are given in parentheses. ** $p<0.01$.

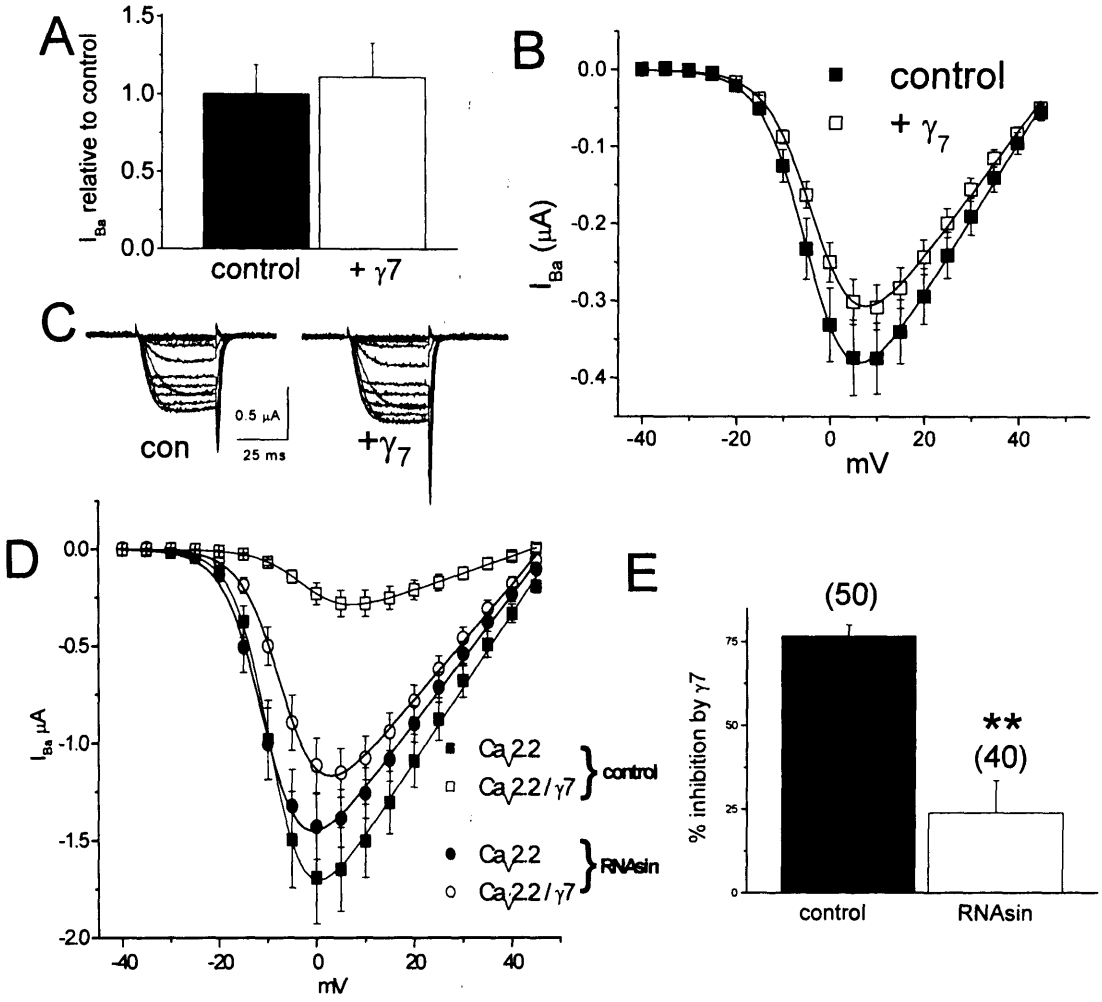

Fig. A.5. Lack of effect of γ7 on $Ca_V2.2$ expressed from mRNA. A) $Ca_V2.2$ was expressed from cytoplasmic injection of mRNA, following γ7, β1b and $\alpha_2\delta$-2 intranuclear injection of cDNA. The peak I_{Ba} is shown in 10 mM Ba^{2+}, relative to control for n= 17 control cells, and n= 29 in the presence of γ_7. B) Example currents from -30 to +30 mV for the two conditions shown in B. C) $Ca_V2.2$, β1b, $\alpha_2\delta$-2 and γ7 were all injected as mRNA. The current-voltage relationship is shown for n= 38 controls (■) and n = 35 (○) in the additional presence of γ7. Data are fit by a modified Boltzmann function, with $V_{50,act}$ of -3.6 and -2.3 mV respectively and G_{max} of 9.8 and 8.2 μS, respectively. D) Current-voltage relationship for cells injected into the cytoplasm with either RNAsin (●, ○) or its vehicle (■, □) prior to intranuclear cDNA injection of $Ca_V2.2$ / β1b/$\alpha_2\delta$-2 (●, ■,

n=50, 25) or $Ca_V2.2$ / β1b /$\alpha_2\delta$-2 /γ7 (○, □, n =40, 26). Data are fit by a modified Boltzmann function, with $V_{50,act}$ of -10.2 (●), -8.9 (■), -6.3 (○) and -1.6 (□) mV, respectively and G_{max} of 33.3 (●), 38.3 (■), 30.1 (○) and 8.9 (□) μS, respectively. E) Percentage inhibition by γ7 of I_{Ba} at 0 mV in the presence of either vehicle or RNAsin. ** $p< 0.01$.

References

1. Lodish, H., Berk, A., Zipursky, S. L., Matsudaira, P., Baltimore, D., and Darnell, J. E. (200) *Molecular Cell Biology*, 4th Ed., W. H. Freeman & Co, New York

2. Hodgkin, A. L. and Huxley, A. F. (1952) *J.Physiol* **117,** 500-544

3. Hodgkin, A. L. and Huxley, A. F. (1952) *J.Physiol* **116,** 473-496

4. Hodgkin, A. L. and Huxley, A. F. (1952) *J.Physiol* **116,** 449-472

5. Hodgkin, A. L. and Huxley, A. F. (1952) *J.Physiol* **116,** 497-506

6. MacKinnon, R. (1991) *Nature* **350,** 232-235

7. Liman, E. R., Tytgat, J., and Hess, P. (1992) *Neuron* **9,** 861-871

8. Doyle, D. A., Morais, C. J., Pfuetzner, R. A., Kuo, A., Gulbis, J. M., Cohen, S. L., Chait, B. T., and MacKinnon, R. (1998) *Science* **280,** 69-77

9. Jiang, Y., Lee, A., Chen, J., Cadene, M., Chait, B. T., and MacKinnon, R. (2002) *Nature* **417,** 515-522

10. Zheng, J., Sun, X., Chen, J., Jiang, F., Li, W., and Xie, S. (2002) *Zhonghua Zhong.Liu Za Zhi.* **24,** 24-26

11. Jiang, Y., Lee, A., Chen, J., Ruta, V., Cadene, M., Chait, B. T., and MacKinnon, R. (2003) *Nature* **423,** 33-41

12. Armstrong, C. M. and Bezanilla, F. (1973) *Nature* **242,** 459-461

13. Noda, M., Shimizu, S., Tanabe, T., Takai, T., Kayano, T., Ikeda, T., Takahashi, H., Nakayama, H., Kanaoka, Y., Minamino, N., and . (1984) *Nature* **312,** 121-127

14. Stuhmer, W., Conti, F., Suzuki, H., Wang, X. D., Noda, M., Yahagi, N., Kubo, H., and Numa, S. (1989) *Nature* **339,** 597-603

15. Papazian, D. M., Timpe, L. C., Jan, Y. N., and Jan, L. Y. (1991) *Nature* **349,** 305-310

16. Jiang, Y., Ruta, V., Chen, J., Lee, A., and MacKinnon, R. (2003) *Nature* **423,** 42-48

17. Swartz, K. J. (2004) *Nat.Rev.Neurosci.* **5,** 905-916

18. Shrivastava, I. H., Durell, S. R., and Guy, H. R. (2004) *Biophys.J.* **87,** 2255-2270

19. Ahern, C. A. and Horn, R. (2004) *Trends Neurosci.* **27,** 303-307

20. Monne, M., Hessa, T., Thissen, L., and von Heijne, G. (2005) *FEBS J.* **272,** 28-36

21. Grabe, M., Lecar, H., Jan, Y. N., and Jan, L. Y. (2004) *Proc.Natl.Acad.Sci.U.S.A* **101,** 17640-17645

22. Sands, Z., Grottesi, A., and Sansom, M. S. (2005) *Curr.Biol.* **15,** R44-R47

23. MacKinnon, R. and Miller, C. (1989) *Science* **245,** 1382-1385

24. Heinemann, S. H., Terlau, H., Stuhmer, W., Imoto, K., and Numa, S. (1992) *Nature* **356,** 441-443

25. Schlief, T., Schonherr, R., Imoto, K., and Heinemann, S. H. (1996) *Eur.Biophys.J.* **25,** 75-91

26. Sun, Y. M., Favre, I., Schild, L., and Moczydlowski, E. (1997) *J.Gen.Physiol* **110,** 693-715

27. Catterall, W. A. (2000) *Neuron* **26,** 13-25

28. Nonner, W. and Eisenberg, B. (1998) *Biophys.J.* **75,** 1287-1305

29. McCleskey, E. W. and Almers, W. (1985) *Proc.Natl.Acad.Sci.U.S.A* **82,** 7149-7153

30. Armstrong, C. M. and Bezanilla, F. (1977) *J.Gen.Physiol* **70,** 567-590

31. Zagotta, W. N., Hoshi, T., and Aldrich, R. W. (1990) *Science* **250,** 568-571

32. Hoshi, T., Zagotta, W. N., and Aldrich, R. W. (1991) *Neuron* **7,** 547-556

33. Lopez-Barneo, J., Hoshi, T., Heinemann, S. H., and Aldrich, R. W. (1993) *Receptors.Channels* **1,** 61-71

34. Rettig, J., Heinemann, S. H., Wunder, F., Lorra, C., Parcej, D. N., Dolly, J. O., and Pongs, O. (1994) *Nature* **369,** 289-294

35. West, J. W., Patton, D. E., Scheuer, T., Wang, Y., Goldin, A. L., and Catterall, W. A. (1992) *Proc.Natl.Acad.Sci.U.S.A* **89,** 10910-10914

36. Isom, L. L., De Jongh, K. S., Patton, D. E., Reber, B. F., Offord, J., Charbonneau, H., Walsh, K., Goldin, A. L., and Catterall, W. A. (1992) *Science* **256,** 839-842

37. Chahine, M., George, A. L., Jr., Zhou, M., Ji, S., Sun, W., Barchi, R. L., and Horn, R. (1994) *Neuron* **12,** 281-294

38. Zhang, J. F., Ellinor, P. T., Aldrich, R. W., and Tsien, R. W. (1994) *Nature* **372,** 97-100

39. Kuo, C. C. and Bean, B. P. (1994) *Neuron* **12,** 819-829

40. Serrano, J. R., Perez-Reyes, E., and Jones, S. W. (1999) *J.Gen.Physiol* **114,** 185-201

41. Curtis, B. M. and Catterall, W. A. (1984) *Biochemistry* **23,** 2113-2118

42. Takahashi, M., Seagar, M. J., Jones, J. F., Reber, B. F., and Catterall, W. A. (1987) *Proc.Natl.Acad.Sci.U.S.A* **84,** 5478-5482

43. Wang, M. C., Velarde, G., Ford, R. C., Berrow, N. S., Dolphin, A. C., and Kitmitto, A. (2002) *J.Mol.Biol.* **323,** 85-98

44. Wang, M. C., Collins, R. F., Ford, R. C., Berrow, N. S., Dolphin, A. C., and Kitmitto, A. (2004) *J.Biol.Chem.* **279,** 7159-7168

45. FATT, P. and KATZ, B. (1953) *J.Physiol* **120,** 171-204

46. FATT, P. and GINSBORG, B. L. (1958) *J.Physiol* **142,** 516-543

47. Catterall, W. A. (1998) *Cell Calcium* **24,** 307-323

48. Jones, S. W. (1998) *J.Bioenerg.Biomembr.* **30,** 299-312

49. Carbone, E. and Lux, H. D. (1984) *Nature* **310,** 501-502

50. Nowycky, M. C., Fox, A. P., and Tsien, R. W. (1985) *Nature* **316,** 440-443

51. Plummer, M. R., Logothetis, D. E., and Hess, P. (1989) *Neuron* **2,** 1453-1463

52. Regan, L. J. (1991) *J.Neurosci.* **11,** 2259-2269

53. Regan, L. J., Sah, D. W., and Bean, B. P. (1991) *Neuron* **6,** 269-280

54. Llinas, R., Sugimori, M., Lin, J. W., and Cherksey, B. (1989) *Proc.Natl.Acad.Sci.U.S.A* **86,** 1689-1693

55. Regan, R. F. and Choi, D. W. (1991) *Neuroscience* **43,** 585-591

56. Zhang, J. F., Randall, A. D., Ellinor, P. T., Horne, W. A., Sather, W. A., Tanabe, T., Schwarz, T. L., and Tsien, R. W. (1993) *Neuropharmacology* **32,** 1075-1088

57. Elmslie, K. S., Kammermeier, P. J., and Jones, S. W. (1994) *Neuron* **13,** 217-228

58. Tottene, A., Moretti, A., and Pietrobon, D. (1996) *J.Neurosci.* **16,** 6353-6363

59. Ertel, E. A., Campbell, K. P., Harpold, M. M., Hofmann, F., Mori, Y., Perez-Reyes, E., Schwartz, A., Snutch, T. P., Tanabe, T., Birnbaumer, L., Tsien, R. W., and Catterall, W. A. (2000) *Neuron* **25,** 533-535

60. Zhou, J., Cribbs, L., Yi, J., Shirokov, R., Perez-Reyes, E., and Rios, E. (1998) *J.Biol.Chem.* **273,** 25503-25509

61. Mikami, A., Imoto, K., Tanabe, T., Niidome, T., Mori, Y., Takeshima, H., Narumiya, S., and Numa, S. (1989) *Nature* **340,** 230-233

62. Snutch, T. P., Tomlinson, W. J., Leonard, J. P., and Gilbert, M. M. (1991) *Neuron* **7,** 45-57

63. Williams, M. E., Brust, P. F., Feldman, D. H., Patthi, S., Simerson, S., Maroufi, A., McCue, A. F., Velicelebi, G., Ellis, S. B., and Harpold, M. M. (1992) *Science* **257,** 389-395

64. Tomlinson, W. J., Stea, A., Bourinet, E., Charnet, P., Nargeot, J., and Snutch, T. P. (1993) *Neuropharmacology* **32,** 1117-1126

65. Bech-Hansen, N. T., Naylor, M. J., Maybaum, T. A., Pearce, W. G., Koop, B., Fishman, G. A., Mets, M., Musarella, M. A., and Boycott, K. M. (1998) *Nat.Genet.* **19,** 264-267

66. Mori, Y., Friedrich, T., Kim, M. S., Mikami, A., Nakai, J., Ruth, P., Bosse, E., Hofmann, F., Flockerzi, V., Furuichi, T., and . (1991) *Nature* **350,** 398-402

67. Sather, W. A., Tanabe, T., Zhang, J. F., Mori, Y., Adams, M. E., and Tsien, R. W. (1993) *Neuron* **11,** 291-303

68. Stea, A., Tomlinson, W. J., Soong, T. W., Bourinet, E., Dubel, S. J., Vincent, S. R., and Snutch, T. P. (1994) *Proc.Natl.Acad.Sci.U.S.A* **91,** 10576-10580

69. Bourinet, E., Soong, T. W., Sutton, K., Slaymaker, S., Mathews, E., Monteil, A., Zamponi, G. W., Nargeot, J., and Snutch, T. P. (1999) *Nat.Neurosci.* **2,** 407-415

70. Dubel, S. J., Starr, T. V., Hell, J., Ahlijanian, M. K., Enyeart, J. J., Catterall, W. A., and Snutch, T. P. (1992) *Proc.Natl.Acad.Sci.U.S.A* **89,** 5058-5062

71. Fujita, Y., Mynlieff, M., Dirksen, R. T., Kim, M. S., Niidome, T., Nakai, J., Friedrich, T., Iwabe, N., Miyata, T., Furuichi, T., and . (1993) *Neuron* **10,** 585-598

72. Soong, T. W., Stea, A., Hodson, C. D., Dubel, S. J., Vincent, S. R., and Snutch, T. P. (1993) *Science* **260,** 1133-1136

73. Williams, M. E., Marubio, L. M., Deal, C. R., Hans, M., Brust, P. F., Philipson, L. H., Miller, R. J., Johnson, E. C., Harpold, M. M., and Ellis, S. B. (1994) *J.Biol.Chem.* **269,** 22347-22357

74. Wilson, S. M., Toth, P. T., Oh, S. B., Gillard, S. E., Volsen, S., Ren, D., Philipson, L. H., Lee, E. C., Fletcher, C. F., Tessarollo, L., Copeland, N. G., Jenkins, N. A., and Miller, R. J. (2000) *J.Neurosci.* **20,** 8566-8571

75. Matsuda, Y., Saegusa, H., Zong, S., Noda, T., and Tanabe, T. (2001) *Biochem.Biophys.Res.Commun.* **289,** 791-795

76. Lee, J. H., Daud, A. N., Cribbs, L. L., Lacerda, A. E., Pereverzev, A., Klockner, U., Schneider, T., and Perez-Reyes, E. (1999) *J.Neurosci.* **19,** 1912-1921

77. Cribbs, L. L., Gomora, J. C., Daud, A. N., Lee, J. H., and Perez-Reyes, E. (2000) *FEBS Lett.* **466,** 54-58

78. McRory, J. E., Santi, C. M., Hamming, K. S., Mezeyova, J., Sutton, K. G., Baillie, D. L., Stea, A., and Snutch, T. P. (2001) *J.Biol.Chem.* **276,** 3999-4011

79. Monteil, A., Chemin, J., Leuranguer, V., Altier, C., Mennessier, G., Bourinet, E., Lory, P., and Nargeot, J. (2000) *J.Biol.Chem.* **275,** 16530-16535

80. Monteil, A., Chemin, J., Bourinet, E., Mennessier, G., Lory, P., and Nargeot, J. (2000) *J.Biol.Chem.* **275,** 6090-6100

81. Perez-Reyes, E., Cribbs, L. L., Daud, A., Lacerda, A. E., Barclay, J., Williamson, M. P., Fox, M., Rees, M., and Lee, J. H. (1998) *Nature* **391,** 896-900

82. Perez-Reyes, E. (1998) *J.Bioenerg.Biomembr.* **30,** 313-318

83. Beedle, A. M., Hamid, J., and Zamponi, G. W. (2002) *J.Membr.Biol.* **187,** 225-238

84. Chad, J. E. and Eckert, R. (1984) *Biophys.J.* **45,** 993-999

85. Simon, S. M. and Llinas, R. R. (1985) *Biophys.J.* **48,** 485-498

86. Sala, F. and Hernandez-Cruz, A. (1990) *Biophys.J.* **57,** 313-324

87. Nowycky, M. C. and Pinter, M. J. (1993) *Biophys.J.* **64,** 77-91

88. Naraghi, M. and Neher, E. (1997) *J.Neurosci.* **17,** 6961-6973

89. Rios, E. and Stern, M. D. (1997) *Annu.Rev.Biophys.Biomol.Struct.* **26,** 47-82

90. Dunlap, K., Luebke, J. I., and Turner, T. J. (1995) *Trends Neurosci.* **18,** 89-98

91. Tsien, R. W., Lipscombe, D., Madison, D. V., Bley, K. R., and Fox, A. P. (1988) *Trends Neurosci.* **11,** 431-438

92. Yaari, Y., Hamon, B., and Lux, H. D. (1987) *Science* **235,** 680-682

93. Usachev, Y. M. and Thayer, S. A. (1997) *J.Neurosci.* **17,** 7404-7414

94. Ghosh, A. and Greenberg, M. E. (1995) *Science* **268,** 239-247

95. Bito, H., Deisseroth, K., and Tsien, R. W. (1997) *Curr.Opin.Neurobiol.* **7,** 419-429

96. Franzini-Armstrong, C. and Protasi, F. (1997) *Physiol Rev.* **77,** 699-729

97. Cheng, H., Lederer, M. R., Lederer, W. J., and Cannell, M. B. (1996) *Am.J.Physiol* **270,** C148-C159

98. Hell, J. W., Westenbroek, R. E., Warner, C., Ahlijanian, M. K., Prystay, W., Gilbert, M. M., Snutch, T. P., and Catterall, W. A. (1993) *J.Cell Biol.* **123,** 949-962

99. Bean, B. (1989) *Trends Neurosci.* **12,** 128-130

100. Heidelberger, R. and Matthews, G. (1992) *J.Physiol* **447,** 235-256

101. Chavis, P., Fagni, L., Lansman, J. B., and Bockaert, J. (1996) *Nature* **382,** 719-722

102. Milani, D., Malgaroli, A., Guidolin, D., Fasolato, C., Skaper, S. D., Meldolesi, J., and Pozzan, T. (1990) *Cell Calcium* **11,** 191-199

103. Wheeler, D. B., Randall, A., and Tsien, R. W. (1994) *Science* **264,** 107-111

104. Westenbroek, R. E., Hell, J. W., Warner, C., Dubel, S. J., Snutch, T. P., and Catterall, W. A. (1992) *Neuron* **9,** 1099-1115

105. Westenbroek, R. E., Sakurai, T., Elliott, E. M., Hell, J. W., Starr, T. V., Snutch, T. P., and Catterall, W. A. (1995) *J.Neurosci.* **15,** 6403-6418

106. Hanson, J. E. and Smith, Y. (2002) *J.Comp Neurol.* **442,** 89-98

107. Huguenard, J. R. (1996) *Annu.Rev.Physiol* **58,** 329-348

108. Perez-Reyes, E., Kim, H. S., Lacerda, A. E., Horne, W., Wei, X. Y., Rampe, D., Campbell, K. P., Brown, A. M., and Birnbaumer, L. (1989) *Nature* **340,** 233-236

109. Lacerda, A. E., Kim, H. S., Ruth, P., Perez-Reyes, E., Flockerzi, V., Hofmann, F., Birnbaumer, L., and Brown, A. M. (1991) *Nature* **352,** 527-530

110. Stea, A., Dubel, S. J., Pragnell, M., Leonard, J. P., Campbell, K. P., and Snutch, T. P. (1993) *Neuropharmacology* **32,** 1103-1116

111. Castellano, A., Wei, X., Birnbaumer, L., and Perez-Reyes, E. (1993) *J.Biol.Chem.* **268,** 12359-12366

112. Castellano, A., Wei, X., Birnbaumer, L., and Perez-Reyes, E. (1993) *J.Biol.Chem.* **268,** 3450-3455

113. Zamponi, G. W., Soong, T. W., Bourinet, E., and Snutch, T. P. (1996) *J.Neurosci.* **16,** 2430-2443

114. Felix, R. (1999) *Receptors.Channels* **6,** 351-362

115. Klugbauer, N., Lacinova, L., Marais, E., Hobom, M., and Hofmann, F. (1999) *J.Neurosci.* **19,** 684-691

116. Rousset, M., Cens, T., Restituito, S., Barrere, C., Black, J. L., III, McEnery, M. W., and Charnet, P. (2001) *J.Physiol* **532,** 583-593

117. Sharp, A. H., Black, J. L., III, Dubel, S. J., Sundarraj, S., Shen, J. P., Yunker, A. M., Copeland, T. D., and McEnery, M. W. (2001) *Neuroscience* **105,** 599-617

118. Ruth, P., Rohrkasten, A., Biel, M., Bosse, E., Regulla, S., Meyer, H. E., Flockerzi, V., and Hofmann, F. (1989) *Science* **245,** 1115-1118

119. Hullin, R., Singer-Lahat, D., Freichel, M., Biel, M., Dascal, N., Hofmann, F., and Flockerzi, V. (1992) *EMBO J.* **11,** 885-890

120. Dolphin, A. C. (2003) *J.Bioenerg.Biomembr.* **35,** 599-620

121. De Waard, M., Pragnell, M., and Campbell, K. P. (1994) *Neuron* **13,** 495-503

122. Chien, A. J., Gao, T., Perez-Reyes, E., and Hosey, M. M. (1998) *J.Biol.Chem.* **273,** 23590-23597

123. Hanlon, M. R., Berrow, N. S., Dolphin, A. C., and Wallace, B. A. (1999) *FEBS Lett.* **445,** 366-370

124. Van Petegem, F., Clark, K. A., Chatelain, F. C., and Minor, D. L., Jr. (2004) *Nature* **429,** 671-675

125. Opatowsky, Y., Chen, C. C., Campbell, K. P., and Hirsch, J. A. (2004) *Neuron* **42,** 387-399

126. Chen, Y. H., Li, M. H., Zhang, Y., He, L. L., Yamada, Y., Fitzmaurice, A., Shen, Y., Zhang, H., Tong, L., and Yang, J. (2004) *Nature* **429,** 675-680

127. Pragnell, M., De Waard, M., Mori, Y., Tanabe, T., Snutch, T. P., and Campbell, K. P. (1994) *Nature* **368,** 67-70

128. Qin, N., Platano, D., Olcese, R., Stefani, E., and Birnbaumer, L. (1997) *Proc.Natl.Acad.Sci.U.S.A* **94,** 8866-8871

129. Walker, D., Bichet, D., Campbell, K. P., and De Waard, M. (1998) *J.Biol.Chem.* **273,** 2361-2367

130. Walker, D., Bichet, D., Geib, S., Mori, E., Cornet, V., Snutch, T. P., Mori, Y., and De Waard, M. (1999) *J.Biol.Chem.* **274,** 12383-12390

131. Stephens, G. J., Page, K. M., Bogdanov, Y., and Dolphin, A. C. (2000) *J.Physiol* **525 Pt 2,** 377-390

132. Birnbaumer, L., Qin, N., Olcese, R., Tareilus, E., Platano, D., Costantin, J., and Stefani, E. (1998) *J.Bioenerg.Biomembr.* **30,** 357-375

133. Brice, N. L., Berrow, N. S., Campbell, V., Page, K. M., Brickley, K., Tedder, I., and Dolphin, A. C. (1997) *Eur.J.Neurosci.* **9,** 749-759

134. Ellis, S. B., Williams, M. E., Ways, N. R., Brenner, R., Sharp, A. H., Leung, A. T., Campbell, K. P., McKenna, E., Koch, W. J., Hui, A., and . (1988) *Science* **241,** 1661-1664

135. Gao, B., Sekido, Y., Maximov, A., Saad, M., Forgacs, E., Latif, F., Wei, M. H., Lerman, M., Lee, J. H., Perez-Reyes, E., Bezprozvanny, I., and Minna, J. D. (2000) *J.Biol.Chem.* **275,** 12237-12242

136. Qin, N., Yagel, S., Momplaisir, M. L., Codd, E. E., and D'Andrea, M. R. (2002) *Mol.Pharmacol.* **62,** 485-496

137. Gurnett, C. A., De Waard, M., and Campbell, K. P. (1996) *Neuron* **16,** 431-440

138. Gurnett, C. A., Felix, R., and Campbell, K. P. (1997) *J.Biol.Chem.* **272,** 18508-18512

139. De Jongh, K. S., Warner, C., and Catterall, W. A. (1990) *J.Biol.Chem.* **265,** 14738-14741

140. Jay, S. D., Sharp, A. H., Kahl, S. D., Vedvick, T. S., Harpold, M. M., and Campbell, K. P. (1991) *J.Biol.Chem.* **266,** 3287-3293

141. Brickley, K., Campbell, V., Berrow, N., Leach, R., Norman, R. I., Wray, D., Dolphin, A. C., and Baldwin, S. A. (1995) *FEBS Lett.* **364,** 129-133

142. Felix, R., Gurnett, C. A., De Waard, M., and Campbell, K. P. (1997) *J.Neurosci.* **17,** 6884-6891

143. Klugbauer, N., Marais, E., and Hofmann, F. (2003) *J.Bioenerg.Biomembr.* **35,** 639-647

144. Lorenzon, N. M. and Beam, K. G. (2000) *Kidney Int.* **57,** 794-802

145. Ophoff, R. A., Terwindt, G. M., Vergouwe, M. N., van Eijk, R., Oefner, P. J., Hoffman, S. M., Lamerdin, J. E., Mohrenweiser, H. W., Bulman, D. E., Ferrari, M., Haan, J., Lindhout, D., van Ommen, G. J., Hofker, M. H., Ferrari, M. D., and Frants, R. R. (1996) *Cell* **87,** 543-552

146. Yue, Q., Jen, J. C., Thwe, M. M., Nelson, S. F., and Baloh, R. W. (1998) *Am.J.Med.Genet.* **77,** 298-301

147. Zhuchenko, O., Bailey, J., Bonnen, P., Ashizawa, T., Stockton, D. W., Amos, C., Dobyns, W. B., Subramony, S. H., Zoghbi, H. Y., and Lee, C. C. (1997) *Nat.Genet.* **15,** 62-69

148. Noebels, J. L. (1984) *Nature* **310,** 409-411

149. Fletcher, C. F., Lutz, C. M., O'Sullivan, T. N., Shaughnessy, J. D., Jr., Hawkes, R., Frankel, W. N., Copeland, N. G., and Jenkins, N. A. (1996) *Cell* **87,** 607-617

150. Doyle, J., Ren, X., Lennon, G., and Stubbs, L. (1997) *Mamm.Genome* **8,** 113-120

151. Bech-Hansen, N. T., Naylor, M. J., Maybaum, T. A., Pearce, W. G., Koop, B., Fishman, G. A., Mets, M., Musarella, M. A., and Boycott, K. M. (1998) *Nat.Genet.* **19,** 264-267

152. Strom, T. M., Nyakatura, G., Apfelstedt-Sylla, E., Hellebrand, H., Lorenz, B., Weber, B. H., Wutz, K., Gutwillinger, N., Ruther, K., Drescher, B., Sauer, C., Zrenner, E., Meitinger, T., Rosenthal, A., and Meindl, A. (1998) *Nat.Genet.* **19,** 260-263

153. Jurkat-Rott, K., Lehmann-Horn, F., Elbaz, A., Heine, R., Gregg, R. G., Hogan, K., Powers, P. A., Lapie, P., Vale-Santos, J. E., Weissenbach, J., and . (1994) *Hum.Mol.Genet.* **3,** 1415-1419

154. Ptacek, L. J., Tawil, R., Griggs, R. C., Engel, A. G., Layzer, R. B., Kwiecinski, H., McManis, P. G., Santiago, L., Moore, M., Fouad, G., and . (1994) *Cell* **77,** 863-868

155. Fouad, G., Dalakas, M., Servidei, S., Mendell, J. R., Van den, B. P., Angelini, C., Alderson, K., Griggs, R. C., Tawil, R., Gregg, R., Hogan, K., Powers, P. A., Weinberg, N., Malonee, W., and Ptacek, L. J. (1997) *Neuromuscul.Disord.* **7,** 33-38

156. Dung, H. C. and Swigart, R. H. (1972) *Tex.Rep.Biol.Med.* **30,** 23-39

157. Escayg, A., Jones, J. M., Kearney, J. A., Hitchcock, P. F., and Meisler, M. H. (1998) *Genomics* **50,** 14-22

158. Barclay, J., Balaguero, N., Mione, M., Ackerman, S. L., Letts, V. A., Brodbeck, J., Canti, C., Meir, A., Page, K. M., Kusumi, K., Perez-Reyes, E., Lander, E. S., Frankel, W. N., Gardiner, R. M., Dolphin, A. C., and Rees, M. (2001) *J.Neurosci.* **21,** 6095-6104

159. Brill, J., Klocke, R., Paul, D., Boison, D., Gouder, N., Klugbauer, N., Hofmann, F., Becker, C. M., and Becker, K. (2004) *J.Biol.Chem.* **279,** 7322-7330

160. Tomita, S., Fukata, M., Nicoll, R. A., and Bredt, D. S. (2004) *Science* **303,** 1508-1511

161. Songyang, Z., Fanning, A. S., Fu, C., Xu, J., Marfatia, S. M., Chishti, A. H., Crompton, A., Chan, A. C., Anderson, J. M., and Cantley, L. C. (1997) *Science* **275,** 73-77

162. Jay, S. D., Ellis, S. B., McCue, A. F., Williams, M. E., Vedvick, T. S., Harpold, M. M., and Campbell, K. P. (1990) *Science* **248,** 490-492

163. Bosse, E., Regulla, S., Biel, M., Ruth, P., Meyer, H. E., Flockerzi, V., and Hofmann, F. (1990) *FEBS Lett.* **267,** 153-156

164. Powers, P. A., Liu, S., Hogan, K., and Gregg, R. G. (1993) *J.Biol.Chem.* **268,** 9275-9279

165. Iles, D. E., Segers, B., Weghuis, D. O., Suikerbuijk, R., and Wieringa, B. (1993) *Cytogenet.Cell Genet.* **64,** 227-230

166. Iles, D. E., Segers, B., Sengers, R. C., Monsieurs, K., Heytens, L., Halsall, P. J., Hopkins, P. M., Ellis, F. R., Hall-Curran, J. L., Stewart, A. D., and . (1993) *Hum.Mol.Genet.* **2,** 863-868

167. Eberst, R., Dai, S., Klugbauer, N., and Hofmann, F. (1997) *Pflugers Arch.* **433,** 633-637

168. Letts, V. A., Felix, R., Biddlecome, G. H., Arikkath, J., Mahaffey, C. L., Valenzuela, A., Bartlett, F. S., Mori, Y., Campbell, K. P., and Frankel, W. N. (1998) *Nat.Genet.* **19,** 340-347

169. Black, J. L., III and Lennon, V. A. (1999) *Mayo Clin.Proc.* **74,** 357-361

170. Klugbauer, N., Dai, S., Specht, V., Lacinova, L., Marais, E., Bohn, G., and Hofmann, F. (2000) *FEBS Lett.* **470,** 189-197

171. Chu, P. J., Robertson, H. M., and Best, P. M. (2001) *Gene* **280,** 37-48

172. Burgess, D. L., Davis, C. F., Gefrides, L. A., and Noebels, J. L. (1999) *Genome Res.* **9,** 1204-1213

173. Burgess, D. L., Gefrides, L. A., Foreman, P. J., and Noebels, J. L. (2001) *Genomics* **71,** 339-350

174. Moss, F. J., Viard, P., Davies, A., Bertaso, F., Page, K. M., Graham, A., Canti, C., Plumpton, M., Plumpton, C., Clare, J. J., and Dolphin, A. C. (2002) *EMBO J.* **21,** 1514-1523

175. Gustincich, S., Batalov, S., Beisel, K. W., Bono, H., Carninci, P., Fletcher, C. F., Grimmond, S., Hirokawa, N., Jarvis, E. D., Jegla, T., Kawasawa, Y., LeMieux, J., Miki, H., Raviola, E., Teasdale, R. D., Tominaga, N., Yagi, K., Zimmer, A., Hayashizaki, Y., and Okazaki, Y. (2003) *Genome Res.* **13,** 1395-1401

176. Moss, F. J., Dolphin, A. C., and Clare, J. J. (2003) *BMC.Neurosci.* **4,** 23

177. Tomita, S., Chen, L., Kawasaki, Y., Petralia, R. S., Wenthold, R. J., Nicoll, R. A., and Bredt, D. S. (2003) *J.Cell Biol.* **161,** 805-816

178. Green, P. J., Warre, R., Hayes, P. D., McNaughton, N. C., Medhurst, A. D., Pangalos, M., Duckworth, D. M., and Randall, A. D. (2001) *J.Physiol* **533,** 467-478

179. Kious, B. M., Baker, C. V., Bronner-Fraser, M., and Knecht, A. K. (2002) *Dev.Biol.* **243,** 249-259

180. Wei, X. Y., Perez-Reyes, E., Lacerda, A. E., Schuster, G., Brown, A. M., and Birnbaumer, L. (1991) *J.Biol.Chem.* **266,** 21943-21947

181. Lerche, H., Klugbauer, N., Lehmann-Horn, F., Hofmann, F., and Melzer, W. (1996) *Pflugers Arch.* **431,** 461-463

182. Kang, M. G., Chen, C. C., Felix, R., Letts, V. A., Frankel, W. N., Mori, Y., and Campbell, K. P. (2001) *J.Biol.Chem.* **276,** 32917-32924

183. Ahern, C. A., Powers, P. A., Biddlecome, G. H., Roethe, L., Vallejo, P., Mortenson, L., Strube, C., Campbell, K. P., Coronado, R., and Gregg, R. G. (2001) *BMC.Physiol* **1,** 8

184. Arikkath, J., Chen, C. C., Ahern, C., Allamand, V., Flanagan, J. D., Coronado, R., Gregg, R. G., and Campbell, K. P. (2003) *J.Biol.Chem.* **278,** 1212-1219

185. Ursu, D., Sebille, S., Dietze, B., Freise, D., Flockerzi, V., and Melzer, W. (2001) *J.Physiol* **533,** 367-377

186. Held, B., Freise, D., Freichel, M., Hoth, M., and Flockerzi, V. (2002) *J.Physiol* **539,** 459-468

187. Hansen, J. P., Chen, R. S., Larsen, J. K., Chu, P. J., Janes, D. M., Weis, K. E., and Best, P. M. (2004) *J.Mol.Cell Cardiol.* **37,** 1147-1158

188. Seeburg, P. H. (1993) *Trends Neurosci.* **16,** 359-365

189. Hollmann, M. and Heinemann, S. (1994) *Annu.Rev.Neurosci.* **17,** 31-108

190. Palmer, C. L., Cotton, L., and Henley, J. M. (2005) *Pharmacol.Rev.* **57,** 253-277

191. Noebels, J. L., Qiao, X., Bronson, R. T., Spencer, C., and Davisson, M. T. (1990) *Epilepsy Res.* **7,** 129-135

192. Letts, V. A., Kang, M. G., Mahaffey, C. L., Beyer, B., Tenbrink, H., Campbell, K. P., and Frankel, W. N. (2003) *Mamm.Genome* **14,** 506-513

193. Aizawa, M., Ito, Y., and Fukuda, H. (1997) *Neurosci.Res.* **29,** 17-25

194. Di Pasquale, E., Keegan, K. D., and Noebels, J. L. (1997) *J.Neurophysiol.* **77,** 621-631

195. Zhang, Y., Mori, M., Burgess, D. L., and Noebels, J. L. (2002) *J.Neurosci.* **22,** 6362-6371

196. Qiao, X. and Noebels, J. L. (1993) *J.Neurosci.* **13,** 4622-4635

197. Qiao, X., Hefti, F., Knusel, B., and Noebels, J. L. (1996) *J.Neurosci.* **16,** 640-648

198. Qiao, X., Chen, L., Gao, H., Bao, S., Hefti, F., Thompson, R. F., and Knusel, B. (1998) *J.Neurosci.* **18,** 6990-6999

199. Thompson, C. L., Tehrani, M. H., Barnes, E. M., Jr., and Stephenson, F. A. (1998) *Brain Res.Mol.Brain Res.* **60,** 282-290

200. Richardson, C. A. and Leitch, B. (2002) *J.Comp Neurol.* **453,** 85-99

201. Hashimoto, K., Fukaya, M., Qiao, X., Sakimura, K., Watanabe, M., and Kano, M. (1999) *J.Neurosci.* **19,** 6027-6036

202. Chen, L., Chetkovich, D. M., Petralia, R. S., Sweeney, N. T., Kawasaki, Y., Wenthold, R. J., Bredt, D. S., and Nicoll, R. A. (2000) *Nature* **408,** 936-943

203. Choi, J., Ko, J., Park, E., Lee, J. R., Yoon, J., Lim, S., and Kim, E. (2002) *J.Biol.Chem.* **277,** 12359-12363

204. Chetkovich, D. M., Chen, L., Stocker, T. J., Nicoll, R. A., and Bredt, D. S. (2002) *J.Neurosci.* **22,** 5791-5796

205. Tomita, S., Stein, V., Stocker, T. J., Nicoll, R. A., and Bredt, D. S. (2005) *Neuron* **45,** 269-277

206. Schnell, E., Sizemore, M., Karimzadegan, S., Chen, L., Bredt, D. S., and Nicoll, R. A. (2002) *Proc.Natl.Acad.Sci.U.S.A* **99,** 13902-13907

207. Chen, L., El Husseini, A., Tomita, S., Bredt, D. S., and Nicoll, R. A. (2003) *Mol.Pharmacol.* **64,** 703-706

208. Cuadra, A. E., Kuo, S. H., Kawasaki, Y., Bredt, D. S., and Chetkovich, D. M. (2004) *J.Neurosci.* **24,** 7491-7502

209. Ives, J. H., Fung, S., Tiwari, P., Payne, H. L., and Thompson, C. L. (2004) *J.Biol.Chem.* **279,** 31002-31009

210. Yamazaki, M., Ohno-Shosaku, T., Fukaya, M., Kano, M., Watanabe, M., and Sakimura, K. (2004) *Neurosci.Res.* **50,** 369-374

211. Priel, A., Kolleker, A., Ayalon, G., Gillor, M., Osten, P., and Stern-Bach, Y. (2005) *J.Neurosci.* **25,** 2682-2686

212. Tomita, S., Adesnik, H., Sekiguchi, M., Zhang, W., Wada, K., Howe, J. R., Nicoll, R. A., and Bredt, D. S. (2005) *Nature* **435,** 1052-1058

213. Dreyfuss, G., Kim, V. N., and Kataoka, N. (2002) *Nat.Rev.Mol.Cell Biol.* **3,** 195-205

214. Swick, A. G., Janicot, M., Cheneval-Kastelic, T., McLenithan, J. C., and Lane, M. D. (1992) *Proc.Natl.Acad.Sci.U.S.A* **89,** 1812-1816

215. SHIMOMURA, O., JOHNSON, F. H., and SAIGA, Y. (1962) *J.Cell Comp Physiol* **59,** 223-239

216. Ward, W. W. and Cormier, M. J. (1979) *J.Biol.Chem.* **254,** 781-788

217. Prasher, D. C., Eckenrode, V. K., Ward, W. W., Prendergast, F. G., and Cormier, M. J. (1992) *Gene* **111,** 229-233

218. Bastiaens, P. I. and Pepperkok, R. (2000) *Trends Biochem.Sci.* **25,** 631-637

219. Wilson, I. A., Niman, H. L., Houghten, R. A., Cherenson, A. R., Connolly, M. L., and Lerner, R. A. (1984) *Cell* **37,** 767-778

220. Pines, J. and Hunter, T. (1991) *J.Cell Biol.* **115,** 1-17

221. Chen, Y. T., Holcomb, C., and Moore, H. P. (1993) *Proc.Natl.Acad.Sci.U.S.A* **90,** 6508-6512

222. Herscovics, A., Schneikert, J., Athanassiadis, A., and Moremen, K. W. (1994) *J.Biol.Chem.* **269,** 9864-9871

223. Kang, M. G. and Campbell, K. P. (2003) *J.Biol.Chem.* **278,** 21315-21318

224. Kaetzel, C. S., Rao, C. K., and Lamm, M. E. (1987) *Biochem.J.* **241,** 39-47

225. Schroder, M. and Kaufman, R. J. (2005) *Mutat.Res.* **569,** 29-63

226. Harding, H. P., Zhang, Y., Bertolotti, A., Zeng, H., and Ron, D. (2000) *Mol.Cell* **5,** 897-904

227. Scheuner, D., Song, B., McEwen, E., Liu, C., Laybutt, R., Gillespie, P., Saunders, T., Bonner-Weir, S., and Kaufman, R. J. (2001) *Mol.Cell* **7,** 1165-1176

228. Ye, J., Rawson, R. B., Komuro, R., Chen, X., Dave, U. P., Prywes, R., Brown, M. S., and Goldstein, J. L. (2000) *Mol.Cell* **6,** 1355-1364

229. Urano, F., Wang, X., Bertolotti, A., Zhang, Y., Chung, P., Harding, H. P., and Ron, D. (2000) *Science* **287,** 664-666

230. Calfon, M., Zeng, H., Urano, F., Till, J. H., Hubbard, S. R., Harding, H. P., Clark, S. G., and Ron, D. (2002) *Nature* **415,** 92-96

231. Yoshida, H., Haze, K., Yanagi, H., Yura, T., and Mori, K. (1998) *J.Biol.Chem.* **273,** 33741-33749

232. Travers, K. J., Patil, C. K., Wodicka, L., Lockhart, D. J., Weissman, J. S., and Walter, P. (2000) *Cell* **101,** 249-258

233. Yoneda, T., Imaizumi, K., Oono, K., Yui, D., Gomi, F., Katayama, T., and Tohyama, M. (2001) *J.Biol.Chem.* **276,** 13935-13940

234. Harding, H. P., Novoa, I., Zhang, Y., Zeng, H., Wek, R., Schapira, M., and Ron, D. (2000) *Mol.Cell* **6,** 1099-1108

235. Gotoh, T., Oyadomari, S., Mori, K., and Mori, M. (2002) *J.Biol.Chem.* **277,** 12343-12350

236. Berridge, M. J. (2002) *Cell Calcium* **32,** 235-249

237. Raghib, A., Bertaso, F., Davies, A., Page, K. M., Meir, A., Bogdanov, Y., and Dolphin, A. C. (2001) *J.Neurosci.* **21,** 8495-8504

238. Page, K. M., Heblich, F., Davies, A., Butcher, A. J., Leroy, J., Bertaso, F., Pratt, W. S., and Dolphin, A. C. (2004) *J.Neurosci.* **24,** 5400-5409

239. Bustin, S. A. and Nolan, T. (2004) *J.Biomol.Tech.* **15,** 155-166

240. Bertolotti, A. and Ron, D. (2001) *J.Cell Sci.* **114,** 3207-3212

241. Greene, L. A. and Tischler, A. S. (1976) *Proc.Natl.Acad.Sci.U.S.A* **73,** 2424-2428

242. Shafer, T. J. and Atchison, W. D. (1991) *Neurotoxicology* **12,** 473-492

243. Usowicz, M. M., Porzig, H., Becker, C., and Reuter, H. (1990) *J.Physiol* **426,** 95-116

244. Avidor, B., Avidor, T., Schwartz, L., De Jongh, K. S., and Atlas, D. (1994) *FEBS Lett.* **342,** 209-213

245. Liu, H., Felix, R., Gurnett, C. A., De Waard, M., Witcher, D. R., and Campbell, K. P. (1996) *J.Neurosci.* **16,** 7557-7565

246. Garber, S. S., Hoshi, T., and Aldrich, R. W. (1989) *J.Neurosci.* **9,** 3976-3987

247. Lievano, A., Bolden, A., and Horn, R. (1994) *Am.J.Physiol* **267,** C411-C424

248. Colston, J. T., Valdes, J. J., and Chambers, J. P. (1998) *Int.J.Dev.Neurosci.* **16,** 379-389

249. Passafaro, M., Rosa, P., Sala, C., Clementi, F., and Sher, E. (1996) *J.Biol.Chem.* **271,** 30096-30104

250. Casado, M., Lopez-Guajardo, A., Mellstrom, B., Naranjo, J. R., and Lerma, J. (1996) *J.Physiol* **490 (Pt 2),** 391-404

251. Zerangue, N., Schwappach, B., Jan, Y. N., and Jan, L. Y. (1999) *Neuron* **22,** 537-548

252. Ma, D., Zerangue, N., Lin, Y. F., Collins, A., Yu, M., Jan, Y. N., and Jan, L. Y. (2001) *Science* **291,** 316-319

253. Scott, D. B., Blanpied, T. A., Swanson, G. T., Zhang, C., and Ehlers, M. D. (2001) *J.Neurosci.* **21,** 3063-3072

254. Margeta-Mitrovic, M., Jan, Y. N., and Jan, L. Y. (2000) *Neuron* **27,** 97-106

255. Taylor, V., Zgraggen, C., Naef, R., and Suter, U. (2000) *J.Neurosci.Res.* **62,** 15-27

256. Kozak, M. (1986) *Cell* **44,** 283-292

257. Rogers, S., Wells, R., and Rechsteiner, M. (1986) *Science* **234,** 364-368

258. Sun, J. and Liao, J. K. (2002) *Proc.Natl.Acad.Sci.U.S.A* **99,** 13108-13113

259. Pappin, D. J., Hojrup, P., and Bleasby, A. J. (1993) *Curr.Biol.* **3,** 327-332

260. Perkins, D. N., Pappin, D. J., Creasy, D. M., and Cottrell, J. S. (1999) *Electrophoresis* **20,** 3551-3567

261. Hoek, K. S., Kidd, G. J., Carson, J. H., and Smith, R. (1998) *Biochemistry* **37,** 7021-7029

262. Ainger, K., Avossa, D., Diana, A. S., Barry, C., Barbarese, E., and Carson, J. H. (1997) *J.Cell Biol.* **138,** 1077-1087

263. Dreyfuss, G., Matunis, M. J., Pinol-Roma, S., and Burd, C. G. (1993) *Annu.Rev.Biochem.* **62,** 289-321

264. Nakielny, S. and Dreyfuss, G. (1997) *Curr.Opin.Cell Biol.* **9,** 420-429

265. Carson, J. H., Kwon, S., and Barbarese, E. (1998) *Curr.Opin.Neurobiol.* **8,** 607-612

266. Oleynikov, Y. and Singer, R. H. (1998) *Trends Cell Biol.* **8,** 381-383

267. Bassell, G. J., Oleynikov, Y., and Singer, R. H. (1999) *FASEB J.* **13,** 447-454

268. Crino, P. B. and Eberwine, J. (1996) *Neuron* **17,** 1173-1187

269. Ainger, K., Avossa, D., Morgan, F., Hill, S. J., Barry, C., Barbarese, E., and Carson, J. H. (1993) *J.Cell Biol.* **123,** 431-441

270. Barbarese, E., Koppel, D. E., Deutscher, M. P., Smith, C. L., Ainger, K., Morgan, F., and Carson, J. H. (1995) *J.Cell Sci.* **108 (Pt 8),** 2781-2790

271. Colman, D. R., Kreibich, G., Frey, A. B., and Sabatini, D. D. (1982) *J.Cell Biol.* **95,** 598-608

272. Trapp, B. D., Moench, T., Pulley, M., Barbosa, E., Tennekoon, G., and Griffin, J. (1987) *Proc.Natl.Acad.Sci.U.S.A* **84,** 7773-7777

273. Carson, J. H., Cui, H., and Barbarese, E. (2001) *Curr.Opin.Neurobiol.* **11,** 558-563

274. Michelotti, E. F., Michelotti, G. A., Aronsohn, A. I., and Levens, D. (1996) *Mol.Cell Biol.* **16,** 2350-2360

275. Ishikawa, F., Matunis, M. J., Dreyfuss, G., and Cech, T. R. (1993) *Mol.Cell Biol.* **13,** 4301-4310

276. LaBranche, H., Dupuis, S., Ben David, Y., Bani, M. R., Wellinger, R. J., and Chabot, B. (1998) *Nat.Genet.* **19,** 199-202

277. Mayeda, A. and Krainer, A. R. (1992) *Cell* **68,** 365-375

278. Kiledjian, M., DeMaria, C. T., Brewer, G., and Novick, K. (1997) *Mol.Cell Biol.* **17,** 4870-4876

279. Beyer, A. L., Christensen, M. E., Walker, B. W., and LeStourgeon, W. M. (1977) *Cell* **11,** 127-138

280. Burd, C. G., Swanson, M. S., Gorlach, M., and Dreyfuss, G. (1989) *Proc.Natl.Acad.Sci.U.S.A* **86,** 9788-9792

281. Kiledjian, M. and Dreyfuss, G. (1992) *EMBO J.* **11,** 2655-2664

282. Biamonti, G., Ruggiu, M., Saccone, S., Della, V. G., and Riva, S. (1994) *Nucleic Acids Res.* **22,** 1996-2002

283. Kozu, T., Henrich, B., and Schafer, K. P. (1995) *Genomics* **25,** 365-371

284. Kamma, H., Horiguchi, H., Wan, L., Matsui, M., Fujiwara, M., Fujimoto, M., Yazawa, T., and Dreyfuss, G. (1999) *Exp.Cell Res.* **246,** 399-411

285. Munro, T. P., Magee, R. J., Kidd, G. J., Carson, J. H., Barbarese, E., Smith, L. M., and Smith, R. (1999) *J.Biol.Chem.* **274,** 34389-34395

286. Shan, J., Munro, T. P., Barbarese, E., Carson, J. H., and Smith, R. (2003) *J.Neurosci.* **23,** 8859-8866

287. Ma, A. S., Moran-Jones, K., Shan, J., Munro, T. P., Snee, M. J., Hoek, K. S., and Smith, R. (2002) *J.Biol.Chem.* **277,** 18010-18020

288. Alliegro, M. C. and Alliegro, M. A. (1996) *Dev.Biol.* **174,** 288-297

289. Bertolotti, A., Lutz, Y., Heard, D. J., Chambon, P., and Tora, L. (1996) *EMBO J.* **15,** 5022-5031

290. Bertolotti, A., Melot, T., Acker, J., Vigneron, M., Delattre, O., and Tora, L. (1998) *Mol.Cell Biol.* **18,** 1489-1497

291. Zinszner, H., Albalat, R., and Ron, D. (1994) *Genes Dev.* **8,** 2513-2526

292. Yang, L., Embree, L. J., and Hickstein, D. D. (2000) *Mol.Cell Biol.* **20,** 3345-3354

293. Black, J. L., III (2003) *J.Bioenerg.Biomembr.* **35,** 649-660

294. Price, M. G., Davis, C. F., Deng, F., and Burgess, D. L. (2005) *J.Biol.Chem.* **280,** 19711-19720

295. Carson, J. H., Cui, H., Krueger, W., Schlepchenko, B., Brumwell, C., and Barbarese, E. (2001) *Results Probl.Cell Differ.* **34,** 69-81

296. Smith, R. (2004) *Neuroscientist.* **10,** 495-500

297. Husi, H., Ward, M. A., Choudhary, J. S., Blackstock, W. P., and Grant, S. G. (2000) *Nat.Neurosci.* **3,** 661-669

298. Belly, A., Moreau-Gachelin, F., Sadoul, R., and Goldberg, Y. (2005) *Neurosci.Lett.* **379,** 152-157

299. Xu, N., Chen, C. Y., and Shyu, A. B. (2001) *Mol.Cell Biol.* **21,** 6960-6971

300. Buzby, J. S., Brewer, G., and Nugent, D. J. (1999) *J.Biol.Chem.* **274,** 33973-33978

301. Pende, A., Tremmel, K. D., DeMaria, C. T., Blaxall, B. C., Minobe, W. A., Sherman, J. A., Bisognano, J. D., Bristow, M. R., Brewer, G., and Port, J. (1996) *J.Biol.Chem.* **271,** 8493-8501

302. Brewer, G. (1991) *Mol.Cell Biol.* **11,** 2460-2466

303. Lau, P. P., Zhu, H. J., Nakamuta, M., and Chan, L. (1997) *J.Biol.Chem.* **272,** 1452-1455

304. Greeve, J., Lellek, H., Rautenberg, P., and Greten, H. (1998) *Biol.Chem.* **379,** 1063-1073

305. Sommer, B., Kohler, M., Sprengel, R., and Seeburg, P. H. (1991) *Cell* **67,** 11-19

306. Wang, Q., Miyakoda, M., Yang, W., Khillan, J., Stachura, D. L., Weiss, M. J., and Nishikura, K. (2004) *J.Biol.Chem.* **279,** 4952-4961

307. Smith, L. A., Peixoto, A. A., and Hall, J. C. (1998) *J.Neurogenet.* **12,** 227-240

308. Tsunemi, T., Saegusa, H., Ishikawa, K., Nagayama, S., Murakoshi, T., Mizusawa, H., and Tanabe, T. (2002) *J.Biol.Chem.* **277,** 7214-7221

309. Sedzik, J., Uyemura, K., and Tsukihara, T. (2002) *Protein Expr.Purif.* **26,** 368-377

310. Sodhi, M. S., Airey, D. C., Lambert, W., Burnet, P. W., Harrison, P. J., and Sanders-Bush, E. (2005) *Mol.Pharmacol.* **68,** 711-719

311. Canti, C., Page, K. M., Stephens, G. J., and Dolphin, A. C. (1999) *J.Neurosci.* **19,** 6855-6864

312. Meir, A., Bell, D. C., Stephens, G. J., Page, K. M., and Dolphin, A. C. (2000) *Biophys.J.* **79,** 731-746

313. Canti, C., Davies, A., Berrow, N. S., Butcher, A. J., Page, K. M., and Dolphin, A. C. (2001) *Biophys.J.* **81,** 1439-1451